Balancing Safety and Capacity in an Adaptive Signal Control System—Phase 1

U.S. Department of Transportation
Federal Highway Administration

Research, Development, and Technology
Turner-Fairbank Highway Research Center
6300 Georgetown Pike
McLean, VA 22101-2296

FOREWORD

Virtually all previous research addressing intersection safety and capacity has dealt with the two issues independently. Over the past 20 years, advancements in real-time adaptive signal timing strategies for intersections and arterials have improved signal operations by improving traffic flow efficiency, but most optimization algorithms do not include performance measures for safety. At this time, little is known about the relationships between signal timing parameters (e.g., cycle time, offsets, phase sequence, etc.) and safety that can be of benefit to traffic engineering practitioners.

This research, comprising two phases, focuses on the development of real-time signal timing methodologies and algorithms that balance safety and efficiency. This report summarizes phase 1, which examines relationships between signal timing parameters and surrogate measures of safety such as rear-end, angle, and lane-change conflicts. These single variable relationship studies determine the parameters that are most likely to offer benefits in an adaptive, real-time strategy. Phase 1 also identifies an experimental design methodology to compute the effect of a change to signal timing parameters and develops both procedures for calculating performance and algorithms for improving the traffic system based on safety and existing principles of adaptive control used in the Federal Highway Administration (FHWA) Adaptive Control Systems (ACS) Lite system.

The ultimate objective of this research is to develop algorithms that can balance the performance of the traffic control system for both efficiency and safety and that can work with state-of-the-practice signal controllers.

Monique R. Evans
Director, Office of Safety
Research and Development

TECHNICAL DOCUMENTATION PAGE

1. Report No. FHWA-HRT-10-038	2. Government Accession No.	3. Recipient's Catalog No.	
4. Title and Subtitle Balancing Safety and Capacity in an Adaptive Signal Control System—Phase 1		5. Report Date October 2010	
		6. Performing Organization Code:	
7. Author(s) Ziad A. Sabra, Douglas Gettman, R. David Henry, and Venkata Nallamothu		8. Performing Organization Report No.	
9. Performing Organization Name and Address Sabra, Wang & Associates, Inc. 1504 Joh Avenue, Suite 160 Baltimore, MD 21227		10. Work Unit No.	
		11. Contract or Grant No. DTRT57-08-C-10061	
12. Sponsoring Agency Name and Address Federal Highway Administration Office of Safety Research, Development and Technology Turner-Fairbank Highway Research Center 6300 Georgetown Pike Mclean, VA 22101-2296		13. Type of Report and Period Covered Final Report: September 2008–December 2009	
		14. Sponsoring Agency Code HRDS-05	
15. Supplementary Notes The FHWA Contracting Officer's Technical Representative (COTR) was Joe Bared. The project panel that reviewed progress of this report are Eddie Curtis, Raj Ghaman, David Gibson, John Halkias, and Wei Zhang.			

16. Abstract

This research focuses on the development of real-time signal timing methodologies and algorithms that balance safety and efficiency. The research consists of two phases, and this report summarizes the findings of phase 1. First, it examines the relationships between signal timing and surrogate measures of safety: frequency of rear-end, angle, and lane-change conflicts. The Federal Highway Administration (FHWA) Surrogate Safety Assessment Methodology (SSAM) was used to evaluate simulated scenarios to test the relationships between signal timing parameters and the occurrence of traffic conflicts. A single intersection and a three-intersection arterial were examined, and each parameter was tested independently. The analysis effort indicated the following results:

- The ratio of demand to capacity (i.e., the length of the split) is a factor that influences the total number of conflicts. There is an inverse linear relationship between splits and total conflicts.
- Cycle length has the most significant impact on the total number of conflicts. Increasing the cycle length beyond its optimum value on an arterial system has a significant effect in reducing all types of conflicts.
- Detector extension times have only a minor impact on changes to conflict rates.
- The phase-change interval has a marginal effect on the total number of conflicts.
- Left-turn phasing (protected/permitted) has a significant effect on the total number of conflicts.
- An offset has an insignificant effect on conflicts until the change is more than ±10 percent of the cycle length.
- Phase sequence has a significant effect on the total number of conflicts on an arterial.

These results were obtained by modifying each variable independently for specific geometric and volume conditions. As such, these results provide evidence that certain parameters have a positive correlation to changes in surrogate measures of safety, but they do not provide metrics that can be used for real-time signal timing optimization. This report also discusses a methodology based on design of experiments to calculate a safety performance function that can be used for estimating the effect of changes to signal timing parameters in tandem. The report concludes with the development of a multiobjective optimization methodology and the five principle algorithms that constitute the proposed adaptive system for tuning the cycle length, splits, offsets, left-turn phase protection treatment, and left-turn phase sequence of a set of intersections.

| 17. Key Words
Surrogate measures of safety, Adaptive traffic control, Traffic signal timing, Traffic conflicts, Microsimulation traffic models, ACS Lite, Multiobjective optimization, Design of experiments | | 18. Distribution Statement
No restrictions. This document is available through the National Technical Information Service, Springfield, VA 22161. | |
| 19. Security Classif. (of this report)
Unclassified | 20. Security Classif. (of this page)
Unclassified | 21. No. of Pages
106 | 22. Price
N/A |

Form DOT F 1700.7 (8-72)   Reproduction of completed page authorized

SI* (MODERN METRIC) CONVERSION FACTORS

APPROXIMATE CONVERSIONS TO SI UNITS

Symbol	When You Know	Multiply By	To Find	Symbol
LENGTH				
in	inches	25.4	millimeters	mm
ft	feet	0.305	meters	m
yd	yards	0.914	meters	m
mi	miles	1.61	kilometers	km
AREA				
in^2	square inches	645.2	square millimeters	mm^2
ft^2	square feet	0.093	square meters	m^2
yd^2	square yard	0.836	square meters	m^2
ac	acres	0.405	hectares	ha
mi^2	square miles	2.59	square kilometers	km^2
VOLUME				
fl oz	fluid ounces	29.57	milliliters	mL
gal	gallons	3.785	liters	L
ft^3	cubic feet	0.028	cubic meters	m^3
yd^3	cubic yards	0.765	cubic meters	m^3
NOTE: volumes greater than 1000 L shall be shown in m^3				
MASS				
oz	ounces	28.35	grams	g
lb	pounds	0.454	kilograms	kg
T	short tons (2000 lb)	0.907	megagrams (or "metric ton")	Mg (or "t")
TEMPERATURE (exact degrees)				
^oF	Fahrenheit	5 (F-32)/9 or (F-32)/1.8	Celsius	^oC
ILLUMINATION				
fc	foot-candles	10.76	lux	lx
fl	foot-Lamberts	3.426	candela/m^2	cd/m^2
FORCE and PRESSURE or STRESS				
lbf	poundforce	4.45	newtons	N
lbf/in^2	poundforce per square inch	6.89	kilopascals	kPa

APPROXIMATE CONVERSIONS FROM SI UNITS

Symbol	When You Know	Multiply By	To Find	Symbol
LENGTH				
mm	millimeters	0.039	inches	in
m	meters	3.28	feet	ft
m	meters	1.09	yards	yd
km	kilometers	0.621	miles	mi
AREA				
mm^2	square millimeters	0.0016	square inches	in^2
m^2	square meters	10.764	square feet	ft^2
m^2	square meters	1.195	square yards	yd^2
ha	hectares	2.47	acres	ac
km^2	square kilometers	0.386	square miles	mi^2
VOLUME				
mL	milliliters	0.034	fluid ounces	fl oz
L	liters	0.264	gallons	gal
m^3	cubic meters	35.314	cubic feet	ft^3
m^3	cubic meters	1.307	cubic yards	yd^3
MASS				
g	grams	0.035	ounces	oz
kg	kilograms	2.202	pounds	lb
Mg (or "t")	megagrams (or "metric ton")	1.103	short tons (2000 lb)	T
TEMPERATURE (exact degrees)				
^oC	Celsius	1.8C+32	Fahrenheit	^oF
ILLUMINATION				
lx	lux	0.0929	foot-candles	fc
cd/m^2	candela/m^2	0.2919	foot-Lamberts	fl
FORCE and PRESSURE or STRESS				
N	newtons	0.225	poundforce	lbf
kPa	kilopascals	0.145	poundforce per square inch	lbf/in^2

*SI is the symbol for the International System of Units. Appropriate rounding should be made to comply with Section 4 of ASTM E380.
(Revised March 2003)

TABLE OF CONTENTS

LIST OF FIGURES

LIST OF TABLES

LIST OF ACRONYMS AND ABBREVIATIONS

AADT   Average annual daily traffic

ACS   Adaptive control system

ADT   Average daily traffic

Aimsun   Advanced Interactive Microscopic Simulator for Urban and Non-urban Networks

ASC MIB   Actuated signal controller management information base

ATMS   Advanced Traffic Management Systems

CCD   Central composite design

CEP   Conflict ending point

CICAS   Cooperative Intersection Collision Avoidance System

CMF   Crash modification factor

CORSIM   Corridor Simulation

CSP   Conflict starting point

DCS   Detection Control System

DeltaS   Maximum speed differential

DeltaV   Change between conflict velocity

DR   Deceleration rate

FHWA   Federal Highway Administration

FRESIM   Integrated Traffic Simulator

HUTSIM   Helsinki Urban Traffic Simulation

ITE   Institute of Technical Engineers

MaxD   Maximum deceleration rate

MaxS   Maximum speed of vehicle

MDSHA   Maryland State Highway Administration

OPAC   Optimization Policies for Adaptive Control

PET	Postenchroachment time
PHF	Peak-hour factor
PI	Performance Index
RHODES	Real Time Hierarchical Optimized Distributed Effective System
SCATS®	Sydney Coordinated Adaptive Traffic System
SCOOT	Split Cycle Offset Optimization Technique
SPUI	Single-point urban interchanges
SSAM	Surrogate Safety Analysis Model
TEXAS	Traffic Experimental Analytical Simulation
TOD	Time of day
TRANSIMS	Transportation Analysis and Simulation System
TTC	Time to collision
V/C	Volume to capacity
Y+AR	Yellow plus all red

1.0 INTRODUCTION

1.1 ADAPTIVE SIGNAL CONTROL SYSTEMS AND SAFETY

Over the past 20 or more years, several adaptive traffic control algorithms have been developed and used for traffic signal control around the world, including Split Cycle Offset Optimization Technique (SCOOT), Sydney Coordinated Adaptive Traffic System (SCATS®), Federal Highway Administration (FHWA) adaptive control systems (ACS) such as Optimization Policies for Adaptive Control (OPAC), Real Time Hierarchical Optimized Distributed Effective System (RHODES), and, most recently, ACS Lite. While these systems differ in operation, they share the common objective of increasing throughput capacity and optimizing traffic flow by responding to current traffic demands rather than assuming predetermined traffic volumes.

The SCOOT algorithm simultaneously optimizes three parameters: (1) splits, (2) offsets, and (3) cycle. At every intersection and for every phase, the split optimizer determines whether to make the change earlier, later, or as currently planned. The split optimizer implements the decision, which adjusts the phase time by a few seconds to minimize the degree of saturation on the approaches to the intersection. Similarly, the offset optimizer determines whether to alter all the offsets by a fixed amount every cycle. The offset optimizer uses information stored in cyclic flow profiles to compare the sum of the performance measures on all adjacent links of an arterial system of intersections for the current offsets and possible changed offsets to determine if the changed offsets will improve traffic flow efficiency. The cycle optimizer varies the cycle time of all the intersections in a traffic section or arterial in small intervals each cycle in an attempt to ensure that the most heavily loaded intersection in the system is operating at less than 90 percent saturation. SCOOT includes a variety of other optimization and congestion management features, all of which are focused on improving efficiency with no assessment of the effect on traffic safety.

SCATS® uses different techniques with a similar goal of improving efficiency of traffic flow and minimizing total system delay. It is based on a split plan selection, matching traffic patterns to a library of signal timing plans, rather than incremental tuning. By measuring real-time traffic flows at the intersection (notably using stop-bar detectors), SCATS® determines the degree of saturation of each traffic phase and selects the signal plan that best minimizes the total degree of saturation at each intersection. Offset and cycle time adjustment algorithms work in a similar fashion to SCOOT but, again, have no assessment of the impact of system decisions on safety. Both SCATS® and SCOOT make decisions at an intersection no more than once per cycle.

FHWA ACS algorithms OPAC and RHODES were developed to provide real-time adaptive traffic control at intersections on a second-by-second basis. Similar to SCOOT and SCATS®, RHODES and OPAC estimate the effect of signal timing changes on efficiency of traffic performance with no assessment of traffic safety effects. RHODES and OPAC make frequent decisions about phase timing (green durations) with consideration of parameters such as cycle time, offsets, and splits, but they do not explicitly consider these parameters in their optimization. OPAC and RHODES focus on modeling the traffic state (length of queues and approach demands) in the system and minimizing the total delay to vehicles in a rolling-horizon optimization fashion.

The FHWA ACS Lite optimization algorithm was developed to address some of the shortcomings of the ACS algorithms. It is based on a simple traffic model with few tunable parameters requiring little calibration. ACS Lite uses three levels of optimization to refine and update traffic signal timing: (1) a time-of-day tuner, (2) a run-time refiner, and (3) a transition manager. The time-of-day tuner is intended to keep baseline timing plans updated by learning from past run-time refiner actions. At the time this report was written, the time-of-day tuner had not yet been implemented in the ACS Lite system. The run-time refiner makes adjustments to signal timing parameters every few cycles based on cyclic flow profiles and stop-bar occupancy data similar to the information collected by SCOOT and SCATS®. The transition manager is intended to select the best method of transitioning between two traffic signal timing plans when the run-time refiner makes an adjustment to the timings. ACS Lite may be slow to respond to rapid changes in traffic flows, but it requires fewer detectors and much less infrastructure, configuration, and calibration than other real-time adaptive traffic control systems.

Each of these systems has been developed to optimize traffic flow, minimize traffic delay, and improve efficiency of traffic signal operations. It is unknown, however, if maximizing traffic efficiency in real time compromises safety in any way. For example, an adaptive system might tend to generate relatively short cycle lengths because short cycles tend to minimize delay. An adaptive system might also generate network-wide solutions that will have many stops but with an average stop of a short duration. Are such solutions less safe than a throughput-maximizing solution that would have fewer stops in the network but higher average delay? Evaluating such issues and developing an adaptive control strategy that balances maximizing traffic flow efficiency and safety is the primary purpose of this project.

1.2 THE SAFETY EFFECTS OF TRAFFIC SIGNAL TIMING PARAMETERS

The body of literature analyzing the effects of signal timing settings on intersection safety is very limited. The analysis of safety from a real-time context is an emerging topic that is primarily addressed from a vehicle-centric approach. In the authors' opinion, the best example of research on the effects of signal timing on safety is the development of the Detection Control System (DCS) by Texas Transportation Institute.[1] This system detects the type of vehicle (large truck or regular passenger vehicle) approaching an intersection and modifies the clearance time of the service phase appropriately to reduce the occurrence of large trucks caught in the dilemma zone. Bonneson's studies have shown that this type of real-time adaptive control is effective at improving the relative safety of an intersection (e.g., 80 percent reduction in red-light running by heavy trucks) with limited negative effect on the intersection's efficiency and, in some cases, even improvements in total delay and stops.[1] These results were found with the application of the DCS system in rural areas that have high-speed main line approaches carrying significant truck traffic and relatively low-volume side street flows. This real-time adaptive control approach was found to be effective because it focuses on one particular signal timing parameter (i.e., yellow and red clearance). Urban and suburban applications of the DCS approach are not likely to see similar results due to differences in the operational environment.

Research on real-time predictions of when a crash is going to occur is very limited. Some research has been pursued to develop relationships with aggregate variables such as average speed, occupancy, or volume data in a freeway context. These studies showed that these relationships provided poor predictive power ($R^2 < 0.5$), as observed in the regression model approach.[2,3]

2

Beyond these studies, current research in real-time crash prediction is focused on vehicle-centric approaches such as the Cooperative Intersection Collision Avoidance System (CICAS). CICAS warns drivers when they are about to violate a red light by a high-speed communications link between the traffic signal and individual vehicles. Future extensions of this type of interaction between vehicles and the traffic signal, under the broad umbrella of IntelliDrive[SM][1] technology, provide additional potential for changing signal timing parameters in response to the observation of impending crash conditions. These effects, however, are localized and provide only microscale changes, such as extensions to clearance times. This approach is not really applicable to making changes to aggregate-level traffic control parameters such as cycle time, splits, and offsets. When there is a significant penetration of IntelliDrive[SM] equipment in the vehicle fleet of the traveling public, this technology may offer more promise for providing a balance of safety and efficiency in traffic signal operation.

For these reasons, the analysis of traffic conflicts has emerged as the best possible surrogate measurement technique for predicting unsafe situations when making changes to signal timing parameters. It is hypothesized that locations that experience a higher rate of traffic conflicts will typically have a higher rate of crashes. Several field studies have shown that conflict rates do have a relationship with an increased rate of crashes, although this relationship is still debated by safety analysis statisticians.[(4)] Although the correlation is relatively weak (as is the correlation of crash prediction models to real crash rates), it is positive. Although the conflict analysis technique is based on manual observation, it is still the best tool available for safety analysis in lieu of collecting crash records.

The recent FHWA research on surrogate measures of safety from simulation models concluded from literature review that conflict analysis represents the most appropriate and intuitive approach for assessing the safety performance of new and innovative intersection designs.[(5,6)] Since a new geometric design, signal system operational setting, or control method has no crash history to draw from, there is essentially no way to predict safety performance except for some combinations of existing regression-based relationships and crash modification factors (CMFs) using engineering judgment. Thus, FHWA's Surrogate Safety Analysis Model (SSAM) project focused on providing a safety analysis tool for simulation-based comparative studies.

The SSAM software tool processes trajectory information from a microscopic simulation model to compute the frequency of various types of conflicts (crossing, lane changing, and rear end) and severity indicators. Time to collision (TTC), postencroachment time (PET), speed differential, and several other measures can be used to compare one traffic facility design to another. The results of the FHWA studies showed that the frequency measures were more reliable than the severity indicators, but many interesting effects were observed, such as a change in statistical significance at varying levels of traffic volume.[(5, 6)] That is, the conclusion that one design is more safe than another may change when the real-time traffic volume is higher or lower. For example, it was found that single-point urban interchanges (SPUI) had lower conflict rates than traditional interchanges at low volumes but higher rates at high volumes.

The validation study as part of the SSAM development project showed a reasonably weak correlation of conflict data with crash records for a battery of statistical tests, including rank-

[1] IntelliDrive is a service mark of the U.S. Department of Transportation.

correlation and deriving regression models for crashes from conflict data.[6] This validation analysis did not, however, study any effects of the differences in signal timings at the 83 intersections used in the study.

The SSAM research did evaluate differences in safety performance of several signal timing-related parameters as follows:[5,6]

- Leading versus lagging left turns.

- Three-phase versus four-phase diamond intersection control.

- Protected versus permitted left turns.

The remainder of the test cases focused on comparing geometric design features of intersections. As expected, leading and lagging left turns were found to have no appreciable difference in conflict rates for a test case performed at an isolated intersection. Results for three-phase and four-phase control at a diamond interchange were found to be inconclusive because low volumes indicated superiority of three-phase control while four-phase control was found to produce lower rates of conflicts at higher volumes. For the current project, however, it is actually a positive result that the three-phase and four-phase approaches had different safety dominance at different traffic volume levels, since this means that in a real-time setting, an algorithm might switch the interchange operation from a three- to four-phase operation to improve safety performance. Finally, it was found that protected left turns reduced the rate of crossing conflicts over permissive lefts, which was also expected.

1.3 RESEARCH OBJECTIVES

The overall objective of this research was to develop real-time adaptive signal timing methodologies and algorithms that balance safety and efficiency. This research consists of two phases, and this report summarizes only the findings of phase 1. The first step of phase 1 was to identify the relationships between traffic signal parameters (cycle, spilt, offset, detector extension time, change and clearance intervals, left-turn phase sequence, and left-turn phase protection alternatives) and safety (rear-end, angle, and lane-change conflicts). FHWA's SSAM was used to evaluate various simulated scenarios to test the relationships between the signal timing parameters and the occurrence of traffic conflicts in the simulation model.

Since there is a limited amount of research on relationships between signal timing and safety (considering both surrogate measures and crash records), these initial test cases were necessary to identify evidence of a relationship between a particular signal timing parameter and a statistically significant change in safety performance. After identifying parameters that hold the promise of an effect on safety and efficiency, the next objective was to identify an approach for combining these relationships into a multivariate performance function that can be used to predict the safety implications, or the change in conflict rates, of modifications to signal timing.

This performance function could be used in tandem with efficiency assessment functions to provide a computational engine that can be used to assess the performance of a given set of signal timing parameters with respect to the current traffic conditions. A multiobjective adaptive

control algorithm was developed to balance the two objectives, although it is important to note that the two objectives may not necessarily be competing in all areas of the parameter space. Next, the algorithms are to be implemented in an offline and/or online solution with modern controller hardware and software and tested for proof of the concept. Finally, validation studies are needed to verify that the proposed algorithms have a positive effect on safety in real-world deployments.

This research project achieved the first three objectives of the effort: (1) to identify a short list of signal timing parameters that are positively correlated with safety, (2) to develop a plan for combining the results into a safety performance function, and (3) to develop a multiobjective algorithm that provides a balanced solution between safety and efficiency in the context of real-time adaptive traffic control. Depending on the outcome of this initial effort, development of the performance function, algorithm implementation, field testing, and validation studies will be performed in future phases of the research.

1.4 ORGANIZATION OF THE REPORT

This report is organized into the following six sections:

- **Section 1:** provides an overview of the project and a statement of the research objectives.

- **Section 2:** explores the relationships between signal timing parameters and safety.

- **Section 3:** discusses the signal timing and traffic simulation tools used in the analysis.

- **Section 4:** discusses the various case scenarios considered in the project.

- **Section 5:** summarizes the findings of the analysis and simulations.

- **Section 6:** discusses the concept of algorithms for developing a multiobjective optimization and safety performance function. It outlines a detailed experimental design approach and methodology, and it summarizes the various methodologies for developing both offline and real-time multiobjective optimization and safety performance algorithms.

2.0 SIGNAL TIMING AND SAFETY

2.1 OVERVIEW

Attributing safety effects to changes in signal timing and phasing parameters and separating these effects from those attributable to the intersection environment is not a simple exercise. For example, a crash pattern at an intersection might be attributed to poorly placed signal displays for an approach where drivers cannot discern the display until the last moment, or the crash pattern might be attributed to a poorly timed offset causing vehicles to stop unnecessarily. The complexity of adaptive signal control compounds the difficulty of this investigation because rather than remaining fixed, the timings change on a cycle-by-cycle basis.

Table 1 illustrates some of the hypothesized relationships between signal timing parameters and safety, as measured by traffic conflicts. For example, it may be found that rear-end crashes tend to be more common when shorter cycles and splits are used. If this finding were valid, then a logical conclusion would be to employ signal timing parameters that result in longer phase times (longer cycles and splits) to reduce the rate of rear-end crashes or conflicts. It is also likely that the correlation between safety and signal timing parameters will have to consider the level of traffic demand with respect to the value of the parameters.

Table 1. Potential relationships between signal timing parameters and conflict types.

Signal Timing Parameter	Rear-end Conflicts	Right-angle Conflicts	Sideswipe Conflicts	Left-turn Conflicts	Pedestrian Conflicts
Cycle length	ü	ü	none	ü	ü
Splits	ü	ü	ü	ü	ü
Offset	ü	ü	none	ü	ü
Detector gap extension	ü	ü	none	ü	none
Coordination transition logic	ü	none	ü	none	ü
Change intervals	ü	ü	none	ü	ü
Phase sequence	ü	ü	none	ü	none
Left-turn operation mode	ü	ü	none	ü	ü

Generally, rear-end crashes and conflicts were expected to be impacted the most heavily by changes in signal timing parameters, as shown in table 1. Therefore, it was important to identify measures from real-time detector output data that were correlated with rear-end crashes and conflicts. For example, higher lane occupancies and uniform speeds at concentrated times during the signal cycle on a coordinated approach indicate the presence of dense platoons, offsets that are working as intended, and, thus, less potential for rear-end crashes. Conversely, larger headways and less uniform lane occupancies during the signal cycle due to incorrect offsets might indicate higher potential for rear-end crashes. This and other similar relationships were investigated in this research and were used to develop a methodology to mathematically determine changes to signal timing parameters that balance safety and efficiency.

Similar explanatory reasoning can be applied to each of the cells in table 1 to determine a potential correlation between a signal timing parameter and a specific type of conflict or crash. For example, continuous changes in signal timing splits in an adaptive control system might generate conflicts between vehicles and pedestrians due to the fact that pedestrians and motorists typically expect consistency in signal timing intervals on a cycle-by-cycle basis. Shortening a left-turn split may induce a higher rate of left-turn crashes due to drivers making more risky maneuvers. Extending the main street split may induce red-light running on the side street. There are opportunities to reduce stops, delays, and blocking problems by changing the sequence of signal phases, including switching a left-turn phase between leading and lagging, skipping phases, or servicing a phase twice in a signal cycle. Changing the phase order may be particularly helpful to reduce blocking problems, for priority vehicle operations, or to support advanced traffic control strategies at closely spaced intersections such as freeway interchanges. The typical reason for not changing phase sequences is the belief that doing so violates driver expectancy and confuses pedestrians. In reality, there is little research to support these concerns. Altering phase sequences may have a positive impact on safety by reducing blocking and spillback between intersections and by decreasing driver frustration, which are both factors that contribute to crash potential. This research investigated these operational conditions and identified a methodology to detect and mitigate such occurrences in real time.

2.2 SAFETY PERFORMANCE ANALYSIS

The literature analyzing safety performance of signal timing settings is limited because of the complexity of the problem due to the potential input variables, the infrequent and random nature of crashes, and the effects of regression to the mean. Causal linkages between potential input variables and crash frequency are not commonly found with strong correlations. Regression to the mean is a particularly challenging complication since locations with high levels of crashes in one reporting period may have a lower level of crashes in the following reporting period with no improvements to the operational or geometric parameters of a location.

2.2.1 Crash Modification Factors

Existing state-of-the-practice safety performance models for signal-controlled intersections predict crashes based on a variety of input variables typically related to the geometric characteristics of the facility and the traffic flows. A typical safety performance model is expressed as a nonlinear regression equation where the primary inputs that predict crash frequency are the crossing flows as follows:

$$\text{Crashes} = a*CMF1*CMF2*CMF3*(Vcross**b)*(Vmain**c) + d \qquad (1)$$

or

$$\text{Crashes} = CMF1*CMF2*CMF3*exp(-a+b*ln(Vcross) + C*(Vmain)) \qquad (2)$$

Variables *a*, *b*, and *c* are parameters that are fit to individual datasets, which are nonnegative numbers typically in the range of [0.5, 1.5]. The coefficients *b* and *c* in most fitted models are ~0.5, so it is commonly asserted that crash frequency is driven by the square-root of the product of the crossing flows. Units of *Vcross* and *Vmain* are typically expressed in average annual daily

traffic (AADT). Typical regression fitting performance is not particularly impressive due to the extremely rare nature of crashes and the myriad exogenous influences that lead to crashes not reflected in any controllable design parameters of an intersection. Good performance of a safety prediction function may result in R^2 values of 0.45–0.5.

Past studies have most often analyzed CMFs in a one-by-one fashion. For example, if the base condition for a signalized intersection is to share the left lane with a through lane—a scenario that is becoming more and more rare since the safety effect is substantial—the addition of a left-turn bay at a certain location might be predicted to reduce the crash rate by, say, 30 percent. So, a CMF for a left-turn bay would be expressed as a 0.7 multiplicative factor to the base model.

Other CMFs are applied similarly in a multiplicative fashion, so it is possible that a 30 percent reduction for the left-turn bay can be offset by, for example, a 25 percent increase due to on-street parking. There have been no CMFs developed for common signal timing inputs such as cycle time, offsets, splits, phase sequence, or detector extension times.

To estimate the safety of various traffic facilities, including facilities that have not yet been built, research has focused on the establishment of safety performance functions that relate the number of crashes or crash rate to a number of operational (e.g., AADT, average speed) and non-operational independent variables via a typically complex regression equation, including but not limited to AADT, occupancy, volume to capacity (V/C) ratios, and products of crossing volumes.[4,5] Calibration is then required to choose the equation parameters for the best statistical fit to the available data.

Studies performed by Gettman et al. identified research that was done on Bayesian methods and advanced statistical techniques (e.g., classification and regression trees) for revising crash estimates based on observations as a way to develop safety estimates for facilities with no crash data.[4,5] Other methods for combining crash rates and other measures into safety level of service measures or common indices based on one type of crash (e.g., property damage only) have also been proposed. These approaches all use macroscopic measurements of total flows rather than recording individual vehicle movements or events to develop safety level of service estimates. Despite the large body of safety modeling research, absolute numbers of crashes and crash rates are still difficult to predict accurately. This has led to increased interest in obtaining surrogate measures that reflect the safety of a facility or at least the increased probability of higher-than-average crash rates for a facility.

2.2.2 Traffic Conflicts

By definition, a *conflict* is an observable situation in which two or more road users approach each other in time and space to such an extent that there is risk of collision if their movements remain unchanged. The traffic conflicts technique is a methodology for field observers to identify conflict events at intersections by watching for strong braking and evasive maneuvers. Conflict methods have a long history of development, including research on topics such as recommended data collection methods, definitions of various types of conflicts, severity measures, how conflict measures are related to crash counts, how conflicts are related to specific crash types, standards for data collection, and standard definitions of conflict indices as used to compare the performance of multiple facilities.

The fact that the subjectivity of field observers introduces additional uncertainty into the collection of data on conflicts leads to a debate of the connection between conflict measures and crash predictions. Conflict studies are, however, still used to rank locations with respect to safety to identify construction upgrades. There is general consensus that higher rates of traffic conflicts can indicate lower levels of safety for a particular facility, given that conflicts generally result from a lack of or misunderstanding of communication between different road users.[4]

Tabulation of total numbers of traffic conflicts indicates frequency, one part of the safety issue. The other element of the safety issue is the severity of the conflicts that occur. The primary conflict severity measure that has been proposed is TTC.[7,8] Some researchers have indicated that TTC is the surrogate measure of safety, while others refute that lower TTC indicates higher severity of crashes, primarily because speed is not included in the measure.[8,9] That is to say that lower TTC certainly indicates a higher probability of collision but cannot be directly linked to the severity of the collision. Gettman et al. also state that others identify the deceleration rate (DR) as the primary indicator of severity instead of TTC.[5] Some of the common measures defining and characterizing a conflict are presented in table 2.

Table 2. Measures of conflict severity.[5]

Candidate Measures of Conflict Severity	Description
Gap time	Time lapse between the completion of encroachment by turning vehicle and the arrival time of crossing vehicle if they continue with same speed and path.
Encroachment time	Time duration during which turning vehicle infringes upon the right-of-way of through vehicle.
DR	Rate at which crossing vehicle must decelerate to avoid collision.
Proportion of stopping distance	Ratio of the distance available to maneuver to the distance remaining to the projected location of collision.
PET	Time lapse between the end of encroachment of turning vehicle and the time that through vehicle actually arrives at the potential point of collision.
Initially attempted PET	Time lapse between the commencement of encroachment by turning vehicle plus the expected time for through vehicle to reach the point of collision and the completion time of encroachment by turning vehicle.
TTC	Expected time for two vehicles to collide if they remain at their present speed and on the same path.

2.3 SURROGATE MEASURES FROM MICROSCOPIC SIMULATION

Microscopic simulation is generally required for generating and collecting conflict severity statistics and/or other surrogate measures that require detailed information on vehicle acceleration, deceleration, position, etc. as a substitute for field studies. Simulation models have been built specifically for the simulation of a particular conflict type. Other models are based on varying approaches to the computation of conflicts.[5,6] One model by Fazio et al. contains a comprehensive treatment of conflict types and surrogate measures for both signalized and

unsignalized intersections.[10] Special-purpose simulations are problematic in application since the level of detail and variety of modeling variables available to the user are typically compromised.

Some efforts prior to the FHWA SSAM project had focused on the modification of multipurpose traffic simulation models to include conflict statistics or other surrogates.[5] A brief overview of these simulation applications and their crash prediction indicators is extracted from the recent SSAM research and shown below.[5] They include the Helsinki Urban Traffic Simulation (HUTSIM); Transportation Analysis and Simulation System (TRANSIMS); Integrated Traffic Simulator (FRESIM), which is part of Corridor Simulation (CORSIM); Network Simulation (NETSIM), which is also now part of CORSIM; Traffic Experimental Analytical Simulation (TEXAS); Advanced Interactive Microscopic Simulator for Urban and Non-urban Networks (Aimsun); and INTEGRATION. A brief description of these models' crash prediction or safety indicator capabilities is as follows:

- **HUTSIM:** The HUTSIM microscopic simulation includes safety indicators that define a detailed driver behavior model (i.e., nanoscopic simulation) for representation of lapses in driver reaction time and errors in response.

- **TRANSIMS:** TRANSIMS uses macroscopic representation of vehicle movements to simulate large-scale network (e.g., an entire city) transportation behavior, but results are not detailed enough for the level of analysis required for signalized intersections.

- **CORSIM:** CORSIM currently outputs a conflict statistic by movement (left, right, through/diagonal), conflicting movement (left, right, through/diagonal), and approach for intersections when micronode analysis is enabled. Micronode analysis is an approach to simulation of the vehicles within the intersection box. CORSIM normally operates by considering the intersection as a point. The vehicle movement logic determines whether the vehicle is clear to enter the intersection and then places the vehicle on the next link after a delay time based on the speed of the vehicle and the width of the intersection or the path distance of the left or right turn. The animation element of CORSIM, Traffic Visualization (TRAFVU), fills in the movements of the vehicles within the intersection for visualization. The micronode module, although based on reasonable approximation principles, is not considered a viable model for intersection vehicle movements. Also, the FRESIM component of CORSIM was previously modified, when the model was called INTRAS, to output merging conflicts for freeway weaving sections.

- **TEXAS:** TEXAS uses the concept of conflicts to determine acceptance of gaps and lane changes by checking for conflicts and then avoiding conflicts. At each check and avoidance step, TTC and distance proximity values, as well as the vehicles' relevant acceleration, deceleration, velocity, position, etc., can be exported to a file.

- **Aimsun:** A recent study illustrates the use of Aimsun for collecting a surrogate measure of safety for ramp junctions.[11] This study extracted the speed differential, maximum speed of the follower vehicle, and DR of the follower vehicle for all ramp-merging events in a test case with and without ramp metering. The "un-safety" measure was the product of the three values. The study illustrates the effectiveness of ramp metering in decreasing the cumulative un-safety during peak rush-hour periods.

· **INTEGRATION:** INTEGRATION has also been augmented to produce estimates of the safety impact of traffic signal coordination. The hypothesis was that reducing the number of vehicle-to-vehicle interactions by reducing total stops would result in fewer total crashes. A module for calculating total crashes based on mean free speed of each intersection approach using previously developed nonlinear regression functions for safety performance was added to INTEGRATION. In addition, look-up tables for type of crash based on speed were added to the simulation model.

The FHWA SSAM project extended upon the approaches used in the preceding simulation models by combining microsimulation and automated conflict analysis to analyze the frequency and character of narrowly averted vehicle-to-vehicle collisions in the simulated traffic situation. The SSAM software application was developed to automate conflict analysis by directly postprocessing vehicle trajectory data from the simulation model. Researchers specified an open standard, universal vehicle trajectory data format designed to provide the location and dimension of each vehicle approximately every tenth of a second. The trajectory file format is currently supported as an export option by four traffic microsimulation models: VISSIM®, Aimsun, Quadstone Paramics, and TEXAS. It is hoped that in the coming years video processing technology will be capable of automatically extracting vehicle trajectory data adequate for SSAM processing from real-world sites. In addition, the approach could be applied to real-time analysis when IntelliDrive[SM] technology is ubiquitous.

2.4 SUMMARY OF PAST RESEARCH IN SURROGATE MEASURES FOR SAFETY

There is limited quantitative research on surrogate measures for safety assessment. The main difficulty is illustrating the correlation between any proposed surrogates and crashes since crashes are rare events. The available literature is focused mainly on various aspects of traffic conflicts and related field studies for obtaining surrogate measures. Given the technical difficulty and cost of field studies, use of simulation models has been proposed, and some previous work has been done to develop specific models for simulating conflicts. The most notable surrogate measure of the severity of a conflict is TTC, although other surrogates such as PET and DR have been used to measure other characteristics of conflict situations. Only limited effort has been expended to modify or enhance existing general-purpose, microscopic simulations to obtain conflict or other surrogate measures for intersections and two-lane roads. The primary difficulty is defining a set of surrogate measures that: (1) have meaningful implications since they are extracted from simulations that were specifically designed to be crash free and (2) have reasonable connectivity to safety assessment of particular facilities using traditional measures (e.g., the frequency and severity of resulting crashes).

Except for the SSAM model, there is currently no calibrated tool that lends itself to modeling and predicting conflicts at signalized intersections to determine correlations between modifications to signal timing parameters and resulting intersection safety. Therefore, this research project applied the SSAM methodology and software to explore the various relationships between safety and signal timing parameters.

3.0 ANALYSIS AND SIMULATION METHODOLOGIES

This section describes the research team's approach to analyzing the various relationships between signal timing parameters and surrogate measures of intersection safety. Details of the SSAM methodology and processing tools are described to provide further context of the analysis effort.

The analysis and simulation methodology followed three steps. First, each test scenario—a combination of traffic conditions and signal timing parameters—was initially input and analyzed in Synchro™, a microscopic and deterministic signal timing optimization model. Based on the data entered for a specific case scenario, Synchro™ was used to either evaluate the test scenario conditions (i.e., compute traffic efficiency performance) and/or to optimize the signal timing settings. Next, the results from the Synchro™ analysis were transferred to VISSIM®, a microscopic and stochastic traffic simulation model. This step was time consuming both in the transfer mode from Synchro™ as well as in having to run the simulations for multiple replications. Nevertheless, VISSIM® was selected as the preferred model due to its ability to represent comprehensive signal timing logic and its resolution of vehicle trajectory data at $^1/_{10}$ s. Six simulation runs were performed in VISSIM® for each test case before the vehicle trajectory data were transferred to the FHWA SSAM analysis software. The last step was to summarize the surrogate measures and to test for statistical significance using the *t*-test method embedded in SSAM. Each iteration of the simulation consisted of 15 min of warm-up period followed with a full hour of simulation time during which the safety performance measures were calculated. Data from the warm-up period were ignored during the analysis.

The choice to use only these three models in this project was based on the research team's knowledge of each model, its ease of use, the model's credibility, and its application to this research. Synchro™ is one of the most commonly used models in the United States for signal timing optimization and evaluation. It is very easy to use to develop several signal timing alternatives. Moreover, the research team is experienced in using Synchro™.

VISSIM® was used because of its ability to provide the data resolution that would support SSAM and to output phase timing performance data, including the cumulative number of green and red durations as well as the mean and average green and red times for each signal group (phase) in a file with the extension .lzv. VISSIM® has a large user base and is well supported in the United States. Compared to models such as CORSIM and SimTraffic®, VISSIM® is not easy to use and migration of data from Synchro™ to VISSIM® was very tasking and time consuming. The task of migrating data from the various Synchro™ signal timing alternatives was the most inefficient process of the research.

SSAM is very easy to use and provides the surrogate measures of safety necessary for comparing alternative signal timing scenarios. Each simulation run in VISSIM® results in a corresponding trajectory file (.trj). SSAM analyzes the batch of VISSIM® trajectory files to identify conflict events and catalogs a variety of event data including, but not limited to, the following surrogate measures of safety: TTC, PET, DR, maximum deceleration rate (MaxD), maximum speed of either vehicle (MaxS), and maximum speed differential of the two vehicles (DeltaS).

TTC is the time to crash into the leading vehicle if the following vehicle does not react by taking an evasive maneuver, assuming constant speeds. *PET* is the time that the following vehicle actually arrives at the point corresponding to a particular calculation of TTC after taking into account that the following vehicle has reacted to the leading vehicle's movements by braking.

When TTC = 0 and/or PET = 0, SSAM determines that a crash has occurred. If TTC > 0, TTC ≤ 1.5 s, and PET ≤ 5.0 s, then SSAM marks the event as a conflict. The 1.5-s TTC threshold and 5.0-s PET threshold are defaults in the SSAM software as recommended by the literature and testing during previous projects.[5,6]

3.1 SYNCHRO™

Synchro™ (developed by Trafficware^Ò, Inc.) is a software package capable of modeling signalized and unsignalized intersections.[12] Synchro™ is commonly used for intersection-capacity and level-of-service analysis and/or signal timing optimization. The software has the ability to compute optimum timings for intersection offsets, cycle lengths, phase splits, and phase sequence. The software can display time-space diagrams that illustrate vehicle progression through a network. Since Synchro™ performs its analysis at a platoon level instead of an individual level, it is characterized as a macroscopic simulation model. Synchro™ version 6.0 was used to code the various alternative scenario models and optimize the signal timings in this project.

3.2 VISSIM®

VISSIM® is a time-step and behavior-based microscopic traffic simulation software.[13] It is characterized as microscopic simulation software because of its ability to model and analyze each entity of the network at an individual level. VISSIM® is capable of simulating multiple modes of traffic, including cars, heavy-goods vehicles, high-occupancy vehicles, bus transit, light rail, heavy rail, rapid transit, cyclists, and pedestrians, for urban as well as rural conditions.

The VISSIM® model consists internally of two distinct components, the traffic simulator and the signal state generator. These components are constantly communicating detector calls and signal status to each other through an interface. The traffic simulator is a microscopic traffic flow simulation model including car following, lane changing, and gap acceptance logic. The signal state generator is signal-control software that polls detector information from the traffic simulator on a discrete time-step basis ($^1/_{10}$ s). It then determines the signal status for the following time-step and returns this information to the traffic simulator. This interaction is the driving force behind modeling a signalized intersection.

VISSIM® version 5.10 release 7 was utilized in this project to code the alternative scenarios and collect the vehicle trajectory data.

3.3 SSAM

3.3.1 Overview

SSAM combines microsimulation and automated conflict analysis to analyze the frequency and character of narrowly averted vehicle-to-vehicle collisions (conflicts) to compute surrogate

measures of the safety of traffic facilities. SSAM determines and quantifies three types of conflicts: crossing (angle), lane changing, and rear end.[5]

SSAM provides the following features:

- A table of all conflicts identified in the batch of analyzed .trj files, including file, time, location, vehicle identifications, and several measures of conflict severity.

- A summary of conflict counts by type and file, with average values of surrogate measures over all conflicts.

- A filtering mechanism that allows the isolation of subsets of conflicts by ranges of surrogate measures of safety, conflict type, network link, or a rectangular region of the network.

- A facility for statistical comparisons of the conflict frequencies and values of surrogate measures of safety for two alternative cases using Student's *t*-distribution for hypothesis testing.

- A display of the location of conflicts on the network map, with icons of different shapes and colors assignable to different conflict types or severities as shown in figure 1.
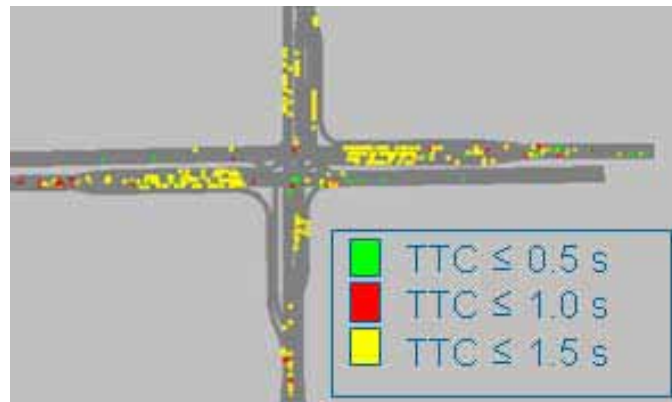
Figure 1. Screenshot. SSAM's color-coded conflicts.

3.3.2 Description of the SSAM Process

This section, extracted from the SSAM validation report and user manual, provides an overview of the typical workflow using the SSAM software, tracing the flow of information through various input data, tasks or operations, and resulting outputs.[6,14] In doing so, many of the screens of the SSAM graphical user interface are introduced. SSAM operates by processing data describing the trajectories of vehicles driving through a traffic facility (e.g., a signalized intersection) and identifying conflicts. The vehicle trajectory input data for SSAM are generated by traffic simulation software in a trajectory file format (using a .trj file extension) specially designed for SSAM. SSAM calculates surrogate measures of safety corresponding to each vehicle-to-vehicle interaction and determines whether or not each interaction satisfies the criteria to be deemed an official conflict. A table of all identified conflicts and their corresponding

surrogate measures of safety is summarized as an output of SSAM. Figure 2 illustrates the workflow for using SSAM.
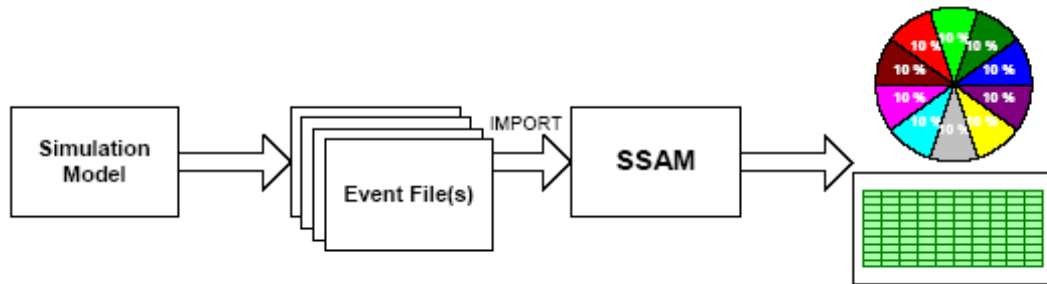
Figure 2. Chart. Operational concept of SSAM.[6]

The user begins the analysis by first enabling output of vehicle interaction (trajectory) data in the simulation model of his or her choice. The traffic engineer then runs the simulation model for a number of iterations—replications with alternate random number seeds—to obtain a statistically sufficient set of simulation output data. The user then launches the standalone SSAM application.

The user defines a new conflict analysis case by using the menus to create a new case file or, alternatively, to open an existing case file. The software uses two threshold values for surrogate measures of safety to delineate which vehicle-to-vehicle interactions are classified as conflicts. These two thresholds are applied to the values TTC and PET. The software provides default threshold values for these measures, which the analyst may override with his or her preferred alternate values. SSAM utilizes a default TTC value of 1.5 s, as suggested in previous research. Once the conflict identification thresholds are determined, the user processes the simulation (trajectory) data to identify vehicle-to-vehicle interactions that satisfy the conflict classification criteria. Each conflict identified during analysis, including data from the trajectory files of all corresponding replications of the simulation, is listed with conflict details, including the time, location, and all surrogate measures of safety for that conflict.

The algorithms used by SSAM to identify conflicts to be processed from the vehicle trajectory files are time intensive depending on the size of the .trj file, which is a function of the number of vehicles in the network model and the amount of time simulated. A high-end computer might require more than 10 min to process data from 5 h of traffic for a single intersection model. Large multi-intersection networks might require hours of processing time. The following steps summarize the technique used to identify conflicts:

Step 1: Determine the dimensions of the analysis area based on the header name in the .trj file. These dimensions define the width and height of a rectangular analysis area and indicate if trajectory data are provided in English or metric units. SSAM constructs a zone grid to cover the entire rectangular analysis area, as shown in figure 3. Individual square zones cover 50-ft by 50-ft areas. By dividing the region into these zones, the number of vehicle-to-vehicle comparisons necessary to identify potential conflicts is reduced considerably.

1 ft = 0.305 m
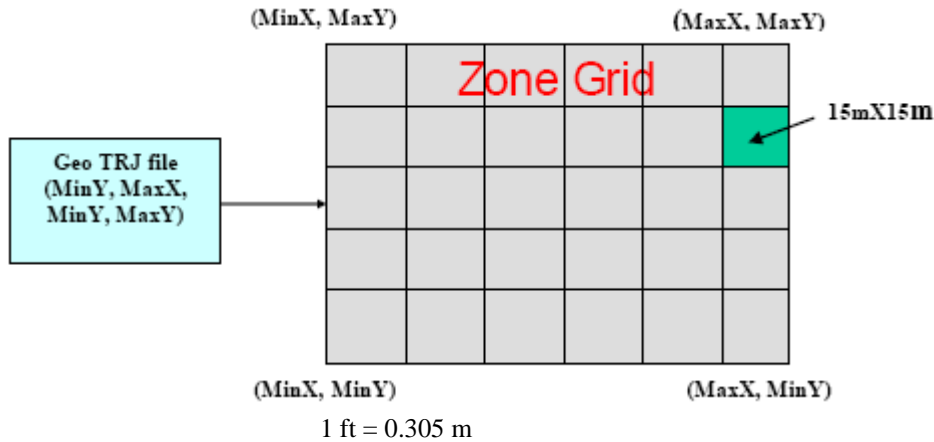
Figure 3. Illustration. SSAM's zone grid.[6]

Step 2: Analyze a single time-step of a trajectory file. For each vehicle in the analysis region, SSAM projects that vehicle's expected location as a function of its current speed if it were to continue traveling along its path for up to the duration of the configured TTC value. A vehicle's projected path is based on a look ahead over the next 10 s of trajectory data. The path, as shown in figure 4, is a set of straight line segments (labeled S) connecting the vehicle's future downstream locations (labeled X). The threshold TTC value is configured by the user of SSAM, typically with a threshold value of order of 1.5 s. Conflicts with TTC values larger than 1.5 s are not generally considered in the safety community to be severe enough events for recording in a traditional field conflict study.
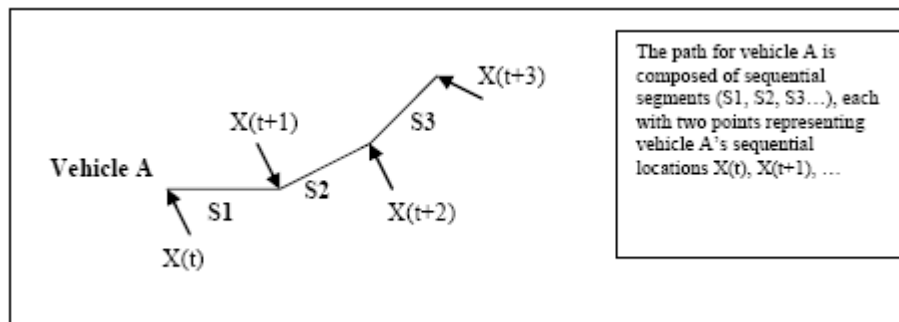
Figure 4. Illustration. Vehicle path.[6]

The process of projecting the distance that a vehicle may progress forward during the specified look-ahead time interval and the calculation of the exact coordinates of that projected vehicle position occur as follows, assuming SSAM is going to analyze the conflicts for vehicle A at time t_1. First, SSAM extracts all data related with vehicle A from the trajectory file, such as vehicle A's location, speed, acceleration, etc., at time t_1 and several time-steps after t_1. Each location is denoted as (x_1,y_1), (x_2,y_2), etc. Then, SSAM projects vehicle A's distance forward along its trajectory, defined by the following locations:

17

1. Each vehicle is defined as a polygon (rectangle) with four corner points (see figure 5).

2. The forward distance that the vehicle will travel is calculated in the MaxTTC interval, denoted as $DIS_1 = V_1 * MaxTTC$ (see figure 5).

3. The vehicle's next time-step location (x_2, y_2) is calculated based on the distance from current location to that location, denoted as $DIS_2 = |Location\ (t+1)-Location\ (t)|$ (see figure 5).

4. If DIS_2 is less than DIS_1, then DIS_2 is subtracted from DIS_1 and the previous two calculations are repeated, updating $DIS_1 = DIS_1-DIS_2$ and $DIS_2 = |Location\ (t+2)-Location\ (t+1)|$ and comparing the new DIS_1 and DIS_2.
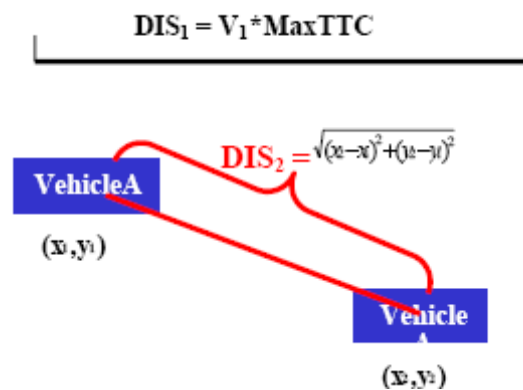
Figure 5. Illustration. DIS_1 and DIS_2. [6]

Step 3: For each vehicle, calculate the rectangular perimeter delineating the location and orientation of that vehicle at its projected future position. Overlay that rectangle on the zone grid, calculating which rectangular zones in the grid will contain at least some portion of that vehicle. For each zone the vehicle will occupy, add that vehicle to a list of occupants maintained for each zone. Any time a vehicle is added into a zone that currently contains one or more other vehicles, check for overlap of the new vehicle (rectangle) with each of the other vehicles (rectangles) in that zone. It is possible that two vehicles may partially occupy the same zone without overlapping. However, two overlapping rectangles indicate that a future collision is projected for this pair of vehicles, and therefore, a potential conflict has been identified, as portrayed in figure 6. SSAM maintains a list of all conflicting vehicle pairs (all conflict events) for the current time-step. For each time-step, the list is prepopulated with all conflicting vehicle pairs from the prior time-step. If the current vehicle being added to the zone grid overlaps with any other vehicle, that vehicle pair would be added to the conflict list for the current time-step, if not already in the list.
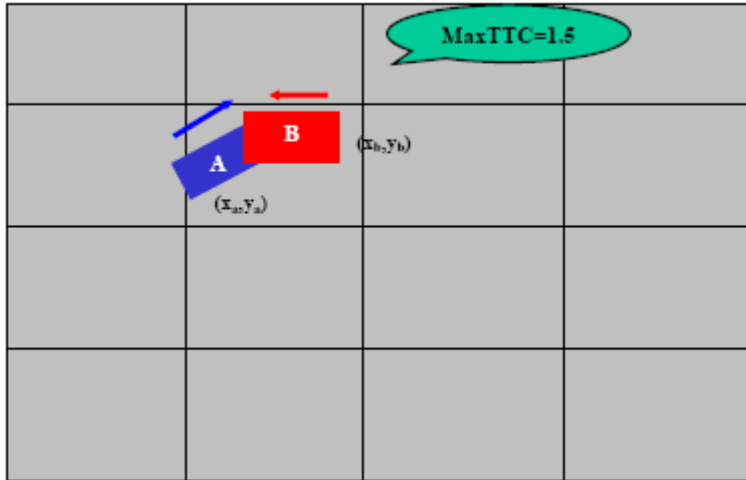
Figure 6. Illustration. Checking a conflict between two vehicles at MaxTTC.[6]

Step 4: Continue so that SSAM can perform more detailed processing of each conflicting vehicle pair in the list for the current time-step. First, update the TTC of the vehicle pair. This is done by iteratively shortening the future projection timeline by a tenth of second and reprojecting both vehicles over successively shorter distances until the pair of vehicles no longer overlaps in their projected locations. In this way, a more accurate TTC value is established for this time-step. This is portrayed in figure 7, where the TTC values have reduced from the maxTTC value of 1.5 s (illustrated in figure 6) to a TTC value of 1.3 s. Instead of the large overlap in figure 6, the vehicles in figure 7 have just barely come into contact. Note that if the projection timeline reduces to 0 s and the vehicles still overlap, this is a crash.
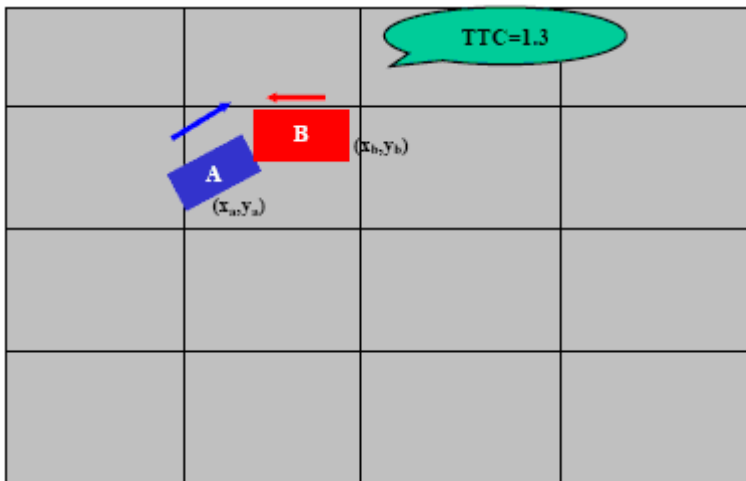
Figure 7. Illustration. Checking a conflict between two vehicles at TTC = 1.3 s (vehicles no longer in conflict).[6]

At this point, various surrogate measures of safety, such as the minTTC, taking the minimum of the current TTC value and that of the prior time-step, are calculated and updated. Also, the current (actual) positions of both vehicles are recorded for postencroachment analysis.

19

If it was found that the vehicle pair does not overlap over any projected time between zero and maxTTC, then this vehicle pair is in the conflict event list by virtue of being in the list during the prior time-step. In this case, the event remains in the list, watching for the trailing vehicle to eventually occupy, or encroach on, a position formerly held by the leading vehicle. The time differential between when the leading vehicle occupied this location and the trailing vehicle arrived is the PET. If a postencroachment was observed, then the minimum PET is updated, and this conflict event remains in the list, as the postencroachment could potentially reduce as the vehicle trajectories progress over time.

If a vehicle pair in the conflict event list is no longer on an imminent collision course and it is clear that PET to any prior positions could not further reduce the minimum PET or if the maximum PET has elapsed, then this vehicle pair is identified for removal from the conflict event list. Prior to removal, all final surrogate measures are computed, including conflict starting and ending points, conflict angles, minimum TTC, and the change between conflict velocity (DeltaV). Also, the conflict is classified at this time as a crossing, rear-end, and/or lane-change conflict. If this conflict event has ended, then the conflict and all surrogate measures are added to the conflict table, and the event is removed from the tracking list.

3.3.3 Definitions of Surrogate Measures Computed by SSAM

SSAM's user manual defines several surrogate measures as follows:[6]

- *TTC* is the minimum time-to-collision value observed during the conflict. This estimate is based on the current location, speed, and future trajectory of two vehicles at a given instant. A TTC value is defined for each time-step during the conflict event. A conflict event is concluded after the TTC value rises back above the critical threshold value. This value is recorded in seconds.

- *PET* is the minimum postencroachment time observed during the conflict. PET is the time between when the first vehicle last occupied a position and the time when the second vehicle subsequently arrived at the same position. A value of zero indicates a collision. PET is associated with each time-step during a conflict. A conflict event is concluded when the final PET value is recorded at the last location where a TTC value was still below the critical threshold value. This value is recorded in seconds.

- *MaxS* is the maximum speed of either vehicle throughout the conflict (i.e., while the TTC is less than the specified threshold). This value is expressed in feet per second or meters per second, depending on the units specified in the corresponding trajectory file.

- *DeltaS* is the difference in vehicle speeds as observed at tMinTTC. More precisely, this value is mathematically defined as the magnitude of the difference in vehicle velocities (or trajectories), such that if *v1* and *v2* are the velocity vectors of the first and second vehicles respectively, then DeltaS = $\| v1 - v2 \|$. For context, consider an example where both vehicles are traveling at the same speed, *v*. If they are traveling in the same direction, DeltaS = 0. If they have a perpendicular crossing path, DeltaS = $(\sqrt{2})v$. If they are approaching each other head on, DeltaS = *2v*.

- *DR* is the initial deceleration rate of the second vehicle, recorded as the instantaneous acceleration rate. If the vehicle brakes (i.e., reacts), this is the first negative acceleration value observed during the conflict. If the vehicle does not decelerate, this is the lowest acceleration value observed during the conflict. This value is expressed in feet per second or meters per second, depending on the units specified in the corresponding trajectory file.

- *MaxD* is the maximum deceleration of the second vehicle, recorded as the minimum instantaneous acceleration rate observed during the conflict. A negative value indicates deceleration (braking or release of gas pedal). A positive value indicates that the vehicle did not decelerate during the conflict. This value is expressed in feet per second or meters per second, depending on the units specified in the corresponding trajectory file.

- *ConflictType*, as shown in figure 8, describes whether the conflict is the result of a rear-end, lane-change, or crossing movement. If link and lane information is not available for both vehicles, then the event type is classified based solely on the absolute value of the ConflictAngle. The type is classified as a rear-end conflict if ||ConflictAngle|| < 30 degrees, a crossing conflict if ||ConflictAngle|| > 85 degrees, or otherwise a lane-change conflict. The simulation model that produced the vehicle trajectory data can generally provide link and lane information for both vehicles, though the coding of these values may vary significantly from one simulation vendor to the next.
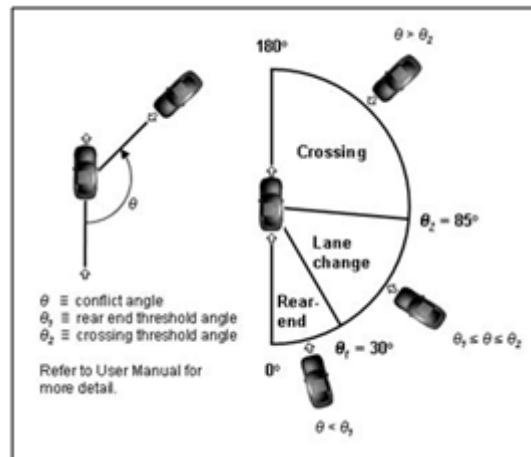
Figure 8. Illustration. Conflict types by angle.

If link and lane information is available, that information is utilized for classification in the case that the vehicles both occupy the same lane of the same link at either the start or end of the conflict event. If the vehicles both occupy the same lane at the start and end of the event, then it is classified as a rear-end event. If either vehicle ends the conflict event in a different lane than it started without having changed links, then the event is classified as a lane-change conflict. If either of the vehicles changes links over the course of the event, then the conflict angle determines the classification as previously described, with the following possible exception.

For two vehicles that begin the conflict event in the same lane, as shown in figure 9, but change links over the course of the event, the classification logic considers only rear-end

or lane-change types, based on the conflict angle and using the threshold value previously mentioned. Note that vehicle maneuvers such as changing lanes into an adjacent turn-bay lane or entering into an intersection area may be considered changing links, depending on the underlying simulation model. In some cases, vehicles that appear to be traveling in the same lane may actually be considered by the simulation model as traveling on different links that happen to overlap.
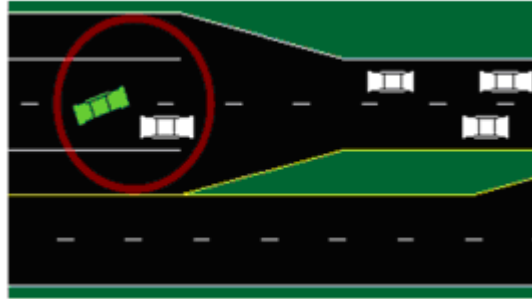
Figure 9. Illustration. Lane-change conflict.

- *MaxDeltaV* is the maximum DeltaV value of either vehicle in the conflict.

- *FirstDeltaV* (*SecondDeltaV*) is the change between conflict velocity (given by speed FirstVMinTTC and heading FirstHeading) and the post collision velocity (given by speed PostCrashV and heading PostCrashHeading). This is a surrogate for the severity of the conflict, calculated assuming a hypothetical collision of the two vehicles in the conflict.

3.3.4 SSAM Data Terms and Definitions

SSAM computes and records the following data or measures for each conflict identified in the vehicle-trajectory input data.[6] This information is provided in the conflicts table on the conflicts panel. It is possible to filter out several of the conflicts based on specified ranges of these values using the Filter tool. These data may also be exported for use in other third-party processing software, such as Microsoft Excel®, where more complicated analysis options may be available. The following are used in SSAM:

- *tMinTTC* is the simulation time when the minimum TTC value for this conflict was observed.

- *xMinPET* is the x-coordinate specifying the approximate location of the conflict at the time when the minimum PET was observed. More specifically, this location corresponds to the center of the first vehicle where the subsequent arrival of the second vehicle to the same location was the shortest encroachment observed.

- *yMinPET* is the y-coordinate specifying the approximate location of the conflict at the time when the minimum PET was observed. More specifically, this location corresponds to the center of the first vehicle where the subsequent arrival of the second vehicle to the same location was the shortest encroachment observed.

- *ConflictAngle* is an approximate angle of hypothetical collision between conflicting vehicles based on the estimated heading of each vehicle. The angle, expressed from the perspective of the first vehicle to arrive at the conflict point, conveys the direction from which the second vehicle is approaching the first vehicle. The angle ranges from -180 to +180 degrees, where a negative angle indicates approach from the left and a positive angle indicates approach from the right. An angle of 180 degrees (or -180 degrees) indicates a direct head-on approach, and an angle of 0 degrees (or -0 degrees) indicates a direct rear approach, as illustrated in figure 10.
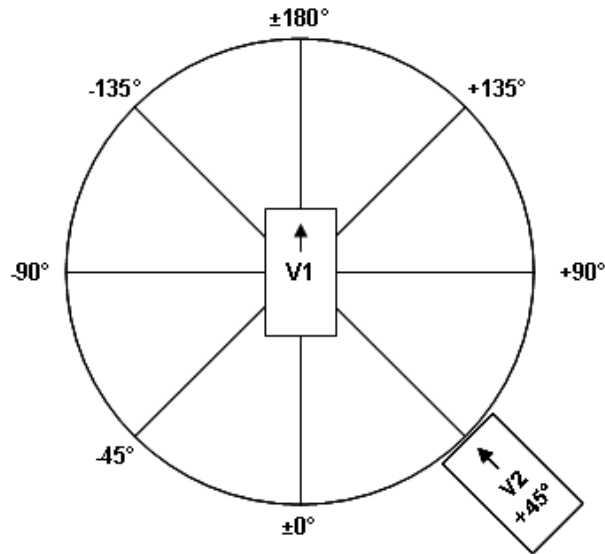
Figure 10. Illustration. Conflict angle.[6]

- *ClockAngle* is an alternative expression of the conflict angle in terms of more familiar clock-hand positions. Again, the angle is expressed from the perspective of the first vehicle, with the clock time indicating the angle from which the second vehicle is approaching. The 12 o'clock position is directly ahead of the first vehicle, the 3 o'clock position is to the right, the 6 o'clock position is directly behind, and the 9 o'clock is to the left, as illustrated in figure 11.
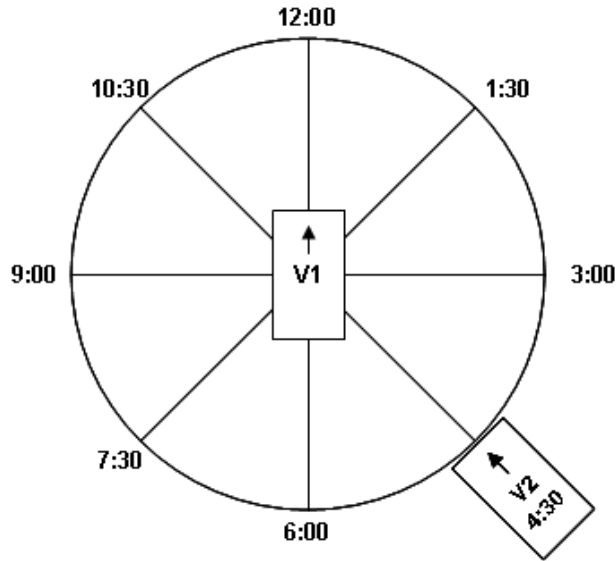
Figure 11. Illustration. Clock angle.[6]

·   *PostCrashV* is an estimate of the postcollision velocity of both vehicles. This estimate assumes that the vehicles did crash at the estimated ConflictAngle, at velocities observed at MinTTC. It also assumes an inelastic collision between the center of mass of both vehicles, where both vehicles subsequently deflect in the same direction and at the same velocity.

·   *PostCrashHeading* is the estimated heading of both vehicles following a hypothetical collision, as discussed in PostCrashV. This heading is expressed as the angle measured counterclockwise from the x-axis (which is assumed to point right), such that 0 degrees is right, 90 degrees is up, 180 degrees is left, and 270 degrees is down. The angle ranges from 0 to 360 degrees.

·   *FirstVID* (*SecondVID*) is the vehicle identification number of the first (second) vehicle. The first vehicle is the vehicle that arrives at the conflict point first. The second vehicle subsequently arrives at the same location. In rare collisions, both vehicles arrive at a location simultaneously, in which case the tie between first and second vehicle is broken arbitrarily.

·   *FirstLink* (*SecondLink*) is a number indicating which link the first (second) vehicle is traveling on at tMinTTC.

·   *FirstLane* (*SecondLane*) is a number indicating in which lane the first (second) vehicle is traveling on at tMinTTC.

·   *FirstLength* (*SecondLength*) is the length of the first (second) vehicle in feet or meters.

·   *FirstWidth* (*SecondWidth*) is the width of the first (second) vehicle in feet or meters.

·   *FirstHeading* (*SecondHeading*) is the heading of the first (second) vehicle during the conflict. This heading is approximated by the change in position from the start of the

conflict to the end of the conflict. Note that in most non-rear-end conflicts, at least one vehicle is turning throughout the conflict. The vehicle's actual heading would vary accordingly throughout the conflict. If the vehicle does not move during the conflict, then the direction in which it is facing is taken as the heading. This heading is expressed as the angle measured counterclockwise from the x-axis (which is assumed to point right), such that 0 degrees is right, 90 degrees is up, 180 degrees is left, and 270 degrees is down. The angle ranges from 0 to 360 degrees.

· *FirstVMinTTC* (*SecondVMinTTC*) is the velocity of the first (second) vehicle at tMinTTC.

· *xFirstCSP* (*xSecondCSP*) is the x-coordinate of the first (second) vehicle at the conflict starting point (CSP). The CSP is the location of the vehicle at tMinTTC.

· *yFirstCSP* (*ySecondCSP*) is the y-coordinate of the first (second) vehicle at the CSP. The CSP is the location of the vehicle at tMinTTC.

· *xFirstCEP* (*xSecondCEP*) is the x-coordinate of the first (second) vehicle at the conflict ending point (CEP). The CEP is the location of the vehicle at either the last time-step where the TTC value is below the specified threshold or where the last postencroachment value was observed, whichever occurs later in the conflict timeline.

· *yFirstCEP* (*ySecondCEP*) is the y-coordinate of the first (second) vehicle at the CEP. The CEP is the location of the vehicle at either the last time-step where the TTC value is below the specified threshold or where the last postencroachment value was observed, whichever occurs later in the conflict timeline.

3.3.5 Validation of the SSAM Approach

SSAM was validated in 2008 using an extensive database of 83 intersections. All were four-legged urban signalized intersections.[6] Researchers conducted theoretical validation, field validation, and sensitivity analysis. The theoretical validation effort considered 11 pairs of intersection designs (e.g., right-turn bay versus no right-turn bay, SPUI versus diamond interchange, roundabout versus diamond interchange). The relative safety assessments of SSAM were compared to assessments using traditional theoretical crash-prediction equations. The results yielded interesting insights. It was often the case that design A might have more total conflicts than design B, while design B had higher severity conflicts than design A, pointing to the need for further research in interpreting and comparing surrogate measures of safety. The field validation effort was concerned with the absolute accuracy of surrogate safety assessment, in contrast to the relative safety assessments of the theoretical validation. A total of 83 intersections were used in the validation study by modeling in VISSIM® and assessing with SSAM. The conflict analysis results of the intersections were compared to actual crash histories, based on insurance claims records, using five statistical tests. This effort also provided an opportunity for benchmark comparison of surrogate safety estimates versus traditional crash-prediction models based on average daily traffic (ADT) volumes. The simulation-based intersection conflicts data provided by SSAM were significantly correlated with the crash data collected in the field, with the exception of conflicts during path-crossing maneuvers (e.g., left turns colliding with opposing through traffic), which were underrepresented in the

simulation results. Intersection rankings based on total conflict frequency were weakly correlated with intersection rankings based on total crash frequency with a Spearman rank coefficient of 0.463 and were similarly correlated for rear-end and lane-change incidents. The relationship between total conflicts and total crashes in the validation study, as shown in equation 3, exhibited a correlation ($R^2 = 0.41$).

$$\frac{Crashes}{Year} = 0.119 \cdot \left(\frac{Conflicts}{Hour}\right)^{1.419} \tag{3}$$

This correlation of conflicts to crashes, albeit weak, is consistent with the range of correlations reported in several studies between ADT and crashes for urban, signalized intersections. This result was achieved despite simulating only morning peak-hour volumes. Crash prediction models based on a yearly average of 24-h ADT volumes exhibited a correlation ($R^2 = 0.68$) with actual crash frequencies. This study also found an average conflict-to-crash ratio of approximately 20,000 to 1, though that ratio varied by conflict type.[6]

The sensitivity analysis compared the performance of 5 intersections (taken from the aforementioned 83) implemented in each of the following microsimulation models: VISSIM®, Aimsun, Paramics, and TEXAS. Crashes, vehicles driving through each other, were found in all simulations, and SSAM proved particularly useful in revealing questionable simulated behavior in the models. This has notably prompted some revisions (so far by TEXAS and VISSIM®) to improve the behavior of the underlying simulation models.[6]

4.0 STUDY SCENARIOS AND SURROGATE MEASURES OF SAFETY

4.1 INTERSECTION AND ARTERIAL CONFIGURATIONS

As previously stated, the objective of this research was to identify relationships between signal timing parameters and surrogate measures of safety such as rear-end, crossing (angle), and lane-change conflicts. There are thousands of combinations of signal timing, traffic demand conditions, and intersection lane configuration scenarios that could be tested. The first phase of this project, limited in both budget and time, focused on testing the relationship and effect of the individual signal timing parameters on safety by means of quantifying surrogate measures of safety. Therefore, the research team identified and selected several test scenarios for a single signalized intersection as well as a three-intersection arterial. Signal timing parameters including cycle length, spilt, offset, detector extension time, and phase-change interval were selected for testing, along with options for left-turn phasing and left-turn phase sequence. Only one geometric configuration, however, was used in this initial analysis as shown in figure 12 and figure 13.
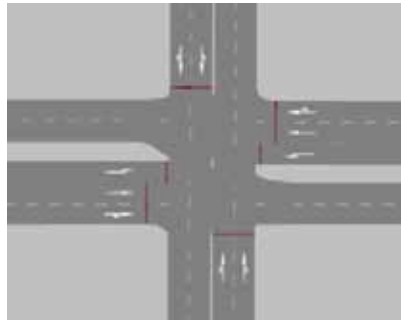
Figure 12. Illustration. Intersection configuration used in simulation tests.
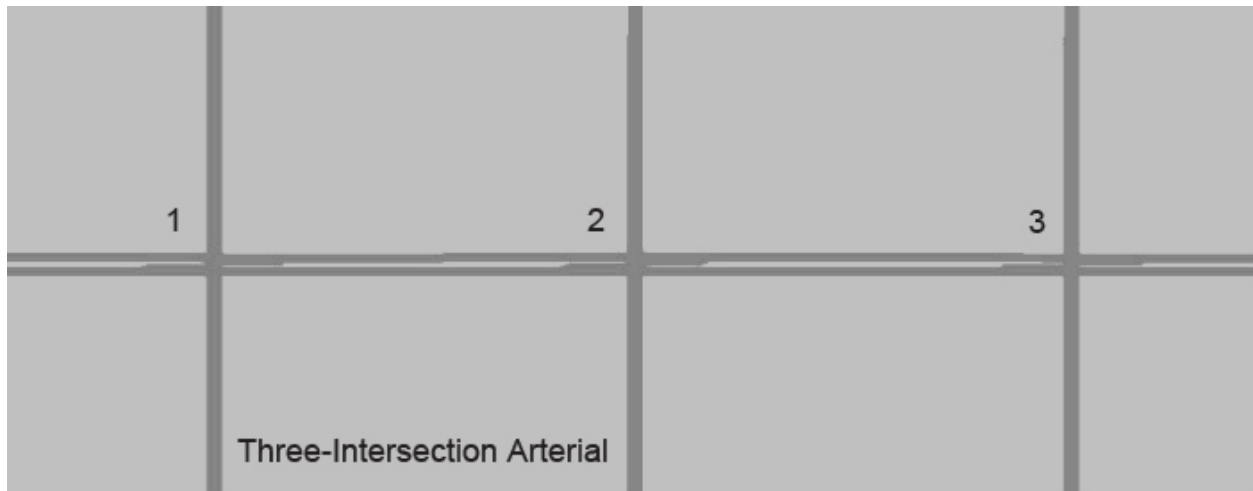
Figure 13. Illustration. Arterial configuration used in simulation tests.

The intersection configuration included two through lanes on the main street, with an exclusive left-turn lane in each approach and right-turn movements sharing the through lanes. The side streets had two through lanes, with left- and right-turn movements sharing the through lanes. Speeds on the main and side streets were 45 mi/h and 30 mi/h, respectively.

The baseline scenario for traffic demand for both the single intersection and the three-intersection arterial assumed a V/C ratio of 0.85 for all movements at the intersection. Left-turn phases on the main streets were lead-lead, while the side streets had permissive left turns only. The baseline condition for the arterial spacing between the first and second intersection and second and third intersection was 1,320 ft and 1,500 ft, respectively.

Table 3 through table 17 summarize each of the conditions tested and the means to identify a relationship between signal timing and safety. Specifically, the following scenarios were tested for their impact on safety, that is, the number of conflicts generated from the SSAM model:

Single intersection:

- Effects of changes in traffic demand.

- Effects of changes in split.

- Effects of changes in cycle length.

- Effects of changes in detector extension times for main street and side street.

- Effects of changes in left-turn phasing: from protected only to protected/permissive.

- Effects of changes in left-turn phasing: from protected only to permissive only.

- Effects of changes in the phase-change interval.

Arterial baseline:

- Effects of changes in traffic demand.

- Effects of changes in offset.

- Effects of changes in left-turn sequence.

4.2 SURROGATE MEASURES OF SAFETY AND STUDY SCENARIOS

Table 3 through table 17 present the test cases that were analyzed in this research. Each table lists the geometry, signal timing parameters, volume levels, and various other inputs tested in the scenario. Below each table is a brief description of the analysis approach for each test related to the use of Synchro™, VISSIM®, and SSAM and the expectations for the results. The primary surrogate measures used in this project were the total numbers of rear-end, crossing, and lane-change conflicts as computed by SSAM. Total average intersection delay per vehicle and the Performance Index (PI), a composite measure of stops, delays, and queues, were recorded from the Synchro™ model, and the approach delay was also recorded from the VISSIM® model. These measures were noted specifically to validate the relative accuracy of input and output from the Synchro™ and VISSIM® models before the trajectory files were analyzed in SSAM. Overall, it was found that the results for the delay measures from both models were relatively similar.

Table 3. Single intersection base condition.

Element	Main/Side Streets	Remarks
Geometry	Main: Three lanes with exclusive left and shared right; 1,000-ft link; 200-ft bays	
	Side: Two lanes with shared left and through; 1,000-ft link	
Traffic volumes	Main: Set volumes to start with approximately V/C = 0.85; peak-hour factor (PHF) = 0.92; trucks at 2 percent	
	Side: Set volumes to start with approximately V/C = 0.85	
Phasing	Main: Four-phase operations with concurrent lead lefts, protected only	
	Side: Single concurrent phase	
V/C ratios	Main: Approximately 0.85	
	Side: Approximately 0.85	
Detection	Main: Advance and stop line; 5-s extension	
	Side: Advance only and stop line; 3-s extension	
Speed	Main: 45 mi/h	
	Side: 30 mi/h	
Signal timing	Fully actuated; yellow plus all red (Y+AR) per Institute of Technical Engineers (ITE) method; minimum green equals 10 s for main line and 7 s for side street; gap extension per Maryland State Highway Administration (MDSHA) look-up chart [15,16]	Fully actuated
Optimization condition	Optimize for best cycle and splits	Use Synchro™ 6
Cycle length	Optimize	Use Synchro™ 6
Splits	Optimize	Use Synchro™ 6
Offsets	Not applicable	
Performance measures	Synchro™ PI; VISSIM® total intersection delay and actual cycle length utilized; SSAM frequency of rear-end, crossing, and lane-change conflicts	

Scenario condition: Set up a base condition with an optimized cycle length and splits.

Expectations: Base condition is used as the basis for comparative analysis with other scenarios.

Synchro™: Record delay and PI for each optimization.

VISSIM®: Export Synchro™ files to VISSIM® and perform six 60-min simulations with random seeding. Record total intersection delay, cycle length utilized, and total vehicles simulated.

SSAM: Export trajectory files from VISSIM® to SSAM for all simulations and average results.

Table 4. Effects of changes in traffic demand under a fixed cycle length.

Element	Main/Side Streets	Remarks
Geometry	Baseline	
	Baseline	
Traffic volumes	Vary V/C ratios to 0.3, 0.5, 0.7, 0.85, and 1.0	
	Vary V/C ratios to 0.3, 0.5, 0.7, 0.85, and 1.0	
Phasing	Baseline	
	Baseline	
V/C ratios	Vary to 0.3, 0.5, 0.7, 0.85, and 1.0	
	Vary to 0.3, 0.5, 0.7, 0.85, and 1.0	
Detection	Baseline	
	Baseline	
Speed	Baseline	
	Baseline	
Signal timing	Optimize splits	Fully actuated
Optimization condition	Use baseline optimized cycle length	Use Synchro™ 6
Cycle length	Use baseline optimized cycle length	Use Synchro™ 6
Splits	Optimize splits	Use Synchro™ 6
Offsets	Not applicable	
Performance measures	Synchro™ PI; VISSIM® total intersection delay and actual cycle length utilized; SSAM frequency of rear-end, crossing, and lane-change conflicts	

Scenario condition: Change settings in Synchro™. Use optimum cycle length, vary demand volumes for V/C ratios of 0.3, 0.5, 0.7, 0.85, and 1.0, and optimize splits. Transfer files to VISSIM®.

Expectations: This condition is expected to determine if there is any relationship between demand volumes and safety using optimized splits within a fixed cycle length. Increasing or reducing traffic demand is expected to create an increase in the frequency of conflicts, especially at the higher V/C ratios but not necessarily at the lower V/C ratios.

Synchro™: Record PI for each optimization.

VISSIM®: Export Synchro™ files to VISSIM® and perform five 60-min runs with random seeding. Record total intersection delay, cycle length utilized, and total vehicles simulated.

SSAM: Export trajectory files from VISSIM® to SSAM for all runs and average results.

Table 5. Effects of changes in splits.

Element	Main/Side Streets	Remarks
Geometry	Baseline	
	Baseline	
Traffic volumes	Baseline	
	Baseline	
Phasing	Baseline	
	Baseline	
V/C ratios	Baseline, 0.85	
	Baseline, 0.85	
Detection	Baseline	
	Baseline	
Speed	Baseline	
	Baseline	
Signal timing	Use baseline cycle	Fully actuated
Optimization condition	No optimization; use baseline cycle; increase cycle length accordingly	Use Synchro™ 6
Cycle length	Increase cycle length based on changing splits	Use Synchro™ 6
Splits	Vary splits by ±10 , ±20, and ±30 percent	Use Synchro™ 6
Offsets	Not applicable	
Performance measures	Synchro™ PI; VISSIM® total intersection delay and actual cycle length utilized; SSAM frequency of rear-end, crossing, and lane-change conflicts	

Scenario condition: Use Synchro™ to add ±10 percent, ±20 percent, and ±30 percent to splits, thus increasing the cycle length but do not optimize it. Transfer files to VISSIM®.

Expectations: This condition is expected to determine if there is any relationship between splits and safety. This scenario should be compared specifically to the base condition in table 3. Increasing or reducing splits from the baseline condition is expected to create a marginal noticeable effect on increasing or reducing the number of conflicts**.**

Synchro™: Make changes in Synchro™ and record PI for each condition.

VISSIM®: Export Synchro™ files to VISSIM® and perform six 60-min runs with random seeding. Record total intersection delay, cycle length utilized, and total vehicles simulated.

SSAM: Export trajectory files from VISSIM® to SSAM for all simulations and average results.

Table 6. Effects of changes in cycle length.

Element	Main/Side Streets	Remarks
Geometry	Baseline	
	Baseline	
Traffic volumes	Vary V/C ratios to 0.3, 0.5, 0.7, 0.85, and 1.0	
	Vary V/C ratios to 0.3, 0.5, 0.7, 0.85, and 1.0	
Phasing	Baseline	
	Baseline	
V/C ratios	Vary to 0.3, 0.5, 0.7, 0.85, and 1.0	
	Vary to 0.3, 0.5, 0.7, 0.85, and 1.0	
Detection	Baseline	
	Baseline	
Speed	Baseline	
	Baseline	
Signal timing	Optimize cycles and splits with each V/C ratio	Fully actuated
Optimization condition	Optimize cycle and splits with each V/C ratio	Use Synchro™ 6
Cycle length	Optimize cycle with each V/C ratio	Use Synchro™ 6
Splits	Optimize splits with each cycle and V/C ratio	Use Synchro™ 6
Offsets	Not applicable	
Performance measures	Synchro™ PI; VISSIM® total intersection delay and actual cycle length utilized; SSAM frequency of rear-end, crossing, and lane-change conflicts	

Scenario condition: Use Synchro™ to vary demand volumes for V/C ratios of 0.3, 0.5, 0.7, 0.85, and 1.0 and optimize cycle length and splits. Transfer files to VISSIM®.

Expectations: This condition is expected to determine if there is any relationship between optimized timing (cycle length and splits) for various traffic volumes and safety. This scenario should be compared specifically to the base condition in table 3. Increasing or reducing traffic demand and also optimizing the timing plans is expected to produce a less noticeable effect on either increasing or reducing the number of conflicts. If so, then it would be clear that cycle length has a direct effect on safety.

Synchro™: Record PI for each optimization.

VISSIM®: Export Synchro™ files to VISSIM® and perform six 60-min runs with random seeding. Record total intersection delay, cycle length utilized, and total vehicles simulated.

SSAM: Export trajectory files from VISSIM® to SSAM for all runs and average results.

Table 7. Effects of changes in the main street detector extension setting.

Element	Main/Side Streets	Remarks
Geometry	Baseline	
	Baseline	
Traffic volumes	Baseline	
	Baseline	
Phasing	Baseline	
	Baseline	
V/C ratios	Baseline, 0.85	
	Baseline, 0.85	
Detection	Change detector gap extension setting by +2, +1, -2, -1.5, and -1 s	
	Baseline	
Speed	Baseline	
	Baseline	
Signal timing	Baseline	Fully actuated
Optimization condition	No optimization; use baseline cycle	Use Synchro™ 6
Cycle length	Baseline	Use Synchro™ 6
Splits	Baseline	Use Synchro™ 6
Offsets	Not applicable	
Performance measures	Synchro™ PI; VISSIM® total intersection delay and actual cycle length utilized; SSAM frequency of rear-end, crossing, and lane-change conflicts	

Scenario Condition: Use VISSIM® directly and change only main street detector setting by +2, +1, -2, -1.5, and -1 s.

Expectations: This condition is expected to determine if there is any relationship between changing detector settings on the main street and safety. This scenario should be compared specifically to the base condition in table 3. Reducing the detector setting (gap extension) is expected to produce a noticeable effect on increasing the number of conflicts.

Synchro™: Make changes in Synchro™ and record PI for each condition.

VISSIM®: Use baseline file in VISSIM®, change detector settings, and perform six 60-min runs with random seeding. Record total intersection delay, cycle length utilized, and total vehicles simulated.

SSAM: Export trajectory files from VISSIM® to SSAM for all runs and average results.

Table 8. Effect of changes in the side street detector extension setting.

Element	Main/Side Streets	Remarks
Geometry	Baseline	
	Baseline	
Traffic volumes	Baseline	
	Baseline	
Phasing	Baseline	
	Baseline	
V/C ratios	Baseline, 0.85	
	Baseline, 0.85	
Detection	Baseline	
	Change detector gap extension setting on side street by +2, +1, -2, -1.5, and -1 s	
Speed	Baseline	
	Baseline	
Signal timing	Baseline	Fully actuated
Optimization condition	No optimization; use baseline cycle	Use Synchro™ 6
Cycle length	Baseline	Use Synchro™ 6
Splits	Baseline	Use Synchro™ 6
Offsets	Not applicable	
Performance measures	Synchro™ PI; VISSIM® total intersection delay and actual cycle length utilized; SSAM frequency of rear-end, crossing, and lane-change conflicts	

Scenario condition: Use VISSIM® directly and change only side street detector setting by +2, +1, -2, -1.5, and -1 s.

Expectations: This condition is expected to determine if there is any relationship between changing detector settings on the side street and safety. This scenario should be compared specifically to the base condition in table 3. Reducing the detector setting (gap extension) is expected to produce a noticeable effect on increasing the number of conflicts.

Synchro™: Make changes in Synchro™ and record PI for each condition.

VISSIM®: Use baseline file in VISSIM®, change detector settings, and perform six 60-min runs with random seeding. Record total intersection delay, cycle length utilized, and total vehicles simulated.

SSAM: Export trajectory files from VISSIM® to SSAM for all runs and average results.

Table 9. Effects of changes in left-turn phasing from protected only to protected/permissive.

Element	Main/Side Streets	Remarks
Geometry	Baseline	
	Baseline	
Traffic Volumes	Baseline	
	Baseline	
Phasing	Change to protected/permissive left turn	
	Baseline	
V/C ratios	1.0, 0.85, 0.7, 0.5, 0.3 (left-turn and opposing volumes only)	Make change for left-turn and opposing volumes only
	Baseline of 0.85	
Detection	Baseline	
	Baseline	
Speed	Baseline	
	Baseline	
Signal timing	Baseline	Fully actuated
Optimization condition	Optimize	Use Synchro™ 6
Cycle length	Optimize cycle length	Use Synchro™ 6
Splits	Optimize	Use Synchro™ 6
Offsets	Not applicable	
Performance measures	Synchro™ PI; VISSIM® total intersection delay and actual cycle length utilized; SSAM frequency of rear-end, crossing, and lane-change conflicts	

Scenario condition: Optimize timing plans with Synchro™ with the change in volumes and left-turn phasing on main street from protected only to protected/permissive left-turn phasing.

Expectations: This condition is expected to determine if there is any relationship between changing left-turn phasing treatment from protected only to protected/permissive and safety. This scenario should be compared specifically to the base condition in table 3. Changing traffic volumes and left-turn phasing treatment from protected only to protected/permissive is expected to produce a noticeable effect on increasing the number of angle conflicts.

Synchro™: Make changes in the base condition in Synchro™ and record PI for each condition.

VISSIM®: Use baseline file in VISSIM®, change left-turn phasing, and perform six 60-min runs with random seeding. Record total intersection delay, cycle length utilized, and total vehicles simulated.

SSAM: Export trajectory files from VISSIM® to SSAM for all runs and average results.

Table 10. Effects of changes in left-turn phasing from protected to permissive left-turn only.

Element	Main/Side Streets	Remarks
Geometry	Baseline	
	Baseline	
Traffic volumes	Baseline	
	Baseline	
Phasing	Change to permissive left turn only	
	Baseline	
V/C ratios	1.0, 0.85, 0.7, 0.5, 0.3 (left-turn and opposing volumes only)	Make change for left-turn and opposing volumes only
	Baseline of 0.85	
Detection	Baseline	
	Baseline	
Speed	Baseline	
	Baseline	
Signal timing	Baseline	Fully actuated
Optimization condition	Optimize	Use Synchro™ 6
Cycle length	Optimize cycle length	Use Synchro™ 6
Splits	Optimize	Use Synchro™ 6
Offsets	Not applicable	
Performance measures	Synchro™ PI; VISSIM® total intersection delay and actual cycle length utilized; SSAM frequency of rear-end, crossing, and lane-change conflicts	

Scenario condition: Optimize timing plans with Synchro™ with the change in volumes and left-turn phasing on main street from protected only to permissive left-turn phasing.

Expectations: This condition is expected to determine if there is any relationship between changing left-turn phasing treatment from protected only to permissive and safety. This scenario should be compared specifically to the base condition in table 3 and the protected/permissive condition in table 9. Changing traffic volumes and left-turn phasing treatment from protected only to permissive is expected to produce a noticeable effect on increasing the number of angle conflicts.

Synchro™: Make changes in the base condition in Synchro™ and record PI for each condition.

VISSIM®: Use baseline file in VISSIM®, change left-turn phasing, and perform six 60-min runs with random seeding. Record total intersection delay, cycle length utilized, and total vehicles simulated.

SSAM: Export trajectory files from VISSIM® to SSAM for all runs and average results.

Table 11. Effects of changes in the phase-change interval.

Element	Main/Side Streets	Remarks
Geometry	Baseline	
	Baseline	
Traffic volumes	Baseline	
	Baseline	
Phasing	Baseline	
	Baseline	
V/C ratios	Baseline, 0.85	
	Baseline, 0.85	
Detection	Baseline	
	Baseline	
Speed	Baseline	
	Baseline	
Signal timing	Change Y+AR on main line by ±2 and ±1 s	Fully actuated
Optimization condition	No optimization; use baseline cycle	Use Synchro™ 6
Cycle length	Baseline	Use Synchro™ 6
Splits	Baseline	Use Synchro™ 6
Offsets	Not applicable	
Performance measures	Synchro™ PI; VISSIM® total intersection delay and actual cycle length utilized; SSAM frequency of rear-end, crossing, and lane-change conflicts	

Scenario Condition: Use VISSIM® directly and change Y+AR on main street.

Expectations: This condition is expected to determine if there is any relationship between changing the change and clearance intervals and safety. This scenario should be compared specifically to the base condition in table 3. Changing the Y+AR intervals is expected to produce a noticeable effect on increasing the number of rear-end and angle conflicts.

Synchro™: Make changes in the base condition in Synchro™ and record PI for each condition.

VISSIM®: Use baseline file in VISSIM®, change Y+AR, and perform six 60-min runs with random seeding. Record total intersection delay, cycle length utilized, and total vehicles simulated.

SSAM: Export trajectory files from VISSIM® to SSAM for all runs and average results.

Table 12. Arterial base condition with arterial traffic demand of V/C = 0.85.

Element	Main/Side Streets; Create Three Intersections	Remarks
Geometry	Three lanes with exclusive left and shared right; 1,000-ft link; 200-ft bays	Link distances should be 0 ft, 1,320 ft, and 1,500 ft between three intersections
	Two lanes with shared left and through; 1,000-ft link	
Traffic volumes	Set volumes to start with approximate V/C = 0.85; PHF = 0.92; trucks at 2 percent	
	Set volumes to start with approximate V/C = 0.85	
Phasing	Four-phase operations with concurrent lead lefts, protected only	
	Single concurrent phase	
V/C ratios	Approximately 0.85	
	Approximately 0.85	
Detection	Advance and stop line; 5-s extension	
	Advance only and stop line; 3-s extension	
Speed	45 mi/h	
	30 mi/h	
Signal timing	Fully actuated; Y+AR per ITE method; minimum green equal 10 s for main line and 7 s for side street; gap extension per MDSHA look-up chart [15,16]	Fully actuated
Optimization condition	Optimize for best cycle and splits for all three intersections	Use Synchro™ 6
Cycle length	Optimize	Use Synchro™ 6
Splits	Optimize	Use Synchro™ 6
Offsets	Optimize	
Performance measures	Synchro™ PI; VISSIM® total intersection delay and actual cycle length utilized; SSAM frequency of rear-end, crossing, and lane-change conflicts	

Scenario condition: Set up a base condition with an optimized cycle length and splits for three intersections with optimized offsets.

Expectations: Base condition is used as the basis for comparative analysis with other scenarios.

Synchro™: Record PI for each optimization.

VISSIM®: Export Synchro™ files to VISSIM® and perform six 60-min runs with random seeding. Record total intersection delay, cycle length utilized, and total vehicles simulated.

SSAM: Export trajectory files from VISSIM® to SSAM for all runs and average results.

Table 13. Arterial base condition with changes in arterial traffic demand to V/C = 1.0.

Element	Main/Side Streets; Create Three Intersections	Remarks
Geometry	Three lanes with exclusive left and shared right; 1,000-ft link; 200-ft bays	Link distances should be 0 ft, 1,320 ft, and 1,500 ft between three intersections
	Two lanes with shared left and through; 1,000-ft link.	
Traffic volumes	Set volumes to start with approximate V/C = 1.00; PHF = 0.92; trucks at 2 percent	
	Set volumes to start with approximate V/C = 1.00	
Phasing	Four-phase operations with concurrent lead lefts, protected only	
	Single concurrent phase	
V/C ratios	Approximately 1.00	
	Approximately 1.00	
Detection	Advance and stop line; 5-s extension	
	Advance only and stop line; 3-s extension	
Speed	45 mi/h	
	30 mi/h	
Signal timing	Fully actuated; Y+AR per ITE method; minimum green equal 10 s for main line and 7 s for side street; gap extension per MDSHA look-up chart [15,16]	Fully actuated
Optimization condition	Optimize for best cycle and splits for all three intersections	Use Synchro™ 6
Cycle length	Optimize	Use Synchro™ 6
Splits	Optimize	Use Synchro™ 6
Offsets	Optimize	
Performance measures	Synchro™ PI; VISSIM® total intersection delay and actual cycle length utilized; SSAM frequency of rear-end, crossing, and lane-change conflicts	

Scenario condition: Set up a base condition with an optimized cycle length and splits for three intersections with optimized offsets.

Expectations: Base condition with higher traffic demand (V/C = 1.00) is used as the basis for the comparative analysis with other scenarios.

Synchro™: Record PI for each optimization.

VISSIM®: Export Synchro™ files to VISSIM® and perform six 60-min runs with random seeding. Record total intersection delay, cycle length utilized, and total vehicles simulated.

SSAM: Export trajectory files from VISSIM® to SSAM for all runs and average results.

Table 14. Effects of changes in offsets with cycle length of 50 s.

Element	Main/Side Streets; Create Three Intersections	Remarks
Geometry	Three lanes with exclusive left and shared right; 1,000-ft link; 200-ft bays	Link distances should be 0 ft, 1,320 ft, and 1,500 ft between three intersections
	Two lanes with shared left and through; 1,000-ft link	
Traffic volumes	Set volumes to start with approximate V/C = 0.85; PHF = 0.92; trucks at 2 percent	
	Set volumes to start with approximate V/C= 0.85	
Phasing	Four-phase operations with concurrent lead lefts, protected only	
	Single concurrent phase	
V/C ratios	Approximately 0.85	
	Approximately 0.85	
Detection	Advance and stop line; 5-s extension	
	Advance only and stop line; 3-s extension	
Speed	45 mi/h	
	30 mi/h	
Signal timing	Fully actuated; Y+AR per ITE method; minimum green equal 10 s for main line and 7 s for side street; gap extension per MDSHA look-up chart [15,16]	Fully actuated
Optimization condition	Optimize for best cycle and splits for all three intersections	Use Synchro™ 6
Cycle length	Cycle 50 s	Use Synchro™ 6
Splits	Base condition	Use Synchro™ 6
Offsets	Change offsets at second intersection by ±10, ±20, and ±30 percent of cycle length	
Performance measures	Synchro™ PI; VISSIM® total intersection delay and actual cycle length utilized; SSAM frequency of rear-end, crossing, and lane-change conflicts	

Scenario condition: Change offsets at second intersection only by ±10, ±20, and ±30 percent of cycle length.

Expectations: It is expected that a change in the offsets will result in an increase in the number of rear-end conflicts.

Synchro™: Record PI for each condition.

VISSIM®: Make changes directly in VISSIM® and perform six 60-min runs with random seeding. Record total intersection delay, cycle length utilized, and total vehicles simulated.

SSAM: Export trajectory files from VISSIM® to SSAM for all runs and average results.

Table 15. Effects of changes in offsets with cycle length of 105 s.

Element	Main/Side Streets; Create Three Intersections	Remarks
Geometry	Three lanes with exclusive left and shared right; 1,000-ft link; 200-ft bays	Link distances should be 0 ft, 1,320 ft, and 1,500 ft between three intersections
	Two lanes with shared left and through; 1,000-ft link	
Traffic volumes	Set volumes to start with approximate V/C = 1.00; PHF = 0.92; trucks at 2 percent	
	Set volumes to start with approximate V/C = 1.00	
Phasing	Four-phase operations with concurrent lead lefts, protected only	
	Single concurrent phase	
V/C ratios	Approximately 0.85	
	Approximately 0.85	
Detection	Advance and stop line; 5-s extension	
	Advance only and stop line; 3-s extension	
Speed	45 mi/h	
	30 mi/h	
Signal timing	Fully actuated; Y+AR per ITE method; minimum green equal 10 s for main line and 7 s for side street; gap extension per MDSHA look-up chart [15, 16]	Fully actuated
Optimization condition	Optimize for best cycle and splits for all three intersections	Use Synchro™ 6
Cycle length	Cycle 105 s	Use Synchro™ 6
Splits	Base condition	Use Synchro™ 6
Offsets	Change offsets at second intersection by ±10, ±20, and ±30 percent of cycle length	
Performance measures	Synchro™ PI; VISSIM® total intersection delay and actual cycle length utilized; SSAM frequency of rear-end, angle, and lane-change conflicts	

Scenario condition: Change offsets at second intersection only by ±10, ±20, and ±30 percent.

Expectations: It is expected that a change in the offsets will result in an increase in the number of rear-end conflicts.

Synchro™: Record PI for each condition.

VISSIM®: Make changes directly in VISSIM® and perform six 60-min runs with random seeding. Record total intersection delay, cycle length utilized, and total vehicles simulated.

SSAM: Export trajectory files from VISSIM® to SSAM for all runs and average results.

Table 16. Effects of changes in left-turn phase sequence to lead-lag, 50-s cycle length.

Element	Main/Side Streets; Create Three Intersections	Remarks
Geometry	Offset baseline	Link distances should be 0 ft, 1,320 ft, and 1,500 ft between three intersections
	Offset baseline	
Traffic volumes	Offset baseline	
	Offset baseline	
Phasing	Change left-turn sequence in Synchro™ to optimized	Induce lead-lag and lag-lead if Synchro™ does not identify as an optimum condition
	Offset baseline	
V/C ratios	1.0, 0.85, 0.7, 0.5, and 0.3	
	1.0, 0.85, 0.7, 0.5, and 0.3	
Detection	Offset baseline	
	Offset baseline	
Speed	Offset baseline	
	Offset baseline	
Signal timing	Offset baseline	Fully actuated
Optimization condition	Offset baseline	Use Synchro™ 6
Cycle length	Offset baseline; cycle length 50 s	Use Synchro™ 6
Splits	Offset baseline	Use Synchro™ 6
Offsets	Optimize	
Performance measures	Synchro™ PI; VISSIM® total intersection delay and actual cycle length utilized; SSAM frequency of rear-end, angle, and lane-change conflicts	

Scenario condition: Base condition with optimized left-turn phase sequence and offsets. Either change directly in VISSIM® after running in Synchro™ or export from Synchro™ to VISSIM®.

Expectations: It is expected that an optimum left-turn phase sequence will result in a reduced number of rear-end and angle conflicts.

Synchro™: Record PI for each optimization.

VISSIM®: Export Synchro™ files to VISSIM® and perform six 60-min runs with random seeding. Record total intersection delay, cycle length utilized, and total vehicles simulated.

SSAM: Export trajectory files from VISSIM® to SSAM for all runs and average results.

Table 17. Effects of changes in left-turn phase sequence to lead-lag, 105-s cycle length.

Element	Main/Side Streets; Create Three Intersections	Remarks
Geometry	Offset baseline	Link distances should be 0 ft, 1,320 ft, and 1,500 ft between three intersections
	Offset baseline	
Traffic volumes	Offset baseline	
	Offset baseline	
Phasing	Change left-turn sequence in Synchro™ to optimized	Induce lead-lag and lag-lead if Synchro™ does not identify as an optimum condition
	Offset baseline	
V/C ratios	1.0, 0.85, 0.7, 0.5, 0.3	
	1.0, 0.85, 0.7, 0.5, 0.3	
Detection	Offset baseline	
	Offset baseline	
Speed	Offset baseline	
	Offset baseline	
Signal timing	Offset baseline	Fully actuated
Optimization condition	Offset baseline	Use Synchro™ 6
Cycle length	Offset baseline; cycle length 105 s	Use Synchro™ 6
Splits	Offset baseline	Use Synchro™ 6
Offsets	Optimize	
Performance measures	Synchro™ PI; VISSIM® total intersection delay and actual cycle length utilized; SSAM frequency of rear-end, angle, and lane-change conflicts	

Scenario condition: Base condition with optimized left-turn phase sequence and offsets. Either change directly in VISSIM® after running in Synchro™ or export from Synchro™ to VISSIM.

Expectations: It is expected that an optimum left-turn phase sequence will result in a reduced number of rear-end and angle conflicts.

Synchro™: Record PI for each optimization.

VISSIM®: Export Synchro™ files to VISSIM® and perform five 60-min runs with random seeding. Record total intersection delay, cycle length utilized, and total vehicles simulated.

SSAM: Export trajectory files from VISSIM® to SSAM for all runs and average results.

5.0 FINDINGS FROM THE SIMULATION ANALYSIS

As previously noted, Synchro™, VISSIM®, and SSAM were used to evaluate the effects of different controller parameters on intersection safety. Specifically, the following seven parameters were studied:

· Cycle length.

· Split/phase maximum.

· Offset.

· Detector gap extension timing.

· Left-turn phase treatment (permissive, protected, or combination).

· Left-turn phase sequence (combination of lead and lag).

· Change and clearance intervals (Y+AR).

For each parameter, a scenario was defined that was intended to allow the safety aspects (either positive or negative) of that parameter to be observable. The figures of merit used as surrogates for crashes were the estimates of conflicts calculated by SSAM, which produces estimates of conflicts in three categories: crossing, rear end, and lane changing. In general, crossing conflicts reflect the potential for right-angle collisions, rear-end conflicts are correlated with rear-end collisions, and lane-change conflicts are related with sideswipe collisions. A statistically significant change in the average number of conflicts of each type was used as the primary indicator that a given signal timing parameter has an effect on safety.

In order to be able to compare the impact of each signal timing parameter, it was necessary to define a base condition. This baseline was intended to reflect a typical urban arterial intersection operating with peak-hour, but not congested, demand conditions. This process was performed first for an individual intersection and then for a three-intersection arterial.

The remainder of this section defines the base scenario and then compares the results of each of the scenarios with the base condition to determine the impact of each signal timing parameter on the total number of intersection conflicts.

5.1 INTERSECTION BASE CONDITION ANALYSIS

The base condition, as shown in figure 14, reflects the average conditions at a typical urban arterial intersection on a four-lane roadway with left-turn pockets. The base demand condition reflects a relatively high demand typical of a peak hour with a V/C ratio of 0.85. The signal timing optimization program Synchro™ was used to determine optimum signal timing parameters. This combination of intersection geometry and demand is intended to reflect a normal peak-period situation.
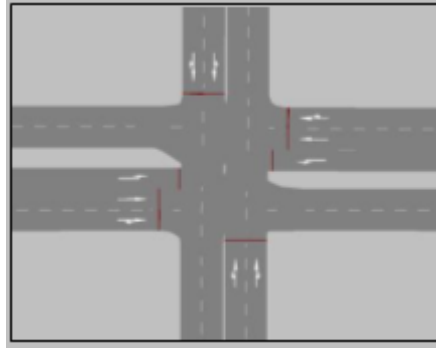
Figure 14. Illustration. Typical intersection layout.

The following is a summary of the base condition:

- Demand volumes as shown in figure 15.

- Two through lanes on side streets with shared right- and left-turn lanes.

- Two through lanes on main streets with a shared right-turn lane and a separate left-turn lane.

- Protected lead-lead left-turn phasing.

- Speed limits of 45 mi/h on main street and 30 mi/h on side street.

- V/C ratio of 0.85 for main and side street.

- Link length of 1,000 ft on each of the intersection approaches.

- Detection set per MDSHA standards.[16]

- Y+AR set per ITE method.[15]

- Signal timing optimized using Synchro™ (resulting in a 65-s cycle length).

- Each simulation conducted for 75 min, including a 15-min warm-up period.

- Six runs performed in VISSIM®, and trajectory files imported to SSAM.
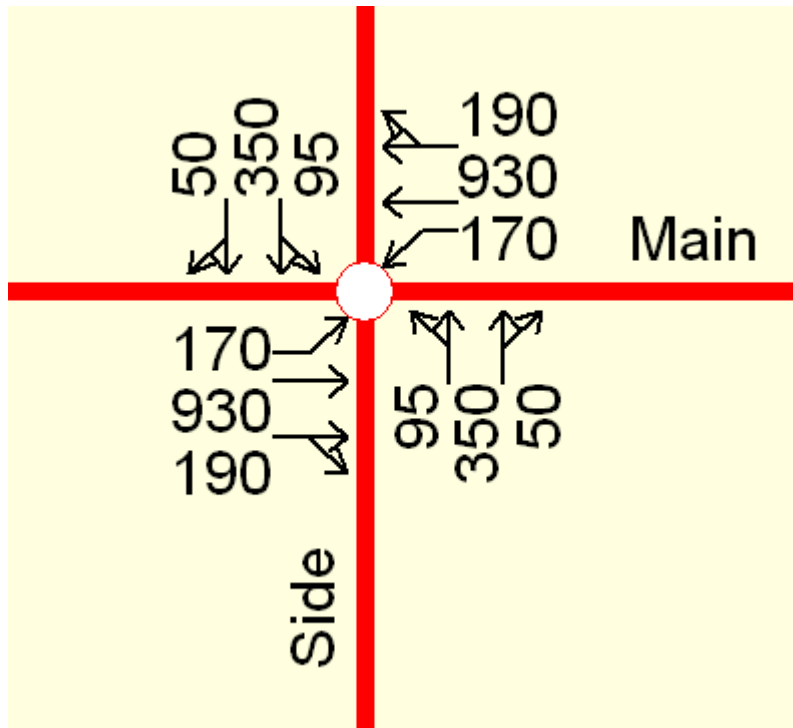
Figure 15. Illustration. Intersection traffic volumes.

Postprocessing the trajectory data from the VISSIM® runs using SSAM resulted in an average total of 132 conflicts—111 rear-end conflicts, 14 crossing conflicts, and 7 lane-change conflicts (see table 18). There were modest differences in the number of conflicts from one simulation to the next. The fewest number of conflicts was 142, and the maximum number was 185. The coefficient of variation, a measure of the dispersion of the conflict data, was found to be 10.5 percent—a reasonable amount for a stochastic simulation.

Table 18. Summary of conflict data for the intersection baseline analysis.

Demand Condition (V/C)	Number of Simulations	Rear-end Conflicts	Crossing Conflicts	Lane-change Conflicts	Total Conflicts
0.85	6	111	14	7	132
0.85	20	113	13	4	130

A further test of 20 iterations was conducted to determine if more iterations would result in larger or smaller standard deviations of the conflict totals. In this test, the average total number of conflicts was 130 and consisted of 113 rear-end, 13 crossing, and 4 lane-change conflicts. The difference between these results and the results of the test using a sample size of six simulations was not statistically significant. Therefore, because of the budget and time constraints of this project, it was determined that a sample size of six 1-h simulations would be adequate to draw statistically significant inferences about the relationships between signal timing and safety. The 1-h simulation for each run was important in order to account for all variations and peak characteristics of traffic and driver behavior within the simulation period. This long simulation period also takes considerable time to run in VISSIM® and subsequently in SSAM. Therefore, considering that a

total of over 400 different runs were conducted in this research, it was important that a proper sample size be selected in order to meet the budget and schedule of the project.

5.1.1 Effects of Changes in Traffic Demand

In the first scenario, the effects of different demand conditions were explored. The demand conditions are expressed in terms of V/C ratios. Three conditions had lower volumes than the base condition (V/C = 0.3, 0.5, and 0.7), and one condition had higher volumes than the base condition (V/C = 1.0). In each case, the signal phasing and cycle length remained the same as the base condition. The cycle length was 65 s, and the split was optimized for each V/C condition. The results, as shown in table 19, indicate that the conflicts were approximately proportional to the volume for this scenario. This is reasonable since one would expect more conflicts as more vehicles are accommodated in the same amount of green time.

Table 19. Average conflicts under different demand conditions.

Demand Condition (V/C)	Rear-end Conflicts	Crossing Conflicts	Lane-change Conflicts	Total Conflicts
0.3	28	1	2	31
0.5	42	5	6	53
0.7	81	8	7	96
0.85 (base)	111	14	7	132
1.0	149	19	2	170

However, it is interesting to note that the number of conflicts increased more rapidly as the V/C ratio approached 1.0. This is illustrated in table 20 by the increasing ratio of conflicts to V/C as the demand condition increases. This shows that the ratio of demand to capacity is another factor that influences the number of conflicts and, therefore, the potential safety of an intersection.

Table 20. Ratio of conflicts to V/C.

Total Conflicts	Demand Condition (V/C)	Ratio of Conflicts to V/C
31	30	31/30 = 1.03
53	50	53/50 = 1.06
96	70	96/70 = 1.31
132	85 (base)	132/85 = 1.55
179	100	179/100 = 1.79

5.1.2 Effects of Changes in Split

In this scenario, the demand was held constant and the signal timings were changed to determine the effect of different splits on conflicts. The splits were adjusted in 10 percent steps from the optimum used in the base condition. The splits were adjusted up and down in proportion to the original split. For example, if the base condition (cycle length = 65 s) had a total green time of 50 s, then the +10 percent simulation would increase the green time by 5 s, resulting in a cycle length of 70 s. The additional 5 s were distributed proportionally among the phases. The results of these simulations are shown in table 21.

Table 21. Conflicts under different split conditions.

Split Condition (Percent)	Cycle Length	Rear-end Conflicts	Crossing Conflicts	Lane-change Conflicts	Total Conflicts
-30	46.0	147	16	12	175
-20	52.5	135	16	10	161
-10	59.0	114	11	8	133
Optimized	65.0	111	14	7	132
+10	72.0	101	10	8	119
+20	78.0	100	10	7	117
+30	84.5	81	10	7	98

This simulation reaffirmed the observation that conflicts increase as the demand-to-capacity ratio increases. The split condition with the least green time (-30 percent) was the condition that experienced the greatest number of conflicts. There is almost an inverse linear relationship between the splits and conflicts. As the split increases, the total number of conflicts decreases. This is not unreasonable since fewer conflicts are expected when the cycle length increases if for no other reason than there are fewer change periods (yellow plus red) per hour with longer cycles. For example, a 50-s cycle will experience 72 change periods per hour while an 80-s cycle will experience 45 change periods per hour. The ratio of maximum to minimum conflicts, 1.8 (175/98), compares well to the ratio of changes, 1.6 (72/45), suggesting that the number of change periods per hour (cycle length) may account for many of the conflicts regardless of other timing parameters. This is illustrated in table 22 with the ratio of conflicts to changes per hour.

Table 22. Ratio of conflicts to changes per hour (various split conditions).

Split Condition (Percent)	Cycle Length	Changes Per Hour	Total Conflicts	Ratio of Conflicts to Changes Per Hour
-30	46.0	78.26	175	2.2
-20	52.5	68.57	161	2.3
-10	59.0	61.02	133	2.2
Optimized	65.0	55.38	132	2.4
+10	72.0	50.00	119	2.4
+20	78.0	46.15	117	2.5
+30	84.5	42.60	98	2.3

The ratio range is 2.2–2.5 with an average of 2.3 for the seven simulations. This ratio is remarkably stable, indicating that the number of changes per hour accounts for many of the conflicts throughout the range of splits.

The effect of splits on safety was tested by holding the cycle length constant and changing the splits on the main street by borrowing up to 42 percent of the side street split (adding up to approximately 9 s to the main street), borrowing the additional time from the side street beyond its minimum time. The results of this effort are shown in table 23. The same process was followed to generate the conflicts on the side street, the results of which are shown in table 24**.**

Table 23. Conflicts with main street split adjustments.

Split Condition (Percent)	Cycle Length	Rear-end Conflicts	Crossing Conflicts	Lane-change Conflicts	Total Conflicts
-42	65.0	93	1	7	101
-27	65.0	80	0	5	85
-13	65.0	71	2	6	79
Optimized	65.0	74	2	4	80
+13	65.0	75	1	5	81
+27	65.0	72	5	3	80
+42	65.0	69	3	5	77

Table 24. Conflicts with side street split adjustments.

Split Condition (Percent)	Cycle Length	Rear-end Conflicts	Crossing Conflicts	Lane-change Conflicts	Total Conflicts
-42	65.0	32	6	5	43
-27	65.0	32	9	5	46
-13	65.0	32	11	3	46
Optimized	65.0	38	16	5	59
+13	65.0	42	15	9	66
+27	65.0	34	22	8	64
+42	65.0	30	20	10	60

As shown in table 23, reducing the time available to the main street increased the number of conflicts by approximately 25 percent (80 to 101). The inverse was also true—increasing the time available to the main street reduced the conflicts (80 to 77). However, the reduction was quite small, approximately 4 percent. This suggests that once the optimum green time has been allocated to a phase, there is little to gain by increasing the green time.

Table 24 shows the effect of split changes to the cross street. With this example, the opposite phenomenon was observed—conflicts increased when green time was increased. This may have been the result of the stochastic process employed with the simulation. One possible reason is that most of the conflicts involved vehicles on the main street, and changing the timing on the cross street would have little or no impact on rear-end and lane-change conflicts involving vehicles on the main street.

5.1.3 Effects of Changes in Cycle Length

The initial investigation of splits suggested that the cycle length has a significant impact on the number of conflicts and, thus, on intersection safety. This scenario was intended to directly address the effects of cycle length. In this scenario, five different demand conditions were evaluated. The demand conditions are expressed as the intersection V/C ratio ranging from a low of 0.3 to a maximum of 1.0. All factors remained identical to the base condition except the adjustments to the demand volumes to achieve the various V/C ratios. For each demand condition, the cycle length and splits were optimized. The results of these simulations are summarized in table 25.

Table 25. Conflicts under different cycle lengths.

Demand Condition (V/C)	Cycle Length	Rear-end Conflicts	Crossing Conflicts	Lane-change Conflicts	Total Conflicts
0.3	38.0	145	19	21	185
0.5	40.0	157	18	16	191
0.7	50.0	127	14	14	155
0.85 (base)	65.0	111	14	7	132
1.0	80.0	94	10	7	111

It is important to note that as the cycle length gets longer, the number of conflicts decreases. These data were subjected to the same ratio test that was used for the split analysis. The results are shown in table 26.

Table 26. Ratio of conflicts to changes per hour (various demand conditions).

Demand Condition (V/C)	Cycle Length	Changes Per Hour	Total Conflicts	Ratio of Conflicts to Changes Per Hour
0.3	38.0	94.74	185	2.0
0.5	40.0	90.00	191	2.1
0.7	50.0	72.00	155	2.2
0.85	65.0	55.39	132	2.4
1.0	80.0	45.00	111	2.5

In this scenario, the ratio range is 2.0–2.5 with an average of 2.2 for the five simulations. This ratio shows very good agreement with the previous scenario, which suggested that the cycle length itself may have the most significant impact on the number of conflicts.

5.1.4 Effects of Changes in the Detector Extension Times

A major signal timing parameter that influences when an actuated phase is terminated is the detector extension time. The optimum value for this parameter for the main street was found to be 5.0 s, according to the MDSHA criteria for signal settings for an arterial road with a speed of 45 mi/h and a detector setback of 330 ft.[16] For the cross street, the setting was 3.0 s at a setback of 90 ft. This parameter was then varied from -2.0 to +2.0 s to determine the impact on conflicts for six different simulations, as shown in table 27 and table 28.

Table 27. Conflicts under different main street detector extension times.

Main Street Extension	Rear-end Conflicts	Crossing Conflicts	Lane-change Conflicts	Total Conflicts
-2.0	117	12	8	137
-1.5	109	14	10	133
-1.0	103	13	10	126
Base	111	14	7	132
+1.0	99	14	11	124
+2.0	100	13	10	123

Unlike several of the previous simulations, which showed correlations between conflicts and the test variable, the relationship is much weaker in this analysis. It would appear that conflicts in general are not very sensitive to changes in the extension time. This is not unreasonable, as longer extension times will result in fewer phase changes and, therefore, longer cycle lengths. Previous analyses have indicated that there is an inverse relationship between conflicts and cycle length. It is surprising however, that the conflicts do not increase more rapidly when the extension period is too short. Changes of up to 1.5 s do not seem to have any effect on conflicts. Even a change as large as 2.0 s has only a minimal impact, increasing the number of conflicts only 4 percent. Similar results were found when the side street extension times were varied, as shown in table 28. These results indicate that extension times have a very minor impact on conflicts.

Table 28. Conflicts under different side street extension times.

Side Street Extension	Rear-end Conflicts	Crossing Conflicts	Lane-change Conflicts	Total Conflicts
-2.0	109	12	9	130
-1.5	109	13	9	131
-1.0	106	13	9	128
Base	111	14	7	132
+1.0	107	13	7	127
+2.0	108	13	7	128

5.1.5 Effects of Changing Left-Turn Phasing

Signal phasing is another characteristic of intersection operation that is likely to have an impact on conflicts. In this scenario, the operation of the intersection under five different demand conditions with three different left-turn phasing plans was considered: protected only (base condition), protected/permissive, and permissive only (no separate left-turn phase), all with exclusive left-turn lanes. The results of these simulations are shown in table 29. Each demand condition and each left-turn phase alternative was optimized for the best cycle length and splits.

Table 29. Total conflicts with protected/permissive phasing versus protected-only phasing.

Demand Condition (V/C)	Total Conflicts Protected Only	Total Conflicts Protected/Permissive	Total Conflicts Permissive Only
0.3	116	112	134
0.5	134	145	192
0.7	145	166	270
0.85	132	172	307
1.0	114	200	309

As shown in this table, the protected/permissive phasing results in a similar number of conflicts when the demand condition is below capacity. This is expected and may be explained by the fact that when the intersection is operating below capacity (below V/C = 0.85), the duration of the protected left-turn phase is adequate to service the majority of left-turn vehicles. Therefore, few vehicles make the left turn during the permissive period, and, thus, the exposure to rear-end and crossing conflicts is minimized. This is not the case, however, when the intersection is operating

at or above capacity. The results indicate that there is a significant difference between the two phase options (114 compared to 200 conflicts). This is not unexpected since the less restricted phasing plan (protected/permissive or permissive only) naturally experiences more potential for conflicts when motorists are faced with these options.

Another way to look at the data in table 29 is to examine the conflicts by type for both protected only and protected/permissive. These results are shown in table 30.

Table 30. Conflict by type for protected only and protected-permissive.

Demand Condition (V/C)	Rear-end Protected Only and Protected/ Permissive	Crossing Protected Only and Protected/ Permissive	Lane-change Protected Only and Protected/ Permissive	Total Protected Only and Protected/ Permissive
0.3	88/87	18/17	10/8	116/112
0.5	105/116	19/18	10/11	134/145
0.7	115/129	18/25	12/12	145/164
0.85 (base)	111/134	14/13	7/9	132/130
1.0	104/158	4/30	6/12	114/200

This table shows that rear-end conflicts account for much of the difference between the two phasing types when the V/C ratio is above 0.85 and that crossing conflicts account for a disproportionate share, particularly with a high V/C ratio. This could be a major safety concern because crossing crashes tend to be more serious than rear-end crashes.

5.1.6 Effects of Permissive Left-Turn Phasing

The previous scenario examined the effects of two types of left-turn phasing. It is also possible to operate the intersection without a separate left-turn phase. Left-turn traffic simply moves when the signal is green and there is a gap in the opposing traffic. The results of these simulations are shown in table 31.

Table 31. Conflicts with permissive left-turn phasing (unprotected left turn).

Demand Condition (V/C)	Rear-end Conflicts	Crossing Conflicts	Lane-change Conflicts	Total Conflicts
0.3	96	23	15	134
0.5	135	35	22	192
0.7	197	48	25	270
0.85 (base)	234	59	24	317
1.0	231	56	22	309

Table 32 presents a comparison of the results of the permissive left turn to the base condition results using protected-only left-turn phasing.

Table 32. Total conflicts with protected/permissive phasing versus protected-only phasing.

Demand Condition (V/C)	Conflicts Protected Only	Conflicts Protected/Permissive	Percent Change
0.3	116	134	332
0.5	134	192	262
0.7	145	270	181
0.85	132	317	140
1.0	114	309	73

These data show a similar pattern to that shown in the previous scenario, except the differences are even more pronounced. It would seem that permissive phasing generates far more conflicts than protected-only phasing. While protected-only was expected to generate fewer conflicts, the magnitude of the differences is greater than was expected, particularly for the low-volume demand condition.

5.1.7 Effects of the Change Intervals on Conflicts

One controller variable that was expected to have a significant impact on conflicts was the Y+AR change interval. Earlier studies by Pilko and Bared indicated that the method used to time the phase-change interval has a significant effect on the total number of conflicts and also concluded that the ITE-prescribed method to time the phase-change interval results in the smallest number of conflicts.[17] The studies conducted in this research were based on the ITE method for the phase-change interval. The simulation results, however, showed that Y+AR has little effect on the number of conflicts. These results are shown in table 33. A 2-s increase in the Y+AR resulted in a 7 percent decrease in the number of conflicts and a 2-s decrease in the Y+AR resulted in a 5 percent increase. Compared to other changes in signal timing parameters, these changes were minimal.

Table 33. Total conflicts with different Y+AR times.

Conflicts	+2 s	+1 s	5.5 s	-1 s	-2 s
Read end	102	107	111	107	117
Crossing	12	14	14	16	11
Lane changing	9	11	7	8	10
Total conflicts	123	132	132	131	138

5.2 ARTERIAL BASE CONDITION ANALYSIS

As with the individual intersection, the analysis of arterial data depends on having a standard against which various parameters can be compared. This situation was modeled as the base condition. It was intended to reflect the average conditions at a typical urban arterial with three intersections on a four-lane roadway with left-turn pockets at the intersections as shown in figure 16 and figure 17. The objective of testing this arterial scenario was to determine the effect of demand changes, offset, and left-turn phase sequence on the number of conflicts.
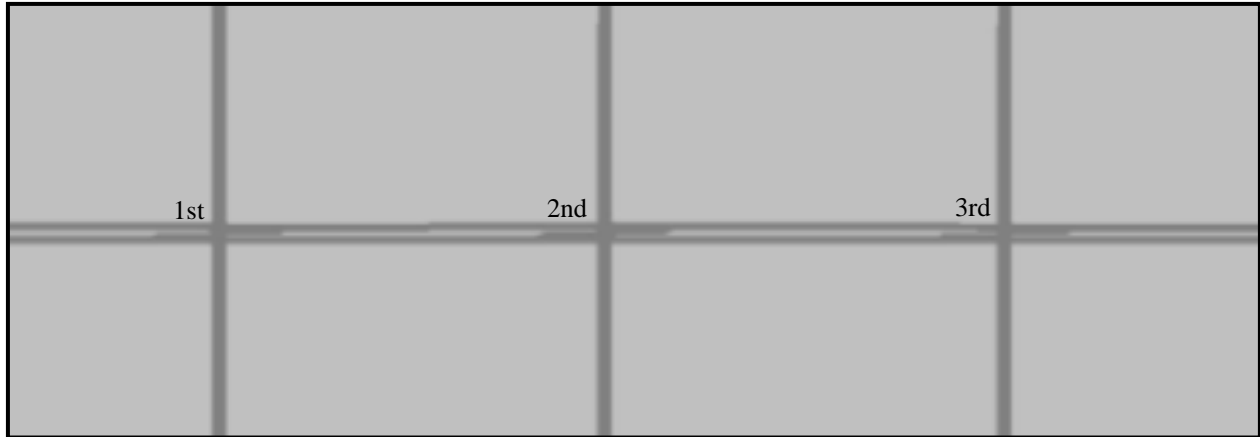
Figure 16. Illustration. Three-intersection arterial.
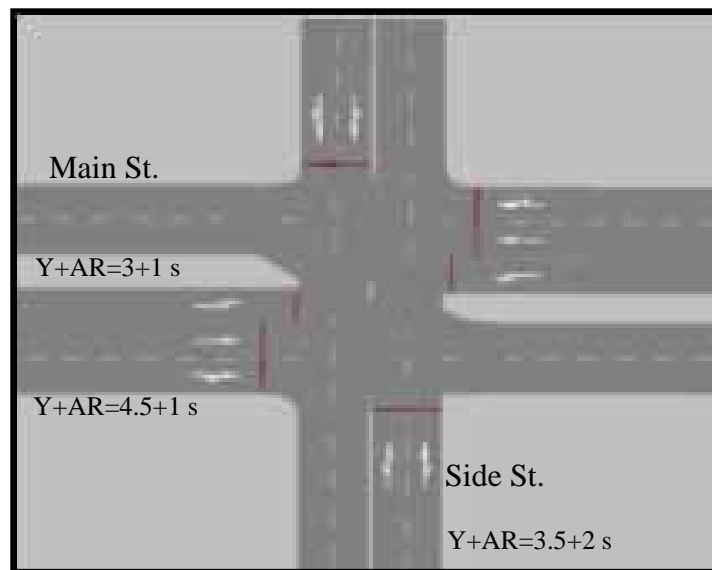
Figure 17. Illustration. Detail of intersection in three-intersection arterial.

The base condition reflected a relatively high demand typical of a peak hour with V/C = 0.85. A cycle length of 50 s was determined to be optimal, based on Synchro™. This combination of intersection geometry and demand was intended to reflect a normal peak-period situation. The study used changes in demand and signal timing parameters to assess the impacts on safety. The base condition is the standard against which the effects of these changes were measured.

Each of the three intersections had the same geometric configuration as the isolated intersection. The spacing between the first and second intersection was 1,320 ft, and the spacing between the second and third intersection was 1,500 ft. The demand volume was selected to achieve a V/C ratio of 0.85 for both the main and side street movements. The left-turn phasing was lead, protected only. Signal timing was optimized using Synchro™. The cycle length was 50 s. As with the single-intersection simulations, conflicts were generated using SSAM.

The base condition is the average of six, 1-h simulations. This condition resulted in a total of 430 conflicts with 342 rear-end conflicts, 38 crossing conflicts, and 50 lane-change conflicts.

5.2.1 Changes in Arterial Demand Expressed as V/C Ratios

The first investigation was to determine the effects of a change in the V/C ratio. The demand conditions for the 50-s cycle (V/C = 0.85) are shown in figure 18, and the demand conditions for the 105-s cycle (V/C = 1.00) are shown in figure 19. The cycle length was optimized in Synchro™. The levels of service under the 50-s and 105-s cycle lengths were C and D, respectively. Also, under these optimized conditions, the average intersection delay was 25 s per vehicle for the 50-s cycle and 50 s per vehicle for the 105-s cycle.
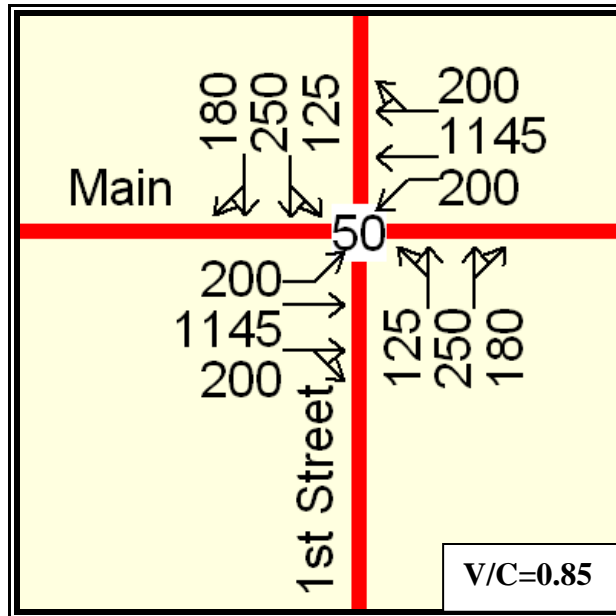
Figure 18. Illustration. Demand volumes for 50-s cycle (vehicles per hour).
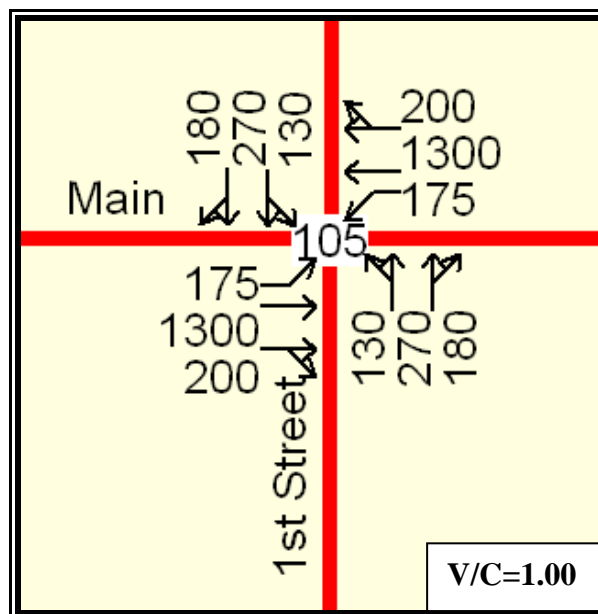
Figure 19. Illustration. Demand volumes for 105-s cycle (vehicles per hour).

The conflicts by type are shown in table 34. Two observations can be made from this table. First, there is a significant reduction in all types of conflicts when the cycle length is increased from 50 s to 105 s in spite of the fact that the demand volume increased. Second, the overall magnitude of the change in the number of conflicts (21 percent) is statistically significant.

Table 34. Arterial conflicts by type.

Demand Condition (V/C) (Cycle Length)	Rear-end Conflicts	Crossing Conflicts	Lane-change Conflicts	Total Conflicts
0.85 (50 s)	342	38	50	430
1.0 (105 s)	288	27	25	340

5.2.2 Effect of Changing Offsets on Conflicts

The next arterial investigation was the impact of changing an offset with a 50-s cycle and retaining the original lead-lead left-turn phase sequence. To do this, the offset at the second signal was adjusted in percentage of the optimum cycle length from -30 to +30 percent, in steps of 10 percent of the cycle length. The conflicts were calculated for each step. The results are shown in table 35.

Table 35. Conflicts under different offset conditions (50-s cycle length).

Offset Condition (Percent)	Rear-end Conflicts	Crossing Conflicts	Lane-change Conflicts	Total Conflicts	Percent Change
-30	343	34	52	429	0
-20	342	38	45	425	-1
-10	322	36	49	407	-5
Optimized	340	38	50	430	—
+10	346	34	50	430	0
+20	384	35	48	467	+9
+30	394	37	46	477	+11

— No change

These results were unexpected. It was anticipated that as the offsets were adjusted away from optimum, more vehicles would have to stop and the number of conflicts would increase accordingly. This happened when the offset was increased but not when the offset was decreased. Moreover, the magnitude of the change in conflicts was much less than what might be expected. This is illustrated in the Synchro™ diagrams shown in figure 20.
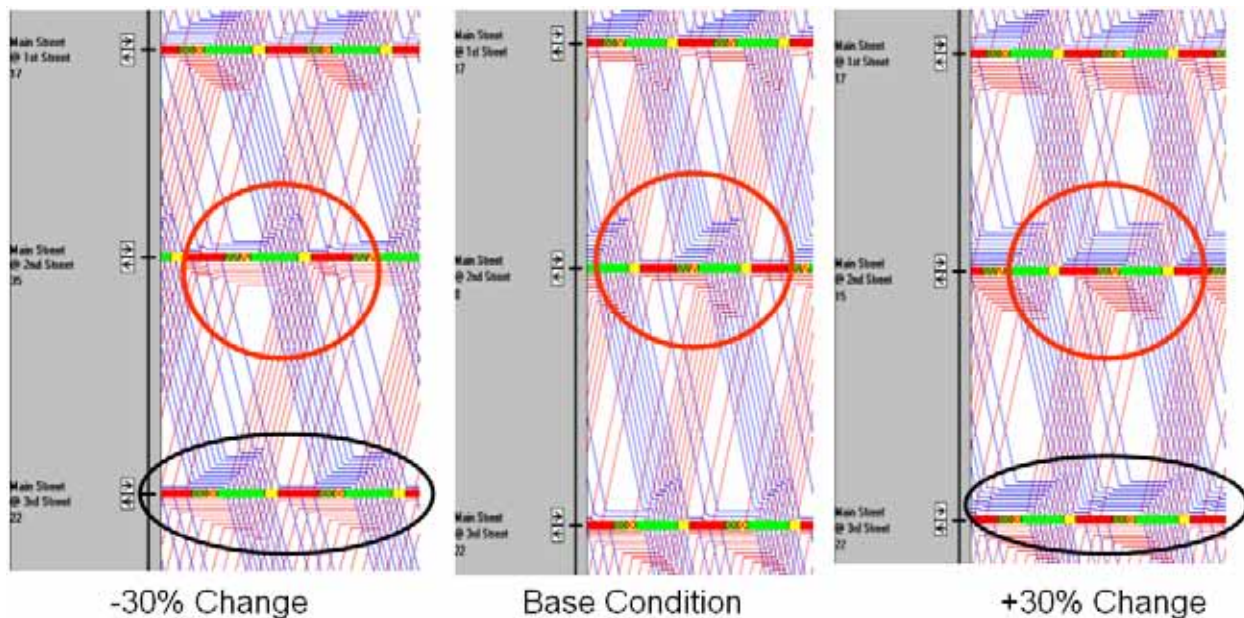
Figure 20. Screenshot. Synchro™'s representation of flows impacted by offset changes.

Notice that there are much greater delays shown in the red circle in the illustration on the right compared to the delays depicted in the illustration on the left due to the queues that are predicted to build up in both directions of travel at the middle intersection. It is not known whether this phenomenon is a result of the specific geometry of the test network or a general fact that positive changes in offset have a more detrimental impact on queues and delays than negative changes to offsets. This phenomenon is important to consider for this research. Since this indicates that the changes to offsets have differential effects on efficiency, it might be reasonable to consider that changes to offsets could have differential effects on safety depending on the direction of adjustment.

To investigate this further, the simulations were repeated using the demand of V/C = 1.0 and a cycle length of 105 s. The results are shown on table 36.

Table 36. Conflicts under different offset conditions (105-s cycle length).

Offset Condition (Percent)	Rear-end Conflicts	Crossing Conflicts	Lane-change Conflicts	Total Conflicts	Percent Change
-30	317	25	28	370	+9
-20	274	29	23	326	-4
-10	271	26	26	323	-5
Optimized	288	27	25	340	—
+10	282	25	26	333	-2
+20	320	26	24	370	+9
+30	319	28	25	372	+9

— No change

The first observation is that the number of rear-end conflicts with the optimum 105-s cycle is 288 while the number of conflicts with the 50-s cycle is 340, a 15 percent reduction by using a longer cycle length. The relative changes, with one exception, are similar in both instances, with the

largest negative changes occurring when the offset is increased by 20 and 30 percent. A tentative conclusion is that the offset has little effect on conflicts until the change is more than +10 or -20 percent.

5.2.3 Effect of Left-Turn Phase Sequence on Conflicts

One additional signal timing parameter, left-turn phase sequence, was expected to have an impact on the number of conflicts. The base condition assumes that there is a lead left-turn phase in each direction on the main street. This is referred to as lead-lead phasing. One alternative that can be used to improve the flow on the arterial is to allow a lead left turn in one direction coupled with a lag left turn in the opposing direction. In both cases, the left-turn phase is protected only. This phasing strategy is only effective when the spacing between the intersections is uneven. In the test scenario, the difference between 1,320 and 1,500 ft is enough of a difference to impact the traffic flow.

As with the other test scenarios, the data were collected for both the 50-s cycle and the 105-s cycle. The results for the 50-s cycle (V/C = 0.85) with optimized offsets are shown in table 37.

Table 37. Arterial conflicts with lead-lag left-turn phasing (50-s cycle, V/C = 0.85)

Demand Condition (V/C)	Rear-end Conflicts	Crossing Conflicts	Lane-change Conflicts	Total Conflicts
0.3	68	3	6	77
0.5	164	11	17	192
0.7	327	25	40	392
0.85	413	33	58	504
1.0	440	37	77	554

This analysis suggests that the conflicts are proportional to demand as long as the through traffic has a progression window, which it had in this scenario by virtue of the lead-lag phasing. However, when compared to the lead-lead alternative, there is an increase in conflicts. The lead-lead (V/C = 0.85) experienced only 430 conflicts compared to 504 with the lead-lag phasing—a 17 percent increase. A similar analysis was conducted for the 105-s cycle (V/C = 1.0), and the results are shown in table 38.

Table 38. Arterial conflicts with lead-lag left-turn phasing (105-s cycle, V/C=1.0).

Demand Condition (V/C)	Rear-end Conflicts	Crossing Conflicts	Lane-change Conflicts	Total Conflicts
0.3	69	1	4	74
0.5	132	2	9	143
0.7	195	14	15	224
0.85	222	25	22	269
1.0	307	27	34	368

The results for the 105-s cycle are similar to the results of the 50-s cycle. There were 340 conflicts with lead-lead phasing. This was only 8 percent fewer than found with lead-lag

phasing. As with all of the previous comparisons, the longer cycle length resulted in fewer conflicts—34 percent fewer in this case.

5.3 STATISTICAL TESTING AND CONFIDENCE IN THE RESULTS

5.3.1 Sample Size and Statistical Results from Multiple Simulations

Each test scenario for measuring the effect of signal timing on conflicts was simulated with multiple iterations, each using different random number seeds, and statistical distributions of the results were collected and analyzed. See figure 21 for a typical summary of results. Initially, a sample size of six simulation runs was selected. The frequency of each type of conflict was averaged and included a standard deviation and coefficient of variances. Subsequently, a sample size of 20 simulation runs was performed, and the results were averaged and compared to the average and statistical distribution for the set of 6 simulation runs. An *F*-test was performed (using 95 percent level of confidence and 10 percent standard error of the mean) to compare the statistical differences of the means. The results indicated no differences. Therefore, because of time and budget constraints, a sample size of six 1-hr simulations was selected for each test scenario in this project.

Scenario 06, VC = 0.30, P/P Left Turn														
				SSAM										
								Conflict Type & Frequency						
Summary Group	Total Conflicts	Total # of Conflicts in Seeding Period	Minus 900sec (Seeding Period)	Unclass-ified	Crossing	# of conflicts in seeding period	Minus 900sec (Seeding Period)	Rear End	# of conflicts in seeding period	Minus 900sec (Seeding Period)	Lane Change	# of conflicts in seeding period	Minus 900sec (Seeding Period)
Filtered-AllFiles	813	149	664	0	119	19	100	634	117	517	60	13	47
Run 1 Filtered R:\2008\76 FHWA_SBIR	144	25	119	0	20	3	17	113	19	94	11	2	9
Run 2 Filtered R:\2008\76 FHWA_SBIR	134	25	109	0	16	3	13	109	19	90	9	2	7
Run 3 Filtered R:\2008\76 FHWA_SBIR	138	25	113	0	22	3	19	104	19	85	12	2	10
Run 4 Filtered R:\2008\76 FHWA_SBIR	121	25	96	0	23	3	20	87	19	68	11	2	9
Run 5 Filtered R:\2008\76 FHWA_SBIR	135	25	110	0	19	3	16	109	19	90	7	2	5
Run 6 Filtered R:\2008\76 FHWA_SBIR	141	25	116	0	19	3	16	112	19	93	10	2	8
Average of 6 runs	136		112				17			87			8
Standard Deviation	8.0		8.0										
Coefficient of Variation	5.9%		7.2%										

Figure 21. Screenshot. Typical summary of statistical distribution data.

5.3.2 Comparison of Base Condition Scenarios and Various Changes in Signal Timing Settings

Variations from the base scenario, such as a change in demand or a change in splits, were compared statistically to identify the significance of the difference from the base condition. The *t*-test was used to compare each surrogate measure of safety and the frequency of conflicts for various changes. The *t*-test calculated the probability of the difference of the two means. In this test, the null hypothesis (H0) indicated that the difference between the means of two samples is zero. Based on the difference level of the two sample variances, *t*-ratios and degree of freedom were calculated in different ways. Whether or not the sample variances were significantly different was verified by using the *F*-test before the *t*-test. When the average number of events in a conflict category and/or total conflicts was less than 0.5 (meaning that out of the 10 replications, an event occurs approximately every other simulation run), the data were marked as N/A, and no test outcome was recorded. An example of the *t*-test results is shown in figure 22.

60

Test of Significance: Effect of change in left turn seq lead-lag optimization (LeadLag Opt 0.85 Vs LeadLag Opt VC 1.00)

SSAM Measures	Mean(Scenario 002_C 105s_LeadLag Opt_VC 1.00)	Variance (Scenario 002_C 105s_LeadLag Opt_VC 1.00)	Replications (Scenario 002_C 105s_LeadLag Opt_VC 1.00)	Mean(Scenario 002_C 105s_LeadLag Opt_VC 0.85)	Variance (Scenario 002_C 105s_LeadLag Opt_VC 0.85)	Replications (Scenario 002_C 105s_LeadLag Opt_VC 0.85)	t value	t critical	Sigfinicant	Mean Difference
TTC	1.11	0.328	2671	1.14	0.305	1955	-1.57	1.66	NO	-0.026
PET	2.38	2.043	2671	2.42	1.942	1955	-0.909	1.66	NO	-0.038
MaxS	7.00	7.725	2671	7.05	7.137	1955	-0.673	1.66	NO	-0.054
DeltaS	4.53	10.135	2671	4.91	10.275	1955	-3.974	1.66	YES	-0.378
DR	-1.68	3.575	2671	-1.94	3.34	1955	4.641	1.66	YES	0.256
MaxD	-2.38	5.427	2671	-2.65	4.938	1955	4.099	1.66	YES	0.277
MaxDeltaV	2.38	2.862	2671	2.57	2.989	1955	-3.844	1.66	YES	-0.196

Conflict Types	Mean(Scenario 002_C 105s_LeadLag Opt_VC 1.00)	Variance (Scenario 002_C 105s_LeadLag Opt_VC 1.00)	Replications (Scenario 002_C 105s_LeadLag Opt_VC 1.00)	Mean(Scenario 002_C 105s_LeadLag Opt_VC 0.85)	Variance (Scenario 002_C 105s_LeadLag Opt_VC 0.85)	Replications (Scenario 002_C 105s_LeadLag Opt_VC 0.85)	t value	t critical	Sigfinicant	Mean Difference
Crossing	32.50	61.1	6	28.67	79.867	6	0.791	1.812	NO	3.833
Rear-end	374.17	331.367	6	270.33	153.07	6	11.556	1.812	YES	103.833
Lane changing	38.50	13.5	6	26.83	17.367	6	5.144	1.812	YES	11.667
Total	445.17	343.767	6	325.83	356.57	6	11.045	1.812	YES	119.333

Figure 22. Screenshot. An excerpt of *t*-test statistical output from SSAM.

5.4 SUMMARY OF SIMULATION STUDIES

The sequence of simulations was intended to identify which signal timing parameters had the most impact on conflicts. To do this, every attempt was made to isolate the impact of each parameter in subsequent tests. Several parameters were identified as having a strong association with conflicts, and several had less convincing associations. One parameter, cycle length, was identified as having a dominant association with conflicts. These results are summarized in table 39**.**

Table 39. Parameter-conflict association.

Signal Parameter	Weak	Moderate	Strong	Dominant
Cycle length				Yes
Split		Yes		
Offset		Yes		
Detector extension	Yes			
Change interval (Y+AR)		Yes		
Left-turn treatment			Yes	
Left-turn sequence			Yes	
V/C ratio		Yes		

Blank cells indicate no association.

Several conclusions may be reached with high confidence based on these simulations. The findings are as follows:

· Cycle length is the dominant factor affecting the number of conflicts.

· Offsets and splits have a direct effect on safety.

- Left-turn phase protection and phase sequence have a significant effect on safety.

- All of these factors interact with one another.

This effort, so far, has only examined the single effect of individual signal timing parameters on conflicts and safety. The combined effect of aggregating multiple parameters with multiple intersection lane configurations was not tested. The next step of this research project must focus on these interactions to examine how these parameters affect each other and how combined changes can reduce the number of conflicts at signalized intersections without adversely affecting operational efficiency. Addressing these issues will require a carefully designed experiment and will provide the foundation for the algorithm development that will enable a real-time adaptive control algorithm to balance safety and efficiency.

The next section of this report describes the experimental design approach for combining the effects of signal timing parameters and specifies the algorithms for combining safety and efficiency measures in a real-time adaptive control system.

6.0 PHASE 2 RESEARCH AND DEVELOPMENT

6.1 OBJECTIVES FOR PHASE 2 RESEARCH

The objective of the second phase of this research is to develop a methodology to balance efficiency of traffic flow and traffic safety in the operation of adaptive traffic signal systems on arterials and grids. In phase 1, the relationships between traffic signal timing parameters and safety performance were explored. Fifteen test cases were constructed to identify isolated correlation effects between changes to one signal timing parameter and a relative change in safety performance. Safety performance in phase 1 was estimated using the FHWA SSAM tool and the VISSIM® traffic microsimulation model. Analysis results in phase 1 indicated that there are measurable and statistically significant differences in the generation of conflict events when modifying several of the signal timing parameters in the test cases. At the same time, changes to the signal timing parameters have appreciable and measurable effects on efficiency of traffic flow as reflected in performance measures such as stops and delay.

The next step in the research is to develop a methodology and algorithms for balancing improvements in efficiency and safety that can be used to adjust signal controller timing parameters in a real-time adaptive manner. This section outlines the plan for the methodology and algorithm development in phase 2 of the research project.

The first step of the methodology is to develop a multiattribute safety performance function. The safety performance function is used to predict and evaluate the relative changes to safety performance when modifying any or all of the traffic signal controller parameters that are considered as inputs. This function would then be used in conjunction with a performance function for traffic efficiency to balance the effects of safety and efficiency when making changes to the signal timing parameters. The first part of this section details the process for developing the multiattribute safety performance function. Subsequent parts describe how the safety performance function and traffic efficiency function can be combined to balance efficiency and safety in a real-time adaptive manner.

6.1.1 Extending the Conflict Analysis Approach to the Next Phase of Research

In this project, a methodology is being developed to balance safety with efficiency in changing signal timing parameters. Whether these parameters are adjusted in real time or infrequently, the first task is to establish the relationships between the signal timing parameters and the change in safety performance. Similarly, a separate performance function for the change in the efficiency (stops and delay) based on the change to the signal timing parameters must be established. In either online or offline signal timing optimization, a traffic performance model is used to predict the performance of various signal settings. A performance model indicates that the efficiency of a given set of input parameters is X', where the current performance of the unchanged parameters is X. If X' is better than X, this direction of change is considered positive and further exploration of changes in that direction are considered. A search method is used to explore all possible, or all reasonable, signal settings until no significant performance improvement can be obtained by further tweaking the parameter values. Different search methods must be selected based on the format of the performance functions. For example, if the functions are all linear equations, very

fast and efficient algorithms are readily available. Nonlinear equations require more sophisticated mathematical techniques. Simulations require iterative approaches that are typically time consuming.

In any case, the next step is to identify the format of the safety performance function to be used in phase 2 of this research. The preliminary analysis done with SSAM has established that certain parameters have positive correlations with changes in safety, but this analysis cannot be used directly to determine the magnitude of effects. In addition, each parameter has been evaluated in isolation. In a real-world, real-time setting, changes to these parameters must be evaluated simultaneously and in an integrated fashion. There are primarily two ways to accomplish the incorporation of a safety performance function in the selection of signal timing parameters:

- Establish a regression equation (nonlinear, linear, neural network, etc.) that relates the change in the conflict rate with the change in the signal timing parameter.

- Configure a simulation model with the newly proposed settings and run both changed and unchanged cases. Use SSAM to compute the change in the conflict rates and compare the before and after performance.

Either option presents a multiobjective optimization problem in which the goal is to identify signal timing settings that either are beneficial for both efficiency and safety or provide a trade-off between improving one or the other according to some preference determination.

6.1.2 Choice of a Safety Performance Function

As identified above, there are two primary choices for establishing a performance function engine for the multiobjective optimization problem. Simulation in-the-loop optimization analysis, using SSAM and a microscopic simulation tool such as VISSIM® in the loop with the optimization search methodology, is a high-fidelity approach. In this approach, SSAM would be used as an exact performance assessment tool that can be used to directly evaluate the changes to conflict rates when modifying one or more traffic signal timing parameters. This approach is very time consuming and has little chance of transferring to online, real-time operation due to the following obstacles:

- Automating the process of configuring the simulation model with the new parameters to be tested, running the model, running SSAM, and collecting the measures includes multiple software packages, proprietary simulation platforms, and expensive software interfaces.

- Processing time required for real-time decision making is non-trivial. Even 5–10 min epochs would be challenging based on the processing times of SSAM by itself as experienced in the SSAM validation project and the first phase of this Small Business Innovation Research.

- Multiple runs are required to obtain statistical significance of the resulting data due to randomness of vehicle flows, driver decision making, and the like. Coupled with processing-time obstacles, the need for multiple runs would make this approach particularly challenging.

The second, and preferred, methodology to establish a safety performance function is to develop a regression-equation relationship between signal timing parameters and safety performance. Such an approach is executable for both offline and online operation. This approach is similar to traditional crash prediction, except that the prediction domain is sufficiently higher fidelity than predicting the crashes that might occur over the next year. Using a regression-equation approach, the safety performance function would evaluate how the conflict occurrence rates would be perturbed over, for example, the next 15 min at the same input traffic demands. In this approach, the following function is established:[18,19]

$$\text{Safety performance index} = f(\text{signal parameters, traffic characteristics}) \qquad (4)$$

The *safety performance index* might be defined as the total number of conflicts at the intersection or as some combination of the different types of conflicts. This functional relationship is likely to require nonlinear terms and interactions between the inputs rather than simply a linear combination of the various input parameters. For example, one will likely need to compute a derived measure of traffic demand or degree of saturation for each phase, rather than directly input the traffic volumes. Before further discussing the methodology for developing the safety performance function, the type of adaptive operation to be developed in phase 2 must be identified.

6.1.3 Candidate Adaptive Control Signal Timing Optimization Strategies

The following are the three primary strategies employed by all adaptive control systems currently in use across the world:

- **Second-by-second optimization**: Control the duration of each timing phase exactly by making adjustments on frequent time scales such as every second up to once per cycle. This approach might replace the traffic signal controller completely or augment the traditional controller with externally applied commands (i.e. hold, force-off, and omit). This approach requires a detailed traffic model that is constantly updated based on detection of each arriving vehicle and information passing between intersections or from all intersections to a central processing unit. This approach describes the method employed by RHODES, OPAC, SCOOT, and System for Priority and Optimization of Traffic.

- **Parameter tuning:** Identify changes to signal timing parameters that improve operations in a locally optimal manner by making small changes to existing settings and allowing the field controller to operate according to its internal rules with the new parameters. This approach downloads new signal settings to the controller on a frequent basis, for example, every 5–15 min. This approach describes the method employed by SCATS®, ACS Lite, MOTION, and Traffic-responsive Urban Control.

- **Pattern matching:** Match patterns of traffic demands and performance measures to signatures or use-threshold settings to switch timing parameters from one set to another prestored on the traffic controller. The traffic controller then operates according to its set of internal rules with the new parameters. This approach commands new timing plan changes to the field controller every 15–30 min. This approach describes the traffic-responsive and/or congestion management operation employed by all modern Advanced Traffic Management Systems (ATMS) central systems such as Kimley-Horn Integrated

Transportation System®, Integrated Interagency Traffic Management System, Advanced Control of Traffic Related Arterials, and ATMS.now.

For this project, only the second two methods are considered viable. The authors believe that real-time, second-by-second control of signal timing for evaluation of safety would only be possible with IntelliDrive[SM] technologies or simple if/then type approaches such as those employed by Zimmerman and Bonneson's DCS system to extend red or yellow clearances due to imminent crash situations.[1] Based on past experience with both RHODES and ACS Lite, it is presumed that real-time safety analysis could not be reliable enough or processed quickly enough to be integrated with a traffic efficiency calculation methodology such as that employed by RHODES or OPAC.

Pattern matching is an approach that has been used in traffic control systems since the development of the minicomputer and the urban traffic control system over 35 years ago. This approach requires a sophisticated user to develop signatures and rules and requires extensive setup and testing. Most traffic responsive modules of ATMS systems are not used to their full potential due to the difficulty in determining what the signatures or thresholds should be, the lack of reliable input data (i.e., volumes) to drive the decision-making algorithms, and the effects of frequent signal controller transition (i.e., offset and cycle seeking) on traffic performance.

A parameter-tuning approach is much more reasonable than either of these two alternatives based on the experience of the researchers in the FHWA ACS Lite development project.[20] Parameter tuning allows the local signal controller to continue to operate the intersection on a second-by-second basis while the external processor handles the more complex decision making to make small adjustments to the signal timing parameters to improve safety, efficiency, or both. A parameter-tuning approach avoids many pitfalls of traffic-responsive methods since it embeds much of the "intelligence" in the algorithms and thus requires less user setup. In addition, drastic transitions from one cycle/offset combination to another are avoided by limiting the parameter changes to only small adjustments from the current settings. Since a parameter-tuning approach only runs its optimization algorithms at minimum once every three or four cycles, the additional processing burden to evaluate safety performance and perform the trade-off analysis to balance efficiency and safety can probably be accommodated in the processing time available.

The general methodology for the adaptive control algorithm that balances safety and efficiency will be as follows:

1. Collect detector data and phase-timing data at regular intervals.

2. Process the detector and phase-timing data into performance measures for efficiency and safety.

3. Evaluate alternative settings for traffic signal timing parameters for improving performance of efficiency, safety, or both.

4. Download new parameter settings to the signal controller.

5. Repeat steps 1–4.

6.1.4 Candidate Signal Timing Parameters that Affect Efficiency and Safety

Phase 2 will develop a traffic-adaptive strategy that tunes the following parameters to improve safety, efficiency, or both:

· Cycle time.

· Splits.

· Offsets.

· Left-turn phase treatment (permissive, protected, or combination).

· Left-turn phase sequence (combination of lead and lag).

These parameters will be tuned every 5–15 min based on phase-timing data and detector data obtained from the signal controller. Similarly, these parameters are frequently tuned in an offline manner in tools such as TRANSYT and Synchro™. In addition to these tuned parameters, the adaptive control system will evaluate delaying or accelerating the change from one time-of-day (TOD) pattern to the next based on the perceived benefits to safety and efficiency.

Experience operating traffic signal control systems and designing signal timing plans for grid and arterial systems has shown that these parameters all have an appreciable effect on efficiency. Performance measures and algorithms for tuning these parameters have been developed in the past, for example, in the FHWA ACS Lite project.[20] These measures will be presented in a later section, where the algorithm is described in more detail.

The initial analysis using the SSAM tool in this research project also indicated that these parameters have an effect on the safety of an intersection, as represented by appreciable and statistically significant changes to the total conflicts that occur when the parameters were changed. Each of these effects on safety was tested and evaluated separately, so the next step will be to test and evaluate their effects in combinations. This is a necessary step in the development of the safety performance regression functions that will be used to predict the effects of changes to the parameters in the adaptive control algorithm.

6.2. EXPERIMENTAL DESIGN

6.2.1 Design of Experiments for Identifying Safety Regression Parameters

As identified previously in this research, the aforementioned input parameters (cycle time, phase sequence, etc.) were found to have individual effects on the safety performance of the signal system in the limited tests that were conducted. These data are not sufficient to identify a generalized prediction of the effect of changing these parameters, evaluated individually or in combinations. For example, one test showed that conflicts increased 25 percent when the cycle time was changed from 70 to 100 s. This result says little about the change in conflicts when the cycle time is changed from 100 to 130 s and at different traffic volumes. In the limited testing that was performed, nonlinear effects were observed in almost all of the parameters evaluated.

So, the rate of change or gradient of conflict is not constant, and thus, a functional relationship must be calibrated.

In statistical regression modeling, this combinatorial problem can be addressed by using a *designed experiment*. A designed experiment attempts to maximize the information gained on each run of the experiment by combining the input factors in special ways so that both the boundaries and the center of the design space are covered by evaluation runs and by performing a minimum number of runs without having to evaluate all possible combinations of the inputs. In the present problem, consider the following representative options for each input parameter for a typical eight-phase dual quad intersection with left-turn phases in all directions:

- Cycle time: long, medium, and short cycle (three options).

- Offset values: zero offset, +25, +50, and +75 percent (four options).

- Split values: V/C low, V/C medium, V/C oversaturated (3 options ´ 8 phases = 6,561 combinations).

- Phase sequence: lead-lead-lead-lead, lead-lag-lead-lead, etc. (16 options).

- Protected/permitted: protected, protected/permitted, permitted (3 options ´ 4 left-turn phases = 81 combinations).

This yields 3 ´ 4 ´ 6,561 ´ 16 ´ 81 = 102,036,672 combinations without including variations in the approach demand volumes. Clearly, this many simulation scenarios do not need to be evaluated to obtain enough information to fit the regression models to the data. Symmetry in the input-parameter structure can be used to reduce the replicates immensely, particularly in the evaluation of the combinations of the split settings. For example, the difference between phase 1 and phase 5 having a certain level of saturation (all other inputs being equal) is the geometric location of the phase at the intersection. To an evaluation algorithm, the situational data appear identical, and—all things such as turning-bay lengths being equal—one would expect the recommended changes to the parameters out of an optimization algorithm to look the same as well.

6.2.2 Design of Experiments to Reduce the Number of Runs

There are many approaches to design of experiments that could be applied. The most common approach for linear regression models is a 2^k fractional factorial design. There are several variations of this approach, but in general, a fractional factorial design is used when single factors are hypothesized to have linear relationships with the output measure. There may be interactive effects between input variables, but no quadratic or other nonlinear terms are assumed to be included for an individual input in the underlying model form. This is not likely the case in the present situation, but more detail on the fractional factorial process is provided for the purpose of explanation.

A fractional factorial designed experiment uses one of two levels of each input variable in each replicate run. Then, a smaller number than the total full factorial matrix of combinations is actually run, such as 2^{k-3} or 2^{k-5}. This smaller number of replicates is based on assumptions about the lack of significance of higher-order combinatorial effects in the resultant model.

A typical model format for 2^{k-n} fractional designs is:

$$Y = A1*x1 + A2*x2 + ... + An*xn + A12*x1*x2 + A13*x1*x3\ b+ \dots\dots + An,n-1*xn*xn-1 \quad (5)$$

In this model, all effects of the input parameters are either linear or cross-product terms of two of the inputs. The current design problem does not exactly match this format since engineering judgment indicates a need for more than two settings for each input parameter to fit an appropriate model.

The runs are then expressed as a matrix of +1 and -1 indicator variables where +1 indicates the high value of a variable and -1 indicates the low value of a variable. For example, in this problem, a high value of a cycle time might be 150 s and a low value would be 60 s. Since the relationships between inputs and outputs are individually assumed to be linear functions in this type of model, it is not necessary to obtain data at 120 s, 90 s, etc. since these outputs can be estimated from the regression equation. The pattern of combinations used in this approach is shown in table 40.

Table 40. Fractional factorial design approach using linear regression models.

Run Number	Cycle	Offset	Split	Phase Sequence	Protected/ Permitted
1	+1	+1	+1	+1	+1
2	-1	+1	+1	+1	+1
3	-1	-1	+1	+1	+1
4	-1	-1	-1	+1	+1
5	-1	-1	-1	+1	+1
6	-1	-1	-1	-1	+1
7	-1	-1	-1	-1	-1
8	+1	-1	-1	-1	-1
9	+1	+1	-1	-1	-1
n					

Clever determination of the combination of +1 and -1 factors of all of the input variables allows maximum information to be gained from just a few iterations of the design space if higher-order interaction terms can be assumed to have negligible impact on the performance of the regression relationship. The use of dummy variables +1 and -1 avoids difficulties with the matrix inverse computations (necessary to solve for the regression coefficients) that arise when input variables have vastly different scales. However, that is not the case in this particular application since all of the potential input parameters are in seconds or can be encoded as integer values. For example, the variable for protected/permitted left turn could be coded as 3 for permitted only, 2 for protected/permitted, and 1 for protected only. To obtain meaningful regression coefficients, it is important to choose the coded values appropriately based on what one would expect to happen to the output variable when the coded value is changed. In this example, the highest value of the code being associated with permitted-only left turns would match earlier results that indicated that conflicts are more plentiful in this situation than in the other two situations.

This is the basic concept of design of experiments: identify the meaningful input variables and potential interaction effects, and identify a matrix of combinations that provides enough data to solve for a set of regression coefficients. Goodness of fit is then typically tested by comparing the model against real results (in this case, the number of conflicts per hour) for a few situations that were not used in developing the model parameters. Engineering judgment indicates that the relationship between the input parameters and the conflict (safety index) output is nonlinear. Although other forms can be chosen, a typical nonlinear regression equation is expressed as:

$$Y = a1*x1 + a2*x2 + ... + an*xn + a11*x1**2 + a12*x2**2 + ... + a1n*xn**2 + b \quad (6)$$

In the design of experiments literature, a more appropriate design for a nonlinear regression model is called the *central composite design* (CCD). This type of design allows the assessment of the curvature of the nonlinear terms by using five potential settings for the input parameters (+sqrt(2), +1, 0, -1, -sqrt(2)). A slightly larger number of runs results from use of CCD instead of fractional factorial design, but the combination of variable settings follows similar patterns, as can be seen in table 41.

Table 41. CCD approach using nonlinear regression models.

Run Number	Cycle	Offset	Split	Phase Sequence	Protected/ Permitted
1	+1	+1	+1	+1	+1
2	-1	-1	+1	+1	+1
3	-1	-1	-1	-1	+1
4	0	0	0	0	0
5	+1.414	+1.414	0	0	0
6	+1.414	+1.414	+1.414	+1.414	0
7	0	0	0	+1.414	+1.414
8	0	0	0	0	+1.414
9	-1.414	-1.414	0	0	0
n					

These values are chosen to maximize the statistical properties of the design of experiments process for quadratic equation. In the actual application, a similar process will be used to choose the run combinations and settings based on the single-variable relationships. After the experimental runs are determined, three VISSIM®/SSAM runs will be performed at each combination of settings, and the average total conflicts and the average of each type of conflict will be obtained. Based on the number of combinations that must be performed, no more than three iterations are sustainable within budgetary and schedule constraints. It is also likely that a single run at each combination could suffice.

The regression coefficients can then be obtained from a statistical analysis package such as SPSS®, SAS®, or Microsoft Excel®. Another smaller set of input combinations is then typically used to test the goodness-of-fit of the resulting model by comparing the actual output from the simulation model with the prediction from the regression equation. These input combinations are not typically used in the development of the regression model.

This functional—total conflicts or a cost-impact weighted combination of the conflict types—would then be used as the safety performance function in the search process that trades off or finds the balance between efficiency and safety for each of the control parameters (cycle time, splits, offsets, phase sequence, and protected/permitted left-turn settings) in determining the new signal settings at each iteration.

6.2.3 Multiobjective Optimization Approach

The parameter-tuning approach for adaptive control is a middle ground between fully adaptive, second-by-second control of traffic signals and rule-based traffic-responsive systems. Fully adaptive real-time control systems require sophisticated simulation modeling to evaluate the effects of changes to the parameters on the performance criteria. For example, in RHODES, queues in each lane at each approach are modeled and traffic is tracked from upstream locations on a second-by-second basis. A dynamic programming algorithm is used to evaluate the resultant traffic delay based on assessment of several options for what the signal timing settings might be in the next 60 s or so. The signal timings that result in minimum delay are selected for implementation. A few seconds later, the entire process is repeated in a rolling-horizon fashion.

RHODES is very sensitive to accurate determination of the queues and requires a multitude of parameters for queue discharge speeds and the like that must be calibrated to field conditions. Past experience leads to the belief that another RHODES- or OPAC-like algorithm is inappropriate for development until data from IntelliDrive^{SM} systems are readily available. On the other hand, a traffic-responsive system can have relatively simple if/then rules that identify when to switch from one traffic-control strategy to another. In predictable situations, this type of operation can be very effective, such as when a certain demand level is tripled or quadrupled very quickly (for example, when a special event is concluded). In generalized situations, however, traffic-responsive systems become onerous to configure, requiring the consideration of every possible situation and the embedding of that information into the system of if/then rules or detector data signatures that are used to match the field conditions with the desired control strategy.

The parameter-turning approach strikes a middle ground by allowing more robust solution of the signal timing settings than traffic-responsive operation but with more predictable behaviors than real-time systems because it starts from a given set of TOD pattern parameters and only tweaks those settings incrementally over time. These tweaks adjust the signal timing operations to react to the statistical fluctuations of traffic flows, correct any errors that have been made in determining the initial settings, and react to special events, incidents, and short-term changes to traffic flow patterns. By operating within a given set of boundaries, such as not changing the signal timings too dramatically from their initial values, the parameter-tuning approach is safer and more reliable than real-time approaches that override the signal controller. In addition, since a parameter-tuning system is not predicated on running a detailed traffic model to evaluate performance, it has fewer challenges with calibration and is less reliant on perfect detection accuracy. As was done with ACS Lite, this project will develop algorithms that select new signal timing settings from simple models of changes to traffic efficiency and the regression-model approach for estimating the changes to safety. For this situation, there is not likely to be a single solution that simultaneously optimizes both objectives. In this case, the goal is a solution in which each objective has been optimized to the extent that if optimized any further, the other objective will suffer as a result. Finding such a solution and quantifying how much better it is

compared to other such solutions—and there will generally be many other feasible options—is the goal when setting up and solving a multiobjective optimization problem.

6.3 FIVE PRINCIPLE ALGORITHMS OF THE ADAPTIVE CONTROL APPROACH TO BALANCE SAFETY AND EFFICIENCY

This section discusses the five principle algorithms included in the proposed adaptive system operation.

6.3.1 Cycle Tuning

Cycle time is most often selected on a section- or arterial-wide basis to facilitate progression and to provide adequate capacity to operate all of the signals in the subsystem under capacity. Most often, cycle times in adaptive control systems are chosen according to a heuristic rule, or in the case of real-time, second-by-second systems, the concept of cycle time is transient—the cycle length can change in each iteration as the system operates more like "free" intersections than in coordination. For example, SCATS® uses a heuristic that might be termed the "90 percent rule." The SCATS® cycle for a section is ratcheted up or down based on keeping the most saturated intersection in the section at a 90 percent degree of saturation. This is a reasonable strategy to follow and guarantees that the cycle selected will not artificially cause congestion in certain approaches. In a simplistic fashion, if the cycle time is increased by X seconds, then every phase on the controller gets a proportion of the additional time. For example, if 4 s are added to the cycle time and there are four phases per ring, one additional second is provided for each phase split. A simple approach for tuning cycle times is depicted in figure 23.

This strategy will tend towards longer cycles during peak periods as traffic demand builds, which is appropriate despite recent research indicating that when the conditions are extremely oversaturated, shorter cycles will provide more efficient throughput. At this point in this research project, the case of extreme oversaturation is ignored and the multiobjective adaptive system is designed for normal operating modes. The research team can return to the consideration of oversaturated conditions after the baseline system is developed and proven effective.
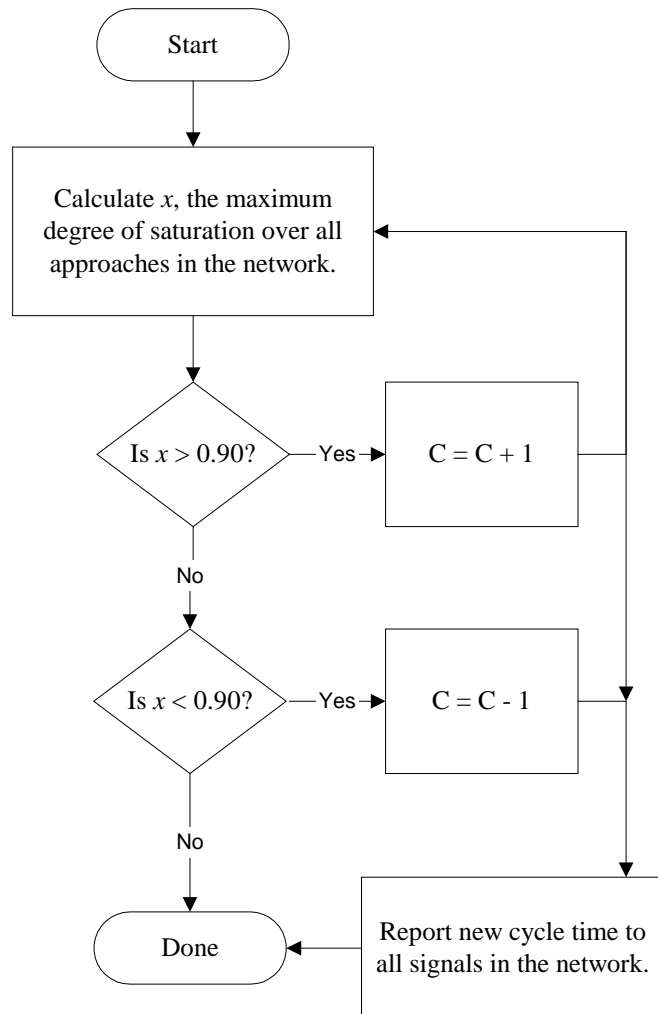
Figure 23. Chart. Generic cycle time tuning algorithm to keep all intersections below 90 percent degree of saturation.

This approach is too simplistic, however, for the following reasons: (1) the consideration of the safety performance of the candidate cycle time must be included, (2) the interaction between the recalculation of the splits must be taken into account before selecting a new cycle setting, and (3) allowing the maximum degree of saturation to be taken from all phases in the system also tends to overreact to minor movements that are at their capacity. A small improvement to this heuristic is to consider some k highest saturation levels—or some determination of critical approaches or movements—throughout the network and only increase the cycle time when a minimum number of those critical links are above the 90 percent level. Similarly, decreasing the system cycle when all approaches are less than 90 percent may not be desirable to maintain adequate progression. To combine the effects of both safety and efficiency, evaluation of the safety performance function is included in the algorithm for adjusting the cycle time as shown in figure 24.
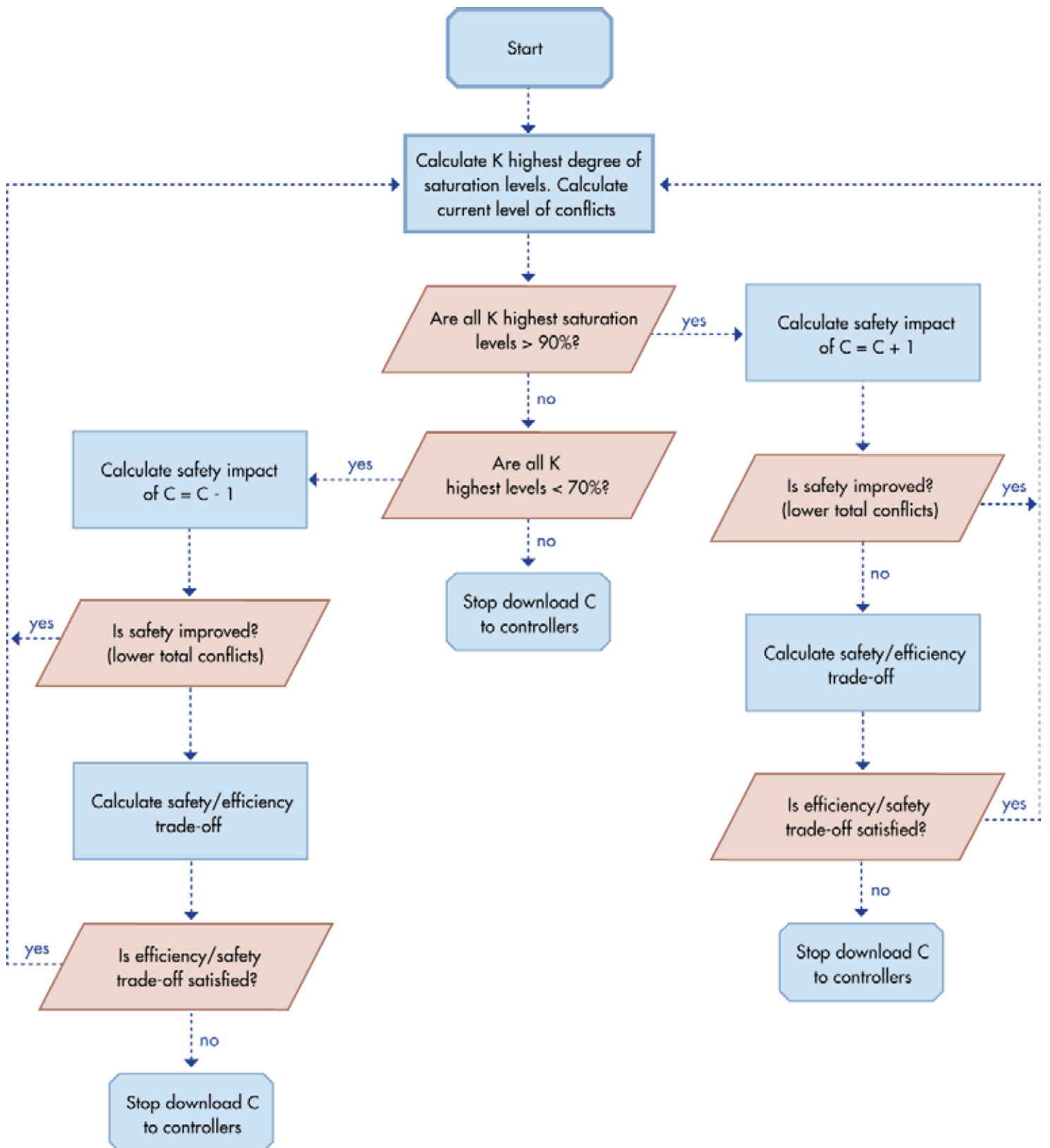
Figure 24. Chart. Flow chart of cycle time tuning algorithm.

In this manner, the possible improvements to both safety and efficiency are considered by first checking the efficiency metric for the cycle time. It must be determined if all of the k highest saturation levels are above or below 90 percent. If there are at least k movements with saturation levels above 90 percent, an increase to the cycle time is considered. If this change results in improvement to the safety metric, reducing the total predicted conflicts, this direction is followed until it begins to degrade safety performance or when one or more of the k highest saturation levels has fallen below 90 percent saturation (or whatever threshold is determined to be appropriate). When the safety performance does not continue to reduce the total number of conflicts, a safety efficiency trade-off metric is computed. Based on the current preferences, it is determined whether to continue to increase the cycle time at the expense of safety. If so, it is increased until the metric falls below the threshold, and then it is stopped.

Similarly, in the opposite direction, reducing the cycle time is considered if there are more than k' (where it could be true that k is not the same as k', but there is currently no judgment to determine that this is the case) movements with saturation level below 70 percent (or whatever threshold is determined to be appropriate). If this is true, a reduction to the cycle time is considered and the system cycle time is reduced until the safety trade-off metric is violated or there are no longer k' movements with saturation level below 70 percent.

6.3.2 Offset Tuning

Cycle time tuning affects all of the intersections in the network if they are all operating in a coordinated mode. Individual intersections that are run "free" can also have their cycle time tuned independently. Tuning offsets improves progression performance along primary routes for phases that are coordinated. Offset tuning algorithms are particularly straightforward. The methodology used in the ACS Lite project will be used in this project.[20]

The concept of the data-driven offset adjustment algorithm is summarized in two simple statements: (1) use detectors several hundred feet upstream of the signal to construct cycle-based profiles of traffic flow arriving to the intersection, and (2) adjust the offset to maximize the number of vehicles arriving during the green phase. This simple concept is then expanded to consider and mitigate the effects of such modifications to the offset value for two-way traffic and the effects of changes at this intersection on adjacent intersections. Periodically, small, incremental adjustments are made to the offset to maximize the total proportion of cyclic flow arriving to a green light.

It is assumed that an initial solution (plan data—cycle, splits, and offset) has already been developed and that the original offset may be less than optimal. A user-configurable maximum deviation from the original setting—either an increase or decrease to the offset value—is defined for each offset to restrict the algorithm from drifting too far away from the original solution.

Figure 25 illustrates the detector locations used for offset tuning. There is one detector station for each coordinated approach. Intersection 1 is referred to as the upstream intersection, and intersection 2 is referred to as the downstream intersection. Traffic volume and occupancy are measured at some point between 1 and 2 by a detector in each lane. These detectors can be located where typical advance detectors are located, 200–300 ft from the intersection. Placing detectors further upstream can improve the quality of the flow rate measurements and reduces

the possibility of vehicles queuing over the detectors when the light is red. It is also not necessary to have one detector per lane returned to the controller in a separate amplifier, but this practice will improve performance of the algorithm.
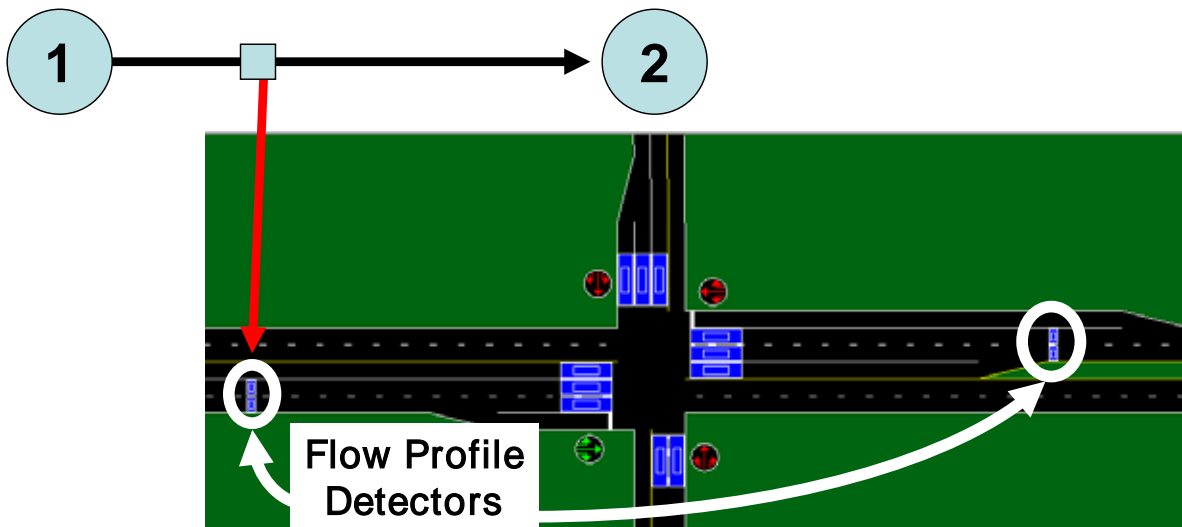

Figure 25. Illustration. Typical flow profile detector locations on coordinated approaches.

Assuming that the traffic signals at both intersections are using the same cycle length and that traffic volumes and turning proportions are reasonably steady over time, it is expected that the detector will measure approximately similar recurring patterns of flow during each cycle. These patterns of flow are referred to as *cyclic flow profiles* or just *flow profiles*.

Figure 26 plots the flow profile data (volume and occupancy observations) as a function of the local cycle time of the controller (time is on the x-axis). The magnitude of the volume and occupancy is indicated by the height of the corresponding bars in each row of the chart. The height of the bars in each row is scaled by the maximum value observed in that row. Equal heights in different rows do not necessarily indicate the same volume or occupancy value. These profiles indicate that it is typical over the last few cycles for traffic to arrive near the beginning of the local cycle time for this approach. Secondary platoons and individual vehicles also show up randomly throughout the cycle, possibly due to turning flow on the cross-street phases of intersection 1 and/or early return to green due to side-street gap-outs.
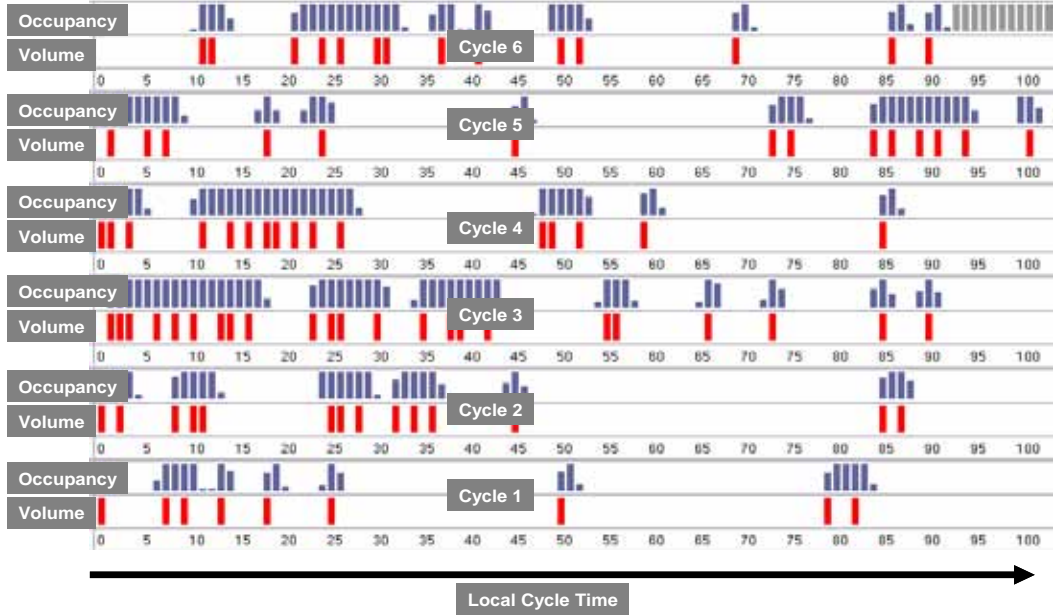
Figure 26. Illustration. Example of volume and occupancy data from a typical advance detector.

Figure 27 illustrates an example of phase timing history observed over the last several cycles at an intersection (note that the data from figure 26 and figure 27 are not from the same location).
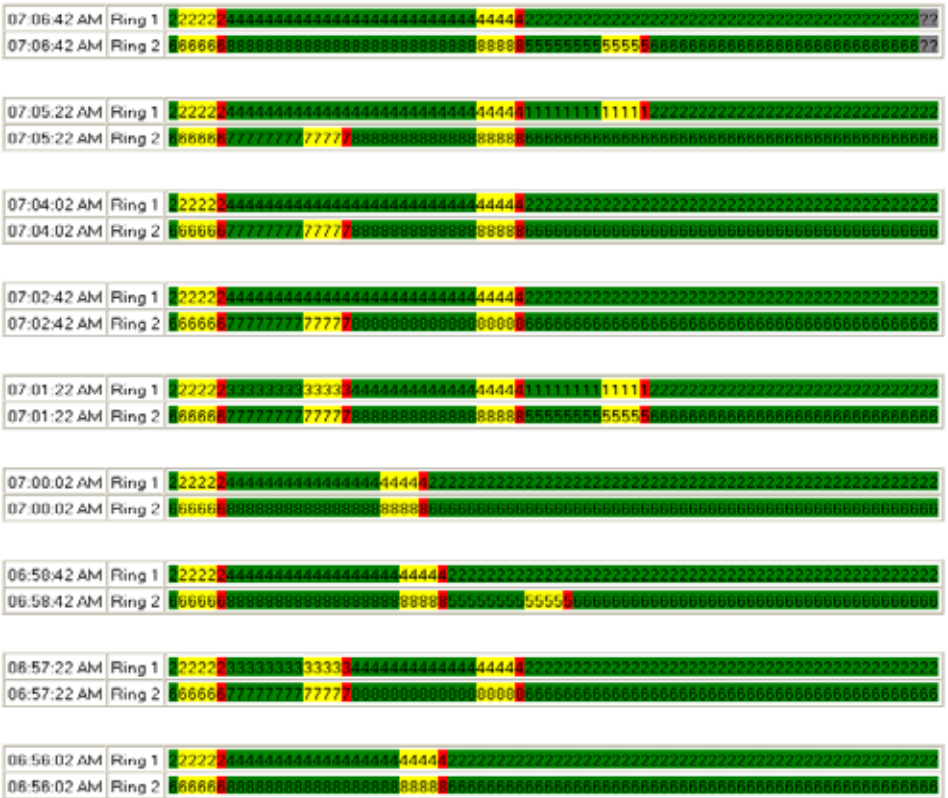

Figure 27. Illustration. Example of phase timing for each of the last several cycles.

77

The number and color of each column in the timeline corresponds to the active phase interval (green, yellow, and red) displayed by each ring at that time in the cycle. All subsequent cycles shown below the first row are actual data recorded from a field test controller with the most recent data at the top and progressing back in time down the display.

Each cycle begins at the local zero time, which is labeled on the left. Note that the duration of non-sync, actuated phases (typically phases other than 2 and 6) are variable, and one or more of these phases may be skipped in any given cycle. Thus, the time at which the controller returns to the sync phases (typically phases 2 and 6) can and does vary from cycle to cycle.

The cyclic flow profiles illustrated in figure 26 are then averaged to generate a single, representative cyclic flow profile for the flow profile detector as shown in figure 27. Each link, and thus each flow profile detector on that link, is associated (via user configuration) with a corresponding phase at the downstream intersection, referred to as the *progression phase*. Figure 28 shows a single cyclic representation of the percent of time that the progression phase was green during the several cycles since the last offset adjustment control decision. The height of the green bar in the display denotes a range of 0–100 percent. Note that in the case of an arterial, the progression phases generally correspond to the coordinated phases on the controller. In a grid network, all major through phases (coordinated and non-coordinated) might be configured as progression phases for their corresponding approaches. Figure 28 shows that during a portion of the cycle, the progression phase is green 100 percent of the time, starting at local time 50 and ending at local cycle time 0 (or 80). During each cycle, one or more non-sync phases typically gaps out early, and in such cases, the controller returns to the coordinated phase earlier than is required, typically termed "early return to green." Figure 28 illustrates this early return to green behavior with the tapering percent-green bars prior to the programmed start of main street green split (local time 50 s). As shown, this progression phase started as early as local cycle time 27 in at least one cycle during the last ~10 cycles.
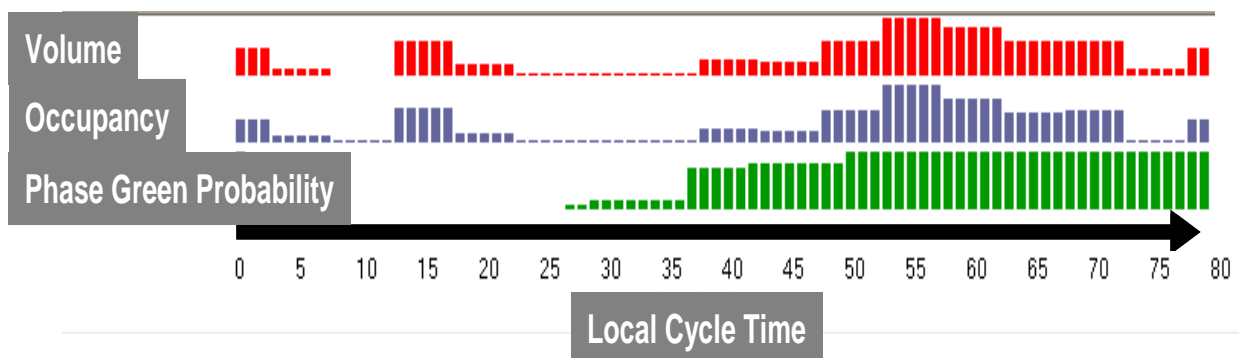

Figure 28. Illustration. Example of cyclic volume and occupancy profiles averaged over the last several cycles.

Figure 28 also displays the detector data from the flow profile detector shifted to account for the unimpeded travel time from the upstream detector location to the theoretical "green point," where a driver would likely decide to stop if the light were yellow and continue if the light were green. This time is configurable by the user based on input of an average travel speed and distance from the detector to the stop line. Detectors that are thus located at the theoretical decision point are not shifted at all, and in cases where the detector is placed closer to the signal

than the green point, this shift may be negative. Note that occupancy, rather than volume, is currently the preferred detector measurement used to generate flow profiles. Thus, the term *flow profile* is used to refer to shifted occupancy cyclic flow measurements rather than volume.

The flow profile scenario shown in figure 28 is an example of the performance of a good offset for one-directional travel. The arriving platoons are indicated by the cluster of relatively tall occupancy bars between local cycle time 40 and local cycle time 75, which corresponds to the green portion of the service phase.

6.3.2.1 Captured Flow

The effectiveness of two offset settings or the relative difference between the two settings at upstream and downstream intersections is quantified by calculating the *progressed flow* or *captured flow*. This performance measure is a surrogate for stops and delay, which cannot be directly measured in the field from point detectors. Specifically, the captured or progressed flow is the amount of flow (in units of vehicle-seconds of occupancy) arriving to the stop line at a given point in the cycle multiplied by the percent of time the progression phase is green at that time during the cycle. The algorithm evaluates different offsets by calculating the captured flow on each approach and selecting the offset that maximizes the total amount of captured flow.

6.3.2.2 Distributed Offset Adjustment

The methodology that will be used is a distributed offset adjustment method. This approach makes offset adjustments for each controller independently with consideration of the effects of each independent decision on adjacent signals. Each controller considers three offset settings: no change, adjust to Δ s earlier, or adjust to Δ s later. The adjustment increment Δ is a user-configurable value (currently specified as 2, 4, or 6 s). The adjustment procedure estimates the amount of cyclic traffic flow progressed for inbound and outbound links of the controller for each of the three adjustment options and chooses the option that maximizes the total progressed flow. As a reliability measure, there must be at least three cycles of error-free vehicle-occupancy data for every flow profile detector at this intersection and adjacent intersections as well as the corresponding phase timing status information to execute the selection algorithm. This provides a minimum level of smoothing. The ACS Lite project field tests determined that this methodology is effective at making adjustments to offsets to improve progression while mitigating the effects of controller transition by only making small adjustments for each tuning.

6.3.2.3 Including Safety in the Assessment of Offset Performance

The approach to tuning offsets previously discussed will be modified to include the evaluation of the safety impact of the adjustment. Similar to the approach for tuning the cycle time, the algorithm will use the safety performance regression equation as the performance calculator. This approach is detailed in the flow chart in figure 29. An enhancement to the methodology used by ACS Lite will also be applied. This adjustment will allow continuous evaluation of offset adjustment options (i.e. ±1 second, ±2 seconds, ±3 seconds, … ±10 seconds, etc.) instead of considering only three options for offset adjustments (i.e +2 seconds, -2 seconds, or zero). As identified by Gettman et al. this extension to the approach will provide more rapid response to offsets that are performing particularly poorly.[20]
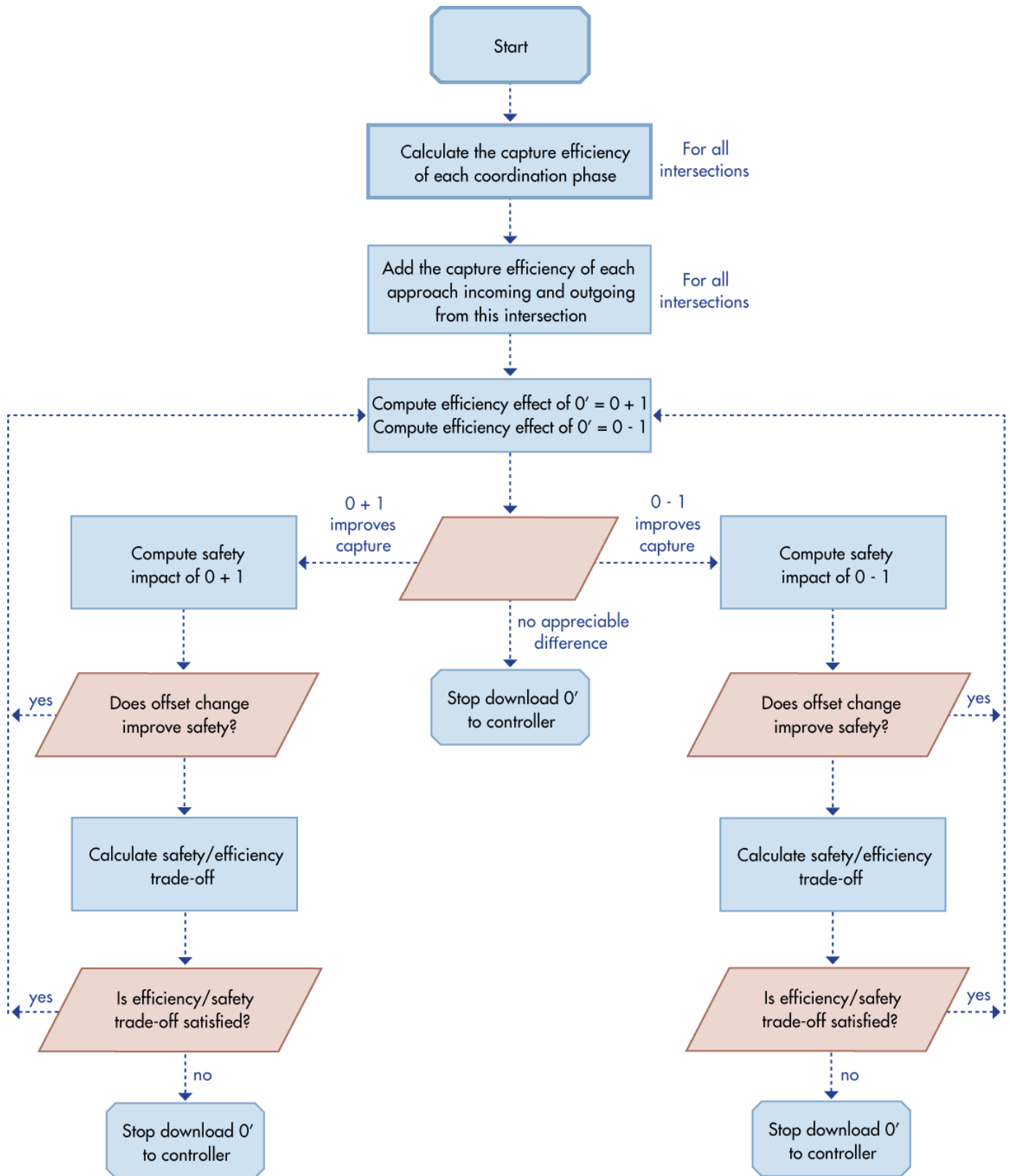
Figure 29. Chart. Offset adjustment algorithm flow chart.

As shown in figure 29, the general approach is to identify the capture efficiency performance of options to move the offset forward or backward. If one or the other improves performance over the "no change" situation (note that it is not common or probable that both moves improve performance), the safety impact of the proposed change is checked. If this change is deemed to improve both safety and efficiency, the algorithm will continue exploring this direction of change for additional improvements. If the change is deleterious to safety, the algorithm checks if the trade-off value is satisfied, asking if the effect on safety is not significant enough to disallow exploration in this direction. The algorithm continues until the effect on safety is deleterious or no longer improves the capture efficiency.

6.3.3 Split Tuning

The approach used to tune splits is driven by collecting the same data used to tune offsets—phase timing information and second-by-second detector occupancy and volume—but the data are collected from detectors at the stop bar of the intersection. This methodology is also derived from the algorithms developed in the ACS Lite project. In general, this approach to tuning split times is derived from the concept used by SCATS® and SCOOT, which is to equalize the degree of saturation on all the phases at the intersection. In shorthand, this approach is termed "equisat." To be specific, the algorithm in ACS Lite minimizes the maximum degree of saturation on any phase rather than driving all of the saturation levels to the same value. This algorithm also allows coordinated phases to have biased splits, so that progression is protected when the saturation level of the coordinated phase is lower than that of side streets. Without such biasing, the performance is slanted toward providing adequate levels of service on side streets, which neglects the throughput issues. The approach works by balancing a measure of degree of saturation that is termed "phase utilization."

6.3.3.1 Split Constraints

There are constraints on split adjustments which can be defined using a phase-barrier diagram. A typical phase-barrier sequence is illustrated, with barriers explicitly labeled, in figure 30.
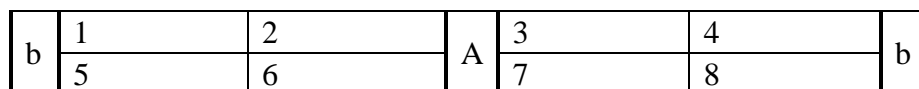
b	1	2	A	3	4	b
	5	6		7	8	

Figure 30. Diagram. Ring diagram with barriers denoted by bold vertical lines.

In discussing the split adjustment algorithms, it is necessary to refer to certain groups of phases. The collection of phases on a particular ring, between two particular barriers, is referred to as a *ring group*. In figure 30, there are four ring groups: (1, 2), (3, 4), (5, 6), and (7, 8).

A *barrier group* is the collection of all phases (or all ring groups) between two particular barriers. In figure 30, there are two barrier groups: (1, 2, 5, 6) and (3, 4, 7, 8). The algorithm uses these groups to swap split time from one phase to another in order to determine the set of split adjustments that satisfy the cycle time.

It is necessary to determine the legal range of adjustments for each split before solving for the set of split values recommended for a given controller. This includes consideration of minimum times, maximum times, and pedestrian crossing restrictions. These constraints are also important

to calculate for each ring and barrier group. While this may seem trivial, it is important to accurately calculate these values before searching the optimization space as consideration of these limits significantly improves the calculation efficiency.

6.3.3.2 Calculation of Duration Constraints

The following algorithm identifies the necessary steps for calculation of the constraints to be considered when searching for the optimum splits at each intersection.

1. **Compute the minimum, current, and (initial) maximum split durations for each phase p, $p \in P$.**

    - Compute $s_p^{min} = \max\{g_p^{min}, g_p^{max\ initial}, g_p^{walk} + g_p^{ped\ clear}\} + y_p + r_p$, for each phase p. Note that the actuated signal controller management information base (ASC MIB) objects uploaded from each controller are in mixed precision (some in seconds, others in tenths of a second). These values are combined in tenths of a second and rounded up to the nearest second. If phase p is omitted in the current pattern, then s_p^{min} is set to zero. The value s_p^{cur} is an ASC MIB object uploaded directly from the controller for each pattern. If phase p is omitted in the current pattern, then s_p^{cur} is set to zero.

    - Initially set $s_p^{max} = g_p^{max} + y_p + r_p$, where g_p^{max} is set depending on the maximum mode (max1, max2, or max inhibit) currently used by the controller. If max inhibit is the current mode, then s_p^{max} is set to 255 s. If phase p is omitted in the current pattern, then s_p^{max} is set to zero. Note that g_p^{max} is specified in seconds, whereas yellow and red intervals can be specified in tenths of a second. These values are combined in tenths of a second and then rounded down to the nearest second such that s_p^{max} is in seconds.

    - Ensure the current split is within the configured minimum and maximum constraints. If it is not true that $s_p^{min} \le s_p^{cur} \le s_p^{max}$, then stop—the configuration data are invalid.

    - If the adjustment process is constrained such that only incremental adjustments from the current value or a maximum cumulative deviation from an underlying baseline split value are allowed, then adjust the minimum and maximum constraints. If the constraint on the cumulative deviation from the baseline split is not satisfied by the current split value, then stop—this constraint is not currently achievable.

    - If there are no detectors associated with the current phase, then stop—this is a configuration error.

2. **Compute the minimum, current, and (initial) maximum durations for each group g.**

- For each ring r, compute the minimum, current, and (initial) maximum ring-group duration for the ring group in barrier group g on ring r as follows: $d_{rg}^{\min} = \sum_{p \in P_{rg}} s_p^{\min}$, $d_{rg}^{\mathrm{cur}} = \sum_{p \in P_{rg}} s_p^{\mathrm{cur}}$, and $d_{rg}^{\max} = \sum_{p \in P_{rg}} s_p^{\max}$.

- Compute the barrier group durations as follows: $d_g^{\min} = \max_{r \in R}\{d_{rg}^{\min}\}$, $d_g^{\mathrm{cur}} = \max_{r \in R}\{d_{rg}^{\mathrm{cur}}\}$, $d_g^{\max} = \min_{r \in \{R : d_{rg}^{\max} > 0\}}\{d_{rg}^{\max}\}$. In general, there will always be at least one phase in each barrier group, hence there will be one ring r such that $d_{rg}^{\max} > 0$, but if not, then set $d_g^{\max} = 0$.

3. **Calculate the revised maximum duration for each barrier group, its corresponding ring groups, and the maximum phase splits of their corresponding phases.**

- Calculate the revised maximum duration for group g under the assumption that each other group must time at least its minimum duration, as follows: $d_g^{\max} = C - \sum_{g' \in \{G : g' \neq g\}} d_{g'}^{\min}$.

- Revise the maximum duration for each ring group on each ring r of the barrier group g, such that it is not greater than the maximum barrier group duration of group g, as follows: $d_{rg}^{\max} = \min\{d_g^{\max}, d_{rg}^{\max}\}$.

- Ensure that the current ring-group duration (i.e., sum of splits) is not greater than the maximum ring-group duration possible with the cycle. If $d_{rg}^{\mathrm{cur}} > d_{rg}^{\max}$, then stop—there is a configuration problem.

- Calculate the revised maximum splits for each phase p in the ring groups from each ring r of the barrier group g, under the assumption that the maximum duration of the ring group may not be exceeded and each other phase in the ring group must time at least its minimum duration. This is calculated as follows: $s_p^{\max} = d_{rg}^{\max} - \sum_{p' \in \{P_{rg} : p' \neq p\}} s_{p'}^{\min}$.

- Ensure that the current split is not greater than the revised maximum split. If $s_p^{\mathrm{cur}} > s_p^{\max}$, then stop—there is a configuration problem.

Once the minimum and maximum phase split duration constraints have been determined using the preceding procedure, the multiring split adjustment algorithm may commence.

6.3.3.3 Estimating Phase Utilization

The split adjustment algorithm that will be used in phase 2 is based on the notion of balancing the utilization of all phases of a signal controller. Prior to discussing the algorithm itself, it is necessary to define the following:

· What is phase utilization?

· How is phase utilization measured?

· How is phase utilization estimated for split durations other than what is currently in use by the controller?

Phase utilization is the effectively utilized percentage of available split time. It is analogous to the degree of saturation concept, which is also referred to as the V/C ratio. Utilization is used instead of degree of saturation since the degree of saturation is calculated using volume and capacity counts or rates. Utilization is calculated using ratios of used green time to available green time. The used green time comes from occupancy of the detector.

Figure 31 illustrates a typical detector layout for measuring phase utilization with a detector placed at the stop bar for each lane. Each detector is associated with the phase that serves traffic flowing through its corresponding lane. Detector dimensions do not have to be the theoretical "best possible length."
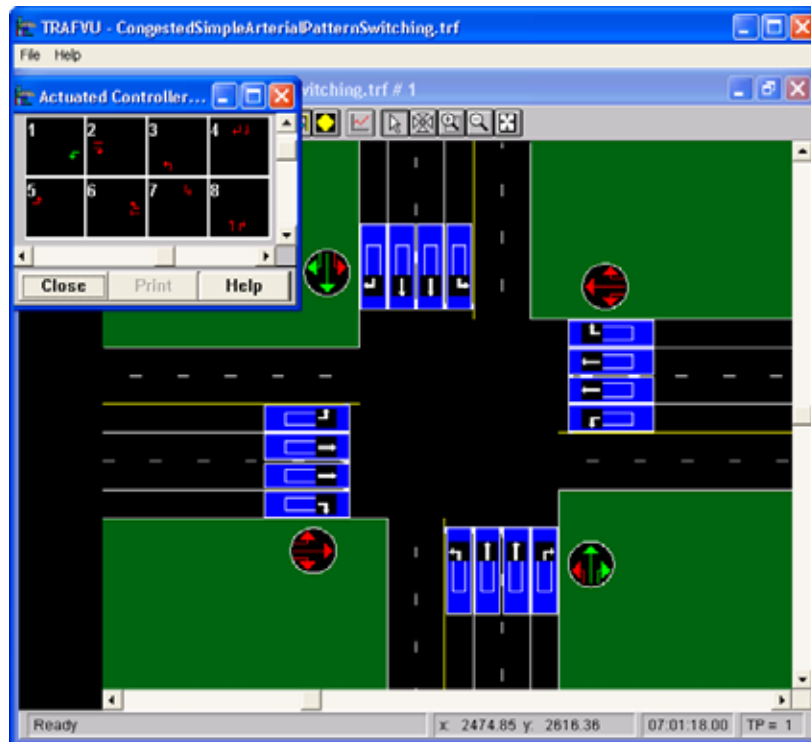

Figure 31. Screenshot. A complete utilization-detector layout for ACS Lite.

The methodology measures the demand for a phase by monitoring the occupancy of the phase during green. Demand is measured in terms of time, rather than volume. Utilization is given by the ratio of demand time to available green time. This is illustrated in figure 32.
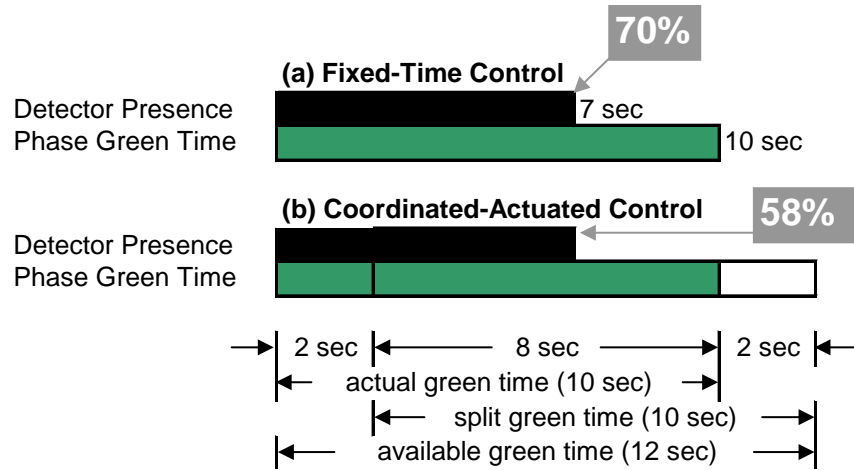
Figure 32. Illustration. Measuring phase utilization for coordinated-actuated controllers.

The system to be developed in phase 2 will poll controllers for phase timing and detector data once per minute and aggregate the data over time, combining several consecutive once-a-minute poll responses to construct estimates of occupancy during green, green phase duration, and utilization.

Figure 32 illustrates an example where 10 s of green is served, during 7 s of which the detector is occupied. For a fixed-time controller, this corresponds to 70 percent utilization. However, in the context of a coordinated, actuated controller, the capacity of the phase is measured as the amount of available green time. In this case, the phase started timing green 2 s early due to a prior phase gapping out early. It could serve up to 12 s of green until it is forced off, but it gaps out after 10 s of green. The notion of available green includes the remaining time to the force-off or maximum green, whichever comes first. It is also important to consider when phases have been skipped due to lack of demand.

Similar to the offset adjustment algorithm, the splits will not be tuned without collection of at least three recent observations of each phase while the controller is in coordination (i.e., when the controller is in transition or preemption, the algorithm will not use these data in tuning splits). Having satisfied this condition, the algorithm then calculates the utilization of alternate split durations for each phase using the following variables and equations, where:

N_p = Number of observations of phase p.

o_{ip} = Occupancy of phase p green time during observation i (0–100 percent).

g_{ip} = Green time served by phase p during observation i (seconds).

a_{ip} = Available green time for phase p during observation i (seconds).

d_p = Average demand (seconds occupied green) per cycle for phase p.

a_p = Average available green time (seconds) per cycle for phase p.

c_p = Clearance time (seconds of yellow and all-red) associated with phase p.

u_{pt} = Utilization estimate for phase p with split of duration t seconds.

6.3.3.4 Estimation of Split Utilization

The calculation of the split utilization is the primary prediction of how well or how poorly an alternative split allocation will perform when implemented. This prediction model is rather simplistic, but it presents a reasonable approximation when traffic is not rapidly increasing or rapidly decreasing in demand. The mathematical process to determine this function is as follows:

1. **If $N_p < 3$, then stop—there is not enough data for split adjustment.**

2. **Compute average demand, $\overline{d}_p = \dfrac{\left(\sum\limits_{i=1}^{N_p} o_{ip} g_{ip} \right)}{N_p}$.**

3. **Compute average available green time, $\overline{a}_p = \dfrac{\left(\sum\limits_{i=1}^{N_p} a_{ip} \right)}{N_p}$.**

4. **For each feasible split duration t, between $s_p^{\min}$ and $s_p^{\max}$, estimate the utilization of that split assuming current demand remains the same and the phase starts, on average, at the same point in the cycle.**

   · If $\overline{a}_p + t - s_p^{\text{cur}} > 0$ (i.e. the available green time of such a split duration is not zero), then

   set $u_{pt} = \dfrac{\overline{d}_p}{\overline{a}_p + t - s_p^{\text{cur}}}$.

   · Otherwise, if $\overline{a}_p + t - s_p^{\text{cur}} \leq 0$ (i.e. there is no available green time), then either set $u_{pt} = 0$ if $\overline{d}_p = 0$ (i.e. there is no demand), or set $u_{pt} = ¥$ if $\overline{d}_p > 0$.

After calculating the estimated utilization levels for all alternate split durations, an iterative algorithm is executed to select the combination of split values that satisfies the constraints on each phase and phase group (i.e., ring and barrier groups) and minimizes the maximum utilization of any phase on the controller. This procedure is discussed in the next section.

6.3.3.5 Balancing Utilization Levels

Each phase is assigned a utilization measure that approximates the degree of saturation of that phase, which ranges from 0 to 100 percent or higher, if oversaturated. Utilization is estimated for each phase for the full range of possible split durations, as discussed in preceding sections. Figure 33 is an example of utilization estimates for a dual-ring, eight-phase controller where the utilization of phase 3 is very high. Figure 34 is a chart of the estimated utilization of phases after the algorithm has adjusted the splits to minimize the maximum utilization of any phase on the controller.
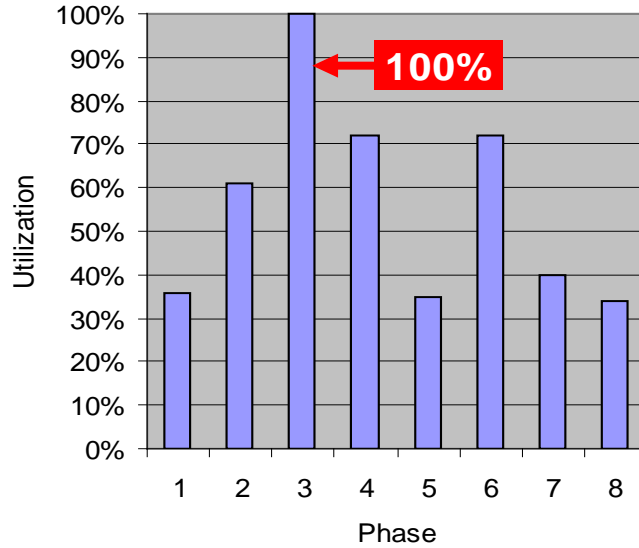
Figure 33. Graph. Utilization of phases before split adjustment.
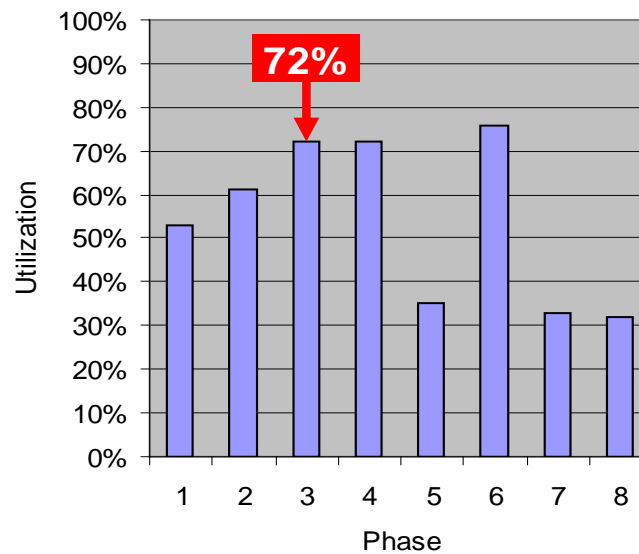
Figure 34. Graph. Utilization of phases after split adjustment.

The changes in split times are listed in table 42. The bold text in table 42 highlights the change of the most utilized phase from 100 percent to 72 percent. Also note that the new maximum phase utilization is now on phase 6, which has increased from 72 percent utilization to an estimated 76 percent utilization. Note that the result of the adjustment is not the exact same utilization level on each phase.

Table 42. Example utilization of phases before and after split adjustment.

Split Times(s)	Phase 1	Phase 2	Phase 3	Phase 4	Phase 5	Phase 6	Phase 7	Phase 8	
Pre-adjustment	14	21	13	22	10	25	15	20	
Post-adjustment	11	21	16	22	10	22	17	21	
Utilization (Percent)	**Phase 1**	**Phase 2**	**Phase 3**	**Phase 4**	**Phase 5**	**Phase 6**	**Phase 7**	**Phase 8**	**Maximum utilization**
Pre-adjustment	36	61	**100**	72	35	72	40	34	100
Post-adjustment	53	61	**72**	72	35	76	33	32	76

As indicated previously, the primary objective of the split adjustment algorithm is to minimize the maximum degree of utilization across all phases. These objectives achieve the general effect of balancing the degree of utilization across phases. Webster suggested as early as 1958 that allocation of splits to equalize the degree of utilization across all phases will have the effect of minimizing delay.[21] In the ACS Lite project, it was found that less than a dozen iterations of the balancing algorithm will typically result in a reallocation that minimizes the maximum phase utilization of the intersection. This does not consume an appreciable amount of CPU time, and thus, the addition of safety analysis should not impact the ability of the system to complete processing in a reasonable time frame.

6.3.3.6 Incorporating Safety Assessment in the Optimization of Splits

Similar to the approach used for cycle time and offset tuning, the algorithm for splits will incorporate evaluation of safety into the optimization by utilizing the safety performance functions developed at the beginning of phase 2. This process is illustrated in the flow chart in figure 35.

First, the reallocation algorithm is run to identify the set of splits that optimizes only efficiency. This set of splits is then input into the safety performance function and evaluated. The safety/efficiency trade-off is also calculated for each split. If the reallocated splits improve total safety, then the splits that have positive safety trade-off are identified for biasing. This means that their utilization values will be artificially increased to force the reallocation algorithm to dedicate more split time to those phases. Since those phases were found to have a positive correlation with improving safety (more time is less conflicts), additional time would be considered to improve safety further. The reallocation algorithm is then re-run with the biased utilization values. If this solution further improves total safety—the negative impacts from shortening the other phases is not enough to cancel out the positive returns—the process is repeated until additional biasing does not result in further safety improvements. Similarly, if the initial reallocation decreases total safety, the phases that have the highest negative trade-off impacts are identified. This process identifies the phases that were shortened in the initial reallocation and boosts their utilization values so that a subsequent reallocation will provide additional split for that phase. That reallocation is then tested again for an improvement to the total safety. If the result is positive, the algorithm stops. If the result is a further detriment, the most negatively impacted phases are biased and the process is repeated.
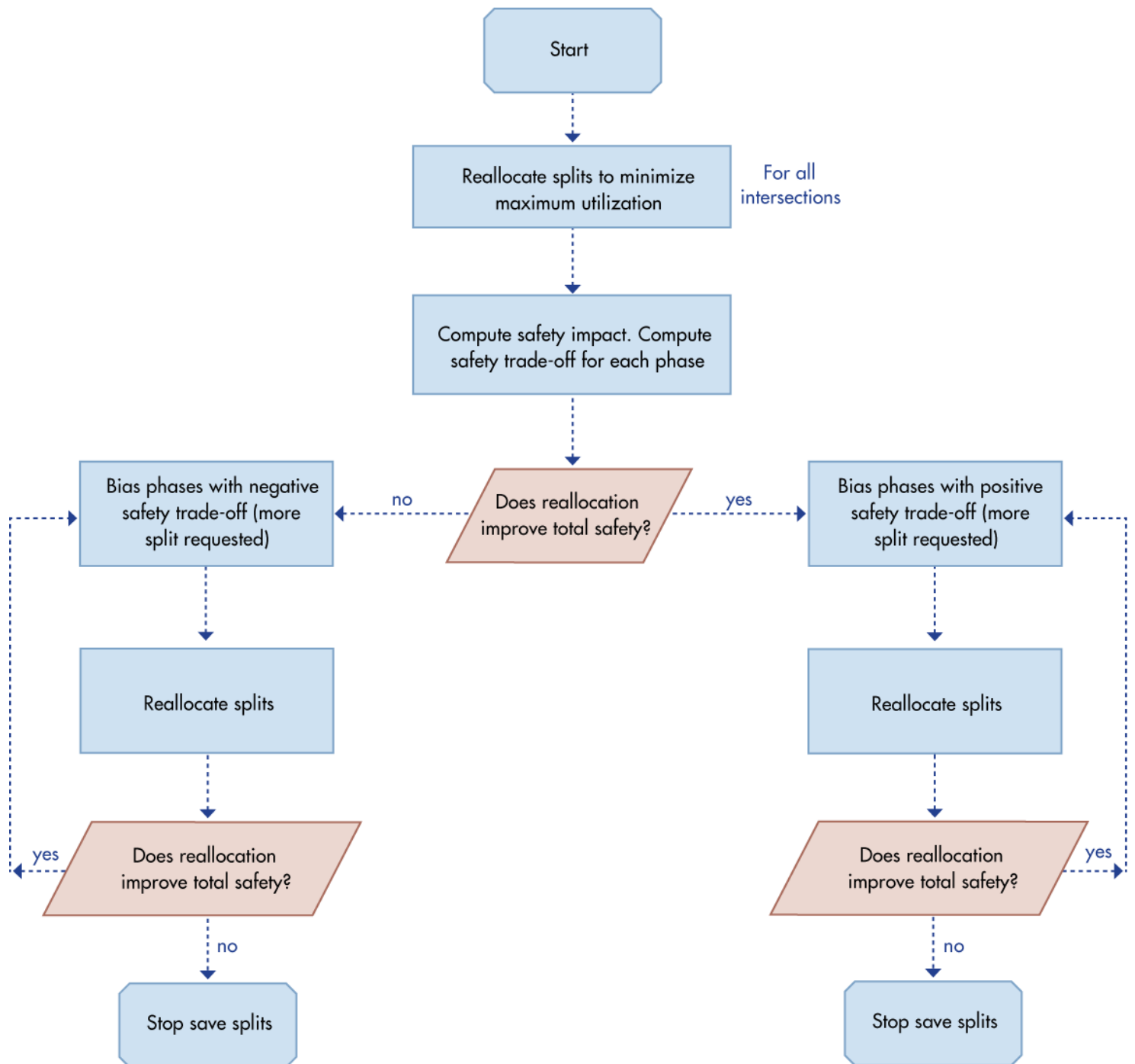
Figure 35. Chart. Flow chart of the split optimization process including safety analysis.

6.3.4 Phase Sequence Changes

Phase sequence affects both progression and delay at an intersection with respect to measures of efficiency. In this study, the sequence was found to also affect the safety of the intersection, particularly when an intersection operates in coordination in a signal system. In the parameter-tuning approach, improvements to both safety and efficiency can be made by analyzing the phase utilization measures for each signal phase and the total capture efficiency of the

coordinated phases. In illustrating the concept of the algorithm, only one barrier group (e.g., phases 1, 2, 5, 6 in a standard dual-ring quad intersection) is considered. The equivalent rules apply to phases 3, 4, 7, 8 in the other barrier group. In lieu of a flow chart, table 43 presents the concept as a table of decision rules.

Table 43. Rules to evaluate to consider changing phase sequence.

Current Sequence/ Potential Next Sequence	Lead-lead (12|56)	Lead-lag (12|65)	Lag-lead (21|56)	Lag-lag (21|65)
Lead-lead (12|56)	N/A	1 has heavier utilization than 5; 16 dominates 25	5 has heavier utilization than 1; 25 dominates 16; adjacent offset changes	26 dominates 16 or 25 (16/25 relatively equal)
Lead-lag (12|65)	Both 1 and 5 have high utilization; 16 is not significantly heavier than 25	N/A	25 dominates 16; adjacent offset changes; significant reversal in flow	1 is very light; adjacent offset changes
Lag-lead (21|56)	25 is not significantly heavier than 16; 1 heavy utilization; adjacent offset changes	1 heavier than 5; adjacent offset changes; 16 dominates 25; significant reversal in flow	N/A	5 is very light and 1 is not heavy utilization
Lag-lag (21|65)	Both 1 and 5 have heavy utilization; adjacent offset changes	1 heavier than 5; 16 dominates 25; adjacent offset changes	5 heavier than 1; 25 dominates 16	N/A

In the left column, the current operating phase sequence is listed: lead-lead, lead-lag, lag-lead, and lag-lag. The top row lists the phase sequence to evaluate for a potential change. The cells of the table indicate the rules that would justify a change from one sequence to another. For example, a change from lead-lead to lag-lead would be predicated if:

- Phase 5 has a heavier utilization than phase 1.

- Phases 2 and 5 have heavier total utilization than phases 1 and 6.

The third element of the table lists when a significant offset change would occur if changing from one sequence to another. In this example case, phase 1 would change to a lagging phase, which moves the offset to coincide with the end of phase 2 (most controllers reference the offset

to the yellow time of the first coordinated phase) instead of the end of both phases 2 and 6. At this intersection, of course, the offset value does not have to change. However, the change in when phase 2 will occur during the cycle will change the time that the traffic arrives at the intersection downstream from phase 2 and also the capture efficiency of the traffic that arrives to phase 6 from the intersection upstream of that phase. For example, if phase 2 services northbound traffic and phase 6 services southbound traffic, the intersection to the north will experience traffic arriving earlier in its cycle and the intersection to the south will have the traffic arriving later in its cycle. Thus, modifications to the phase sequence for the boxes that indicate "adjacent offset changes" will require a reevaluation of the offset selection algorithm.

Similar to the evaluation algorithms for cycle, splits, and offsets, after evaluating the efficiency impact of a potential change to the phase sequence, the effect on safety is checked by evaluating the regression equation. If safety is improved, the change is made. If safety is reduced, the efficiency-safety trade-off level is checked. If this level is acceptable, the change is still made. If it is not, the current sequence is retained.

6.3.5 Protected/Permitted Left-Turn Mode Changes

This study has shown that the mode of left-turn operations has a significant effect on the safety of an intersection, with permitted left turns creating the most conflicts and, not surprisingly, protected left turns creating the fewest conflicts. Efficiency is affected in a slightly different order with permitted being the least efficient, protected being next, and protected/permitted having the highest level of service for the same service volume (assuming the service volume is high enough to require protected/permitted operation). Similar to the algorithm for selecting phase sequence, the algorithm for modifying left-turn accommodation is presented in the form of a table. In table 44, the leftmost column lists the current left-turn treatment for a given left turn. The top row lists the left-turn treatment being considered. The cells of the table list the conditions that would justify a change from one left-turn treatment to the other.

Table 44. Rules to evaluate when considering changing left-turn treatment.

Current Left-turn Treatment/next Left-turn Treatment	Permitted Only	Protected	Protected/Permitted
Permitted only	N/A	Utilization of left-turn lane is heavy	N/A
Protected	Utilization of left-turn phase is very low	N/A	Utilization of left-turn phase is very high; opposing utilization is low to moderate
Protected/permitted	N/A	Utilization of left-turn-protected portion is moderate to low	N/A

Similar to the other algorithms, efficiency measure is evaluated first and then any potential detrimental effects on safety are compared by evaluating the trade-off value. If the trade-off

value of changes detrimental to safety is acceptable, the change to left-turn operational mode is made. Otherwise the current operating mode is retained.

6.4 ADAPTIVE CONTROL SYSTEM SUMMARY

The approach that will be pursued in phase 2 of this research is to develop a parameter-tuning adaptive control system. Safety and efficiency will be balanced by evaluating potential changes to splits, offsets, cycle time, phase sequence, and protected/permitted left-turn modes and implementing those changes that improve efficiency, improve safety, or do both. These five parameters were found to have an appreciable correlation to safety in the phase 1 research using analysis of simulated traffic conflicts. The authors believe that a parameter-tuning approach can be both effective and implementable, as evidenced by the recent development of ACS Lite for FHWA. In this project, a similar approach to ACS Lite will be followed to derive the adaptive decisions at each level of control directly from the field data. This approach uses reasonable surrogate performance measures of both efficiency and safety in lieu of an extensive simulation model that would derive total delay and stops and analyze conflicts.

The following four principle surrogate measures of performance are to be used in the adaptive control system:

- **Phase utilization** is a surrogate measure of efficiency that represents the degree of saturation of a traffic phase. This measure can be derived directly from the occupancy data measured at stop-bar detectors.

- **Progression capture efficiency** is a surrogate measure of efficiency that represents the progression performance of coordinated phases. Capture efficiency can be derived directly from the data measured at upstream detectors on the coordinated phases.

- **Total estimated conflicts per hour** is a surrogate measure that represents the estimated effect of changing a traffic-control parameter on intersection safety. This measure is a regression model that will be derived from an extensive designed experiment in the first stage of the phase 2 research.

- **Safety/efficiency trade-off** is a ratio of the change in efficiency to the change in safety, evaluated as the total societal cost/benefit in dollars. The safety/efficiency trade-off is used as a heuristic to evaluate if there is value in continuing to explore a given search direction or if the point of balance between the two objectives has been reached.

Each of these measures is used in the adaptive control algorithms as detailed in the previous sections. The five optimization stages are executed independently but in sequence and with the feedback steps as shown in figure 36.
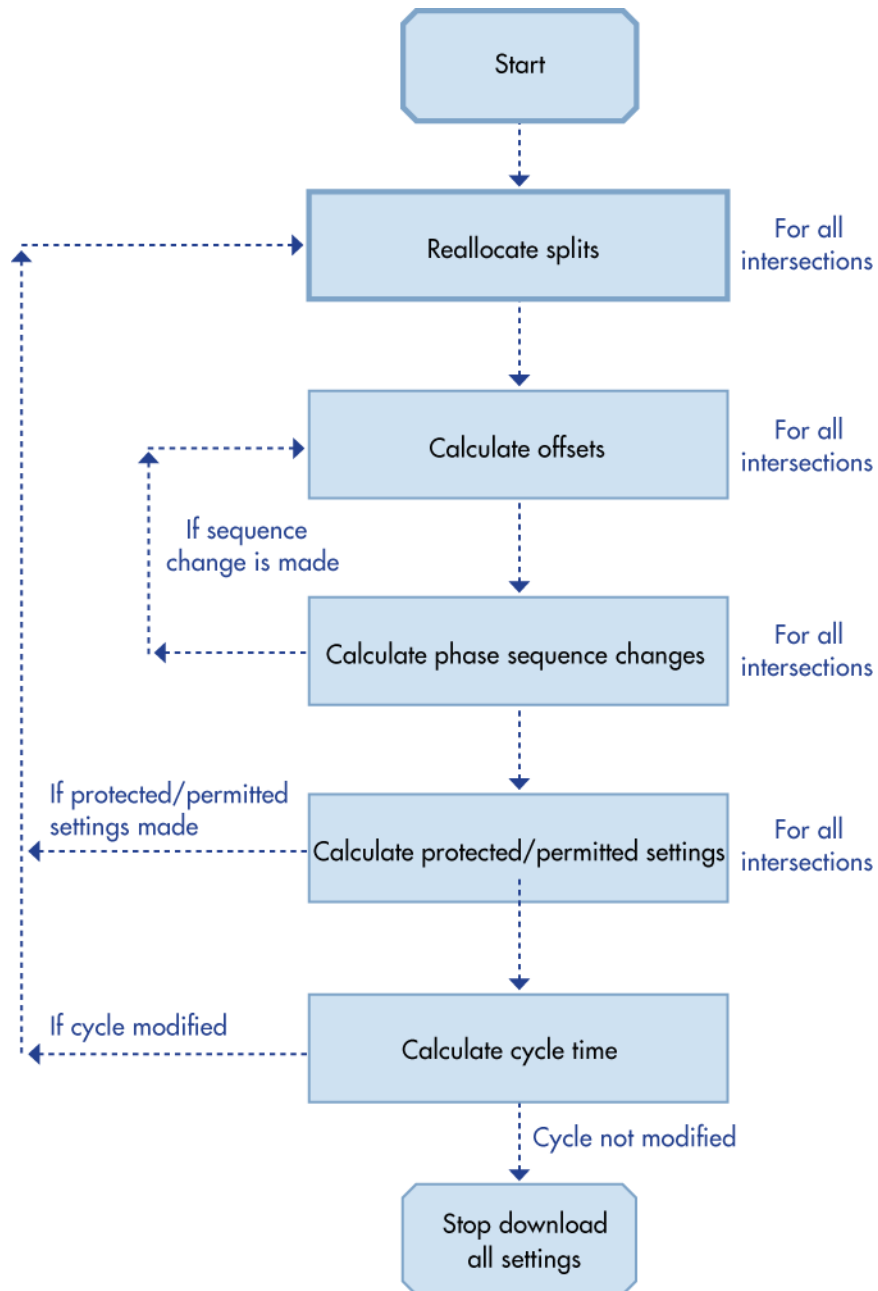
Figure 36. Chart. Flow chart of algorithms execution sequence.

In step 1, the split reallocation algorithm is executed for each intersection in the system. This step identifies if any slack green time can be shifted from one or more phases to another within the current cycle time to minimize the maximum phase utilization at the intersection. Safety is evaluated by checking that the reallocation either provides a safety benefit by reducing total conflicts or that the reallocation does not exceed a prescribed threshold for the safety/efficiency trade-off value.

After this reallocation, the offset adjustment algorithm is executed in step 2 to identify any modifications to the offsets to improve progression. The total capture efficiency of the offset to capture occupancy on the coordinated phases at the subject intersection and its neighbors is

calculated to represent the efficiency of the proposed change. Similar to the split calculation, safety is evaluated by checking that the new offset either provides a safety benefit by reducing total conflicts or that the proposed change does not exceed a prescribed threshold for the safety/efficiency trade-off value. If either of these continues to be true, the algorithm will continue changing the offset in that direction until efficiency is degraded, safety is degraded, or a preset threshold is reached. For example, to minimize transition effects, the changes to offsets at any adjustment interval may be limited to a small value such as 5 s (or X percent of cycle).

After the splits and offsets are calculated, modifications to the phase sequence (step 3) are evaluated with the new split values calculated in step 1. If any phase sequence modifications are identified that adjust the offset (the departure platoons to adjacent intersections), the offset calculation must be reexecuted to determine if this change is of further benefit and can be retained or if the change is detrimental to efficiency or safety performance. If the change is detrimental, the safety/efficiency trade-off can be used to determine if the phase sequence change should be dropped or if it is worth reexecuting the offset search algorithm to find a slightly better solution.

Next, potential changes to the protected/permitted settings for left-turns are evaluated (step 4) using the phase sequence selected in the previous step. If any left-turn settings are deemed beneficial to both efficiency and safety or deemed beneficial to efficiency and within the safety/efficiency trade-off value, the split reallocation algorithm may have to be recalculated, particularly if the left-turn mode is changed from protected to permitted-only. This change, in effect, omits the left-turn phase, setting its split to zero, which frees up additional time in the cycle for other phases. It may not be the best policy to simply provide all of that split for its corresponding companion through phase (e.g., phase 6 if the left turn is phase 1). In turn, if the splits are reallocated at this step, the offsets, phase sequence, and protected/permitted settings are reevaluated as well.

Finally, the cycle time adjustment algorithm is evaluated (step 5). Since cycle time affects all of the intersections in the system, it is important that this adjustment is calculated last, after all of the improvements to individual locations are calculated. As with the phase sequence and protected/permitted settings, if it is deemed beneficial to modify the cycle time, the other algorithms must be reevaluated within the new value for the cycle.

6.5 PHASE 2 RESEARCH APPROACH

The plan for research in phase 2 of the project is as follows:

1. Develop the safety performance function using simulation data.

2. Validate the theoretical predictive performance of the safety function.

3. Develop the multiobjective adaptive algorithms.

4. Evaluate the multiobjective algorithms in offline analysis scenarios.

5. Implement the multiobjective adaptive algorithms in a real-time processing system.

6. Test the multiobjective adaptive algorithms using simulation modeling.

7. Show proof of concept of the approach in a limited field deployment.

Validation of the approach with long-term crash studies will be done in phase 3 after the proof-of-concept demonstration.

6.5.1 Task 1: Develop the Safety Performance Function

In this task, the designed experiment will be specified in more detail than provided in this initial plan, and the simulations of the designed experiment will be run to collect the necessary traffic conflict data on the impact of interactions between the input parameters. Approximately 10 percent of the runs will then be set aside for the theoretical validation process in task 2. The remaining runs will be used to calculate the regression coefficients of the safety performance function. Several functional forms of the regression equation will be tested according to the results of the regression process. It is typical in regression modeling that some variables that were hypothesized to have significant impact turn out, in fact, to have very weak influence on the performance. These variables are then removed from the model, and the coefficients are recalculated.

6.5.2 Task 2: Validate the Safety Performance Function

In task 2, the predictive performance of the safety function will be tested with the ~10 percent of the simulation runs that were held out of the regression process. This step is important to identify the ability of the safety performance model to closely replicate the data obtained directly from running a particular simulation case. If the performance of the model is insufficient, it may be necessary to revisit the variable selection and regression form steps completed in task 1.

6.5.3 Task 3: Develop the Multiobjective Adaptive Algorithms

In task 3, the adaptive control algorithms specified in sections 6.3 and 6.4 will be implemented in software. These algorithms require both detector and phase-timing data as described in each section. This data will be obtained from a microscopic simulation model. The data-processing and evaluation concepts from ACS Lite for split tuning and offset tuning (and cycle time tuning, if it is available when the phase 2 project begins) and the evaluation of the safety performance function and additional tuning steps as outlined in sections 6.3 and 6.4 will be added. The other algorithms, for phase sequence selection and protected/permitted operation, will be new developments, and a new communications processing component will be developed to avoid any proprietary issues with Siemens ITS, the developers of ACS Lite for FHWA.

6.5.4 Task 4: Evaluate the Performance in Offline Scenarios

In this task, microsimulation data will be obtained for several test cases and will be output to files. These data files will be input to the adaptive control calculation engine to verify that the compromise algorithm process executes as expected. Since there is no feedback loop to the simulation process, the results of the changes to the traffic signal parameters cannot be assessed for the real performance, so this task will simply demonstrate that the algorithms are functioning.

6.5.5 Task 5: Implement the Algorithms in a Real-Time Processing System

In this task, the algorithms will be implemented in an online manner with a traffic simulation model in the loop. To streamline the process of moving the algorithms to real-world testing, the algorithms will be interfaced to a virtual traffic controller that is identical to the version of the controller that runs in the field. There are two such controllers available in the market today: D4 from 4th Dimension Traffic and the Econolite ASC/3. Both are able to interface to the VISSIM® microsimulation model environment. Currently, the research team has more experience with the D4 virtual controller, but it will consider both as part of the project. In either case, the interface between the optimization component and the field controller will be an open standard such as the National Transportation Communications for Intelligent Transportation Systems Protocol. This implementation will allow evaluation of the performance of the algorithms before deployment in the street. A similar architecture is envisioned for the system when deployed in the real world. The adaptive control algorithms will reside as part of a central system, similar to the architecture of ACS Lite, by polling detector data and phase timing information from the controllers and downloading new timing parameters on a periodic basis (every 3–5 cycles). This adaptive control component will be part of a central system, unlike ACS Lite, which operates as a master controller.

6.5.6 Task 6: Test the Algorithms' Performance in Simulation Scenarios

In this task, the algorithms will be tested in simulation scenarios. A combination of scenarios for single intersections, small arterial, long arterial, and small networks will be tested. The test cases will replicate field locations that will be candidates for field testing in task 7. The simulation test results will be tabulated and used both to determine if it is worthwhile to deploy the system in the real world and to evaluate its online performance.

6.5.7 Task 7: Show Proof of Concept in a Limited Field Deployment

Assuming acceptable performance of the system in task 6, task 7 will deploy the algorithms to the field to assess their performance in the real world. Since the development of the system in task 5 uses the virtual controller software, there should only be minor modifications necessary to deploy the approach at real intersections. A possible test includes perhaps three to five intersections being controlled by the adaptive system. Before- and after-travel time runs and traffic conflict analysis studies would be executed to evaluate the system performance. The site could then be used for long-term data collection and performance analysis in phase 3.

REFERENCES

1. Zimmerman, K.H. and Bonneson, J.A. (2005). *In-Service Evaluation of a Detection-Control System for High-Speed Signalized Intersections*, Implementation Report No. 5-4022-01-1, Texas Transportation Institute, College Station, TX.

2. Zhou, M. and Sisiopiku, V. (1997). "Relationship Between Volume-to-Capacity Ratios and Accident Rates," *Transportation Research Record 1581*, Transportation Research Board, Washington, DC.

3. Torday, A. and Dumont, A. (2002). *Safety Indicator for Microsimulation-Based Assessments*, Swiss Federal Institute of Technology, Laboratory of Traffic Facilities, LAVOC-EPFL, Lausanne, Switzerland.

4. Migletz, D. et al. (1985). *Relationships Between Traffic Conflicts and Accidents*, Report No. FHWA-RD-84-042, Federal Highway Administration, Washington, DC.

5. Gettman, D. and Head, L. (2003). *Surrogate Safety Measures From Traffic Simulation Models*, Report No. FHWA-RD-03-050, Federal Highway Administration, Washington, DC.

6. Gettman, D., Pu, L., Sayed, T., and Shelby, S. (2008). *Surrogate Safety Assessment Model and Validation: Final Report*, Report No. FHWA-HRT-08-051, Federal Highway Administration, Washington, DC.

7. Tiwari, G. et al. (1995). *Conflict Analysis for Prediction of Fatal Crash Locations in Mixed Traffic Streams*, Proceedings of the 29th Annual Association for the Advancement of Automotive Medicine, Chicago, IL.

8. Cooper, D. and Ferguson, N. (1976). "A Conflict Simulation Model," *Traffic Engineering and Control*, *17*, 306–309.

9. Darzentas, J. et al. (1980). "Minimum Acceptance Gaps and Conflict Involvement in a Single Crossing Maneuver," *Traffic Engineering and Control*, *21*, 58–62.

10. Fazio, J. et al. (1995). "Use of Freeway Conflict Rates as an Alternative to Crash Rates in Weaving Section Safety Analyses," *Transportation Research Record 1401*, Transportation Research Board, Washington, DC.

11. Torday, A. and Dumont, A. (2002). *Safety Indicator for Microsimulation-based Assessments*, Swiss Federal Institute of Technology, Laboratory of Traffic Facilities, LAVOC-EPFL, Lausanne, Switzerland.

12. Trafficware$^{\text{Ò}}$. (2007). SIMTRAFFIC 6. Obtained from: www.trafficware.com. Site last accessed December 10, 2009.

13. PTV AG. (2008). *VISSIM$^{®}$ User Manual*, Version 5.1, Release 7, Karlsruhe, Germany.

14. Gettman, D., Shelby, S., Pu, L., and Joshi, R. (2008). *Surrogate Safety Assessment Model (SSAM)—Software User Manual*, Report No. FHWA-HRT-08-050, Federal Highway Administration, Washington, DC.

15. Pline, J.L., Ed. (2001). *Traffic Control Devices Handbook*, Institute of Transportation Engineers, Washington, DC.

16. Maryland State Highway Administration (2006). *Traffic Control Devices Design Manual*, Annapolis, MD.

17. Pilko, P. and Bared, J. (2009). *Safety Assessment of Intersection Phase-Change Interval Timing Using Simulation*, Proceedings of the Transportation Research Board Conference, Washington, DC.

18. Kaub, A. (2000). *Highway Corridor Safety Levels of Service Based on Annual Risk of Injury*, 79th Transportation Research Board Annual Meeting, Washington, DC.

19. Lee, S. and Berg, W. (1997). *Development of a Safety-Based Level of Service Parameters for Two-Way, Stop-Controlled Intersections*, Paper submitted to 74th Annual Transportation Research Board Meeting, Washington, DC.

20. Gettman, D. et al. (2007). "Data-Driven Algorithms for Real-Time Adaptive Tuning of Offsets in Coordinated Traffic Signal Systems," *Transportation Research Record 2035*, Transportation Research Board, Washington, DC.

21. Webster, F.V. (1958). "Traffic Signal Settings," *Road Research Technical Paper 39*, H.M. Stationary Office, London, England.